Construction of an Integrated Hydrological Model for Sustainable Water Resources Management in the Chirchik River Basin, Uzbekistan

ウスマノフ, サイドイスロムホーン

https://doi.org/10.15017/1807005

出版情報：九州大学, 2016, 博士（工学）, 課程博士
バージョン：

Construction of an Integrated Hydrological Model for Sustainable Water Resources Management in the Chirchik River Basin, Uzbekistan

Saidislomkhon Usmanov

Construction of an Integrated Hydrological Model for Sustainable Water Resources Management in the Chirchik River Basin, Uzbekistan.

A Thesis Submitted
In Partial Fulfillment of the Requirements
For the Degree of
Doctor of Engineering

By
Saidislomkhon Usmanov

to the
DEPARTMENT OF CIVIL AND STRUCTURAL ENGINEERING
GRADUATE SCHOOL OF ENGINEERING
KYUSHU UNIVERSITY
Fukuoka, Japan
January, 2017

DEPARTMENT OF CIVIL AND STRUCTURAL ENGINEERING
GRADUATE SCHOOL OF ENGINEERING
KYUSHU UNIVERSITY
Fukuoka, Japan

CERTIFICATE

The undersigned hereby certify that they have read and recommended to the Graduate School of Engineering for the acceptance of this thesis entitled, "***Construction of Integrated an Hydrological Model for Sustainable Water Resources Management in the Chirchik River Basin, Uzbekistan*** " by **Saidislomkhon Usmanov Mannonovich** in partial fulfillment of the requirements for the degree of **Doctor of Engineering**.

Dated: January, 2017

Thesis Supervisor:

_____
Prof. Yasuhiro Mitani, Dr. Eng.

Examining Committee:

_____
Prof. Tetsuya Kusuda, Dr. Eng.

_____
Associate Prof. Yoshinari Hiroshiro, Dr. Eng.

Table of Contents

ACKNOWLEDGEMENT 4

ABSTRACT 5

LIST OF TABLES 8

LIST OF FIGURES 9

Chapter 1: Introduction 12

1.1 Study area and climate 12

1.2 Demography and economic indicators 14

1.3 Water sources and hydrological characteristics 16

1.4 Geology and soil 22

1.5 Problems of water resources management 27

1.6 Research objectives 30

1.7 Dissertation arrangements 31

1.8 References 32

Chapter 2: Integrated hydrological modeling system 34

2.1 Hydrological model selection 34

2.2 Modeling structures 37

2.3 Actual evapotranspiration 38

2.4 Snow melting and freezing 40

2.5 Unsaturated zone components 41

2.6 Saturated zone components 42

2.7 Overland flow components 42

2.8 MIKE 11 model for river flow simulation 43

2.9 Geostatistical interpolation methods 44

2.9 References 46

Chapter 3: Evaluation of Interpolation Methods for Spatial Modeling of Reference Evapotranspiration Using Modified Hargreaves Equation 48

3.1 Introduction 48
3.2 Spatial distributed reference evapotranspiration 48
3.3 Materials and methods 50
3.4 Results and discussions 52
3.5 Evaluation of interpolation methods 55
3.6 Conclusion 60
3.7 References 61
Chapter 4: Development of Hydrological Model Parameters of Chirchik River Basin, Northern Uzbekistan 62
4.1 Introduction 62
4.2 Simulation specification 62
4.3 Generation of spatial distributed hydrological parameters 63
4.4 Stream flow simulation 82
4.5 Irrigation process 86
4.6 Calibration and validation 87
4.7 Stream flow hydrograph 87
4.8 Groundwater dynamics 89
4.9 Water balance results of Chirchik River Basin 97
4.10 Conclusions 101
4.11 References 102
Chapter 5: Integrated Approach to Detect the Spatial and Temporal Variation of Groundwater Level in Quyi Chirchik District, Uzbekistan 104
5.1 Introduction 104
5.2 Problems in groundwater management 105
5.3 Hydrological model development 107
5.4 Results and discussion 113
5.5 Spatial analyses of groundwater table 120
5.6 Groundwater Quality Assessment by Using Water Quality Index in Quyi Chirchik District 123

5.6 Results and discussion 125
5.7 Correlation of the groundwater table and land use with water quality 129
5.8 Conclusion 131
5.9 References 133
Chapter 6: Conclusions and Future Work 135
6.1 Conclusion 135
6.2 Future works 137

ACKNOWLEDGEMENT

I would like to express my genuine gratitude and appreciation to my doctoral thesis supervisor, Prof. Yasuhiro Mitani without whom this thesis would not have been possible. I would also like extending my sincere gratitude to Prof. Tetsuya Kusuada and Dr. Hiro Ikemi. The support, encouragement and professional advice that I received from my supervisors was of much help in the writing of this thesis. In spite of his tight schedule, he was able to provide proper guidance, advice and help in this research project.

I would also like extending my sincere gratitude to Dr. Ernazar Jumaevich, Professor in Technical university in Uzbekistan, for the providing the good suggestions and giving advice throughout this research journey.

I would like to thank to Dr. Hendra Pachri, Ryunosuke Nakanishi and Hiroyuki Honda students of Civil and Structural Engineering department at the Kyushu University. They were showed a constant help in sorting out all the problems encountered during this study.

I also want to express, my deepest gratitude and appreciation to my dearest mum, Mrs. Makhmuda Usmanova, for their love and proper guidance in life. Also, I would like to thank my lovely wife Nozima Usmanova, for always caring for me, understanding, patient and support during this study period.

ABSTRACT

The Chirchik River Basin is considered one of the country's largest and most important basins. It is located in the northeastern province of Tashkent, Uzbekistan. The economy of the basin relies heavily on agricultural production; employing most of the region's population and consuming the lionshare of available water through irrigation practices. Unsurprising, the Chirchik River basin is facing several potentially severe water related problems, including increased aridity and, land salinization, and declines in agricultural production. Continuously increasing the groundwater level and the inefficient use of river waters are expected to further compound these problems, and their effects. Poor management of water resources due to limited knowledge of hydrological processes has been identified as a root cause of water resource issues in the basin. Efficient management requires accurate estimation and modeling of water balance and main hydrological parameters. In order to achieve reliable and accurate results, irrigation processes, which play an important role in the hydrological cycle, should be included in the model to account for the contribution of irrigation water to other hydrological parameters. In this concern, an integrated hydrological model was developed to study hydrological processes in the basin territory through detailed water balance estimation.

Previously, the empirical coefficient (0.0023) of Hargreaves model (HM) was modified under local climatic conditions of Tashkent province using standard Penman Monteih FAO 56 (FAO-56 PM) model estimates for every month of the years. Then the suitable interpolation methods were determined among deterministic, geostatistical and regression methods to spatial modeling of ETo over Tashkent province using modified HM estimates. Using the estimated reference evapotranspiration, hydrological parameters were estimated of Chirchik River Basin using the integrated hydrological model. The groundwater and surface water interaction and spatial variability of hydrological parameters are also analyzed.

In the last part of the research have introduced the GIS based method and its application in Quyi Chirchik district in Tashkent Province to detect the Spatial and Temporal Variation of Groundwater Level. The research also studies the relationship between spatial and temporal variation of groundwater level and its quality.

The significant findings of the research are presented as follows:

1. The best interpolation model of ETo was obtained from Co-kriking method using elevation data as an auxiliary secondary variable. The results revealed that the incorporation of elevation data improved spatial prediction of ETo in Tashkent province. The modified HM provided the best performance to estimate ETo in Tashkent province as an arid and semiarid climate. Over and under estimations of ETo with the original HM were reduced by 65 % as an average using new empirical coefficients for all 16 weather stations.

2. Actual evapotranspiration was found to be the main water loss factor among water balance components, with an average of 714 mm/year (77% of total water budget). As an arid land, AET is strongly dependent on irrigation water quantity irrespective of rainfall.

3. Actual evapotranspiration is highly variable across the basin, with increases toward to downstream sites. The estimated AET in irrigation areas at downstream sites was almost two times higher than upstream sites. Therefore decreased irrigation water causes increased aridity, particularly in downstream site.

4. The general direction of groundwater flow is toward the Syrdarya River. Base flow from basin boundary into the Syrdarya River was estimated at an average of 55 mm/year. The Chirchik River is gaining upper stream sites by overland flow on average 77 mm/year.

5. The novelty of this study is a development of a local hydrological model for a relatively large river basin covering from upstream to downstream site of the basin and considering agricultural water use and administrative boundaries of the districts. This modeling approach is better describing formation, utilization and discharging of water resources under the impact of different land use process.

6. The spatial analyses show southwestern part of Quyi Chirchik district is impacted by high groundwater table. In 925 ha area groundwater depth were estimated 2.5 meters in end of May. This groundwater depth considered critical level due to its negative effects. Because from this level groundwater expose to evaporation and create good environment for soil salinization process. It should be noted that, about 86 % of these lands corresponds to irrigated agricultural lands. Visual comparison of the model generated groundwater depth map with government elaborated map is spatially

overlapped by 70 %. This shows that this is an accurate approach to detect the high water table impacted areas under irrigation process. This method can be important to water resources managers to perform countermeasures against aridity increase and soil salinization issues.

7. The results shows that 75 % of groundwater samples in Quyi Chirchik district falls in “Fair” classification and 25 % samples falls in “Poor” categories of WQI. This shows that shallow groundwater in the study area is not suitable for drinking purposes. The statistical analyses show that the high value of WQI and TDS of this site has been found mainly from the higher values of sulfate, nitrate, calcium, magnesium and sodium. The excessive concentration of sulfate and nitrate in samples depicts intensive application of inorganic fertilizers. The study also found that a strong correlation exists between the groundwater table depth and TDS. The spatial distributed groundwater table depth and WQI map provide valuable tools for managers to understand the status of water quality specially and assist making adequate decisions.

LIST OF TABLES

Table 1.1 Average GDP of agricultural sub sectors……..14
Table 1.2 Average harvest of the cotton and wheat……15
Table 1.3 Utilization of total water resources by sectors……20
Table 1.4 Water utilization of districts of Chirchik River Basin……..21
Table 3.1 Statistics for mean monthly, vegetation period (VP), and annual ETo (mm) of all 16 meteorological stations for the observation period 2009-2011 across Tashkent province (SD = standard deviation)……51
Table 3.2 Average of new coefficient of HM for all weather stations (values in the table are multiples of 0.001). The first column shows ID of weather stations…….53
Table 3.3 RMSE of prediction produced by each of the interpolation methods for monthly (Jan-Dec), vegetation period (VP) and annual ETo……56
Table 4.1 Technical Characteristics of AVNIR-2 satellite image……68
Table 4.2 Explication of each land use classes……69
Table 4.3 Independent ET parameters……..70
Table 4.4 Degree day coefficients……75
Table 4.5 Hydrogeological parameter of soil in study area……..77
Table 4.6 Soil vertical discretization……..……..78
Table 4.7 Description of branch network in MIKE 11 model……..83
Table 4.8 Performance of streamflow simulation at Chinoz gauging station.....89
Table 4.9 Calibration results of groundwater simulation……..96
Table 4.10 Validation results of groundwater simulation……96
Table 4.11 Contribution of hydrological parameters to water balance……99
Table 5.1 Hydrogeological parameters of Quyi Chirchik district……..108
Table 5.2 Estimated water balance parameters of hydrological model……..114
Table 5.3 Statistics of groundwater simulation……..118
Table 5.4 Relative weight for each chemical parameter……126
Table 5.5 Water quality classification based on WQI……126
Table 5.6 Sample data of groundwater chemicals (mg/l) and estimated WQI……127
Table 5.7 Correlation coefficient matrix……128

LIST OF FIGURES

Figure 1.1 Map of Tashkent Province and districts.....13
Figure 1.2 Potential evaporation of Tashkent Province.....15
Figure 1.3 Precipitation of Tashkent Province.....15
Figure 1.4 Charvak Water reservoir (www.travelpod.com).....18
Figure 1.5 Main rivers and irrigation canals of Chirchik River Basin.....18
Figure 1.6 Coverage area of irrigation channels.....19
Figure 1.7 Discharge of UPCH (total discharge of Chirchik and Ugam Rivers) and Chinoz gauging station.....19
Figure 1.8 Irrigation sources of Tashkent Province.....21
Figure 1.9 Topography of Tashkent Province.....24
Figure 1.10 Geological profile of Chirchik River Basin from mountain zone to foothill area.....26
Figure 1.11 Geological map of Chirchik River Basin.....26
Figure 1.12 Demographic changes of Tashkent Province.....29
Figure 1.13 Groundwater impacted map of Tashkent Province.....29
Figure 1.14 Groundwater impacted areas in districts of Tashkent Province.....30
Figure 2.1 Classification of hydrological models.....36
Figure 2.2 Schematic view of the integrated hydrological model.....36
Figure 2.3 Hydrological processes simulated by MIKE SHE. Source: Refsgaard and Storm (1995).....37
Figure 2.4 Open channel flow along a longitudinal axis indexed by the abscissa x.....43
Figure 3.1 Location of meteorological stations and Digital Elevation Model (DEM) of Tashkent Province, Uzbekistan.....49
Figure 3.2 Comparison of estimated ETo by two methods (values in the table are multiples of 0.001). The x axes has labeled with ID of weather stations.....53
Figure 3.3 Variation of new average coefficients of HM.....54
Figure 3.4 Spatial prediction of average (2009-2011) annual and vegetation period (VP) ETo (mm) across Tashkent Province.....56

Figure 3.5 Spatial prediction of average monthly (2009-2011) ETo (mm) across Tashkent Province……...57
Figure 4.1 Generation process of sub watersheds of Tashkent Province…….64
Figure 4.2 Extraction of the Chirchik River Basin boundary from geospatial data…….64
Figure 4.3 Topography of Chirchik River Basin input in MIKE SHE…….65
Figure 4.4 ALOS AVNIR-2 satellite image…….68
Figure 4.5 Land use map of the Chirchik River Basin……..……..69
Figure 4.6 Values of seasonal changes of LAI……..71
Figure 4.7 Values of seasonal changes of RD…….....71
Figure 4.8 Weather stations of Tashkent Province……..……73
Figure 4.9 Average annual precipitation data of selected weather stations…..……74
Figure 4.10 Average annual ETo data of selected weather stations……74
Figure 4.11 Initial snow storage depth of study area……..……..75
Figure 4.12 Soil map of Chirchik River Basin……..78
Figure 4.13 Depth of the soil map of Chirchik River Basin…….……..……..79
Figure 4.14 Initial groundwater table and wells of Chirchik River Basin……79
Figure 4.15 Preprocessed hydrogeological parameters…….....80
Figure 4.16 River network of simulated branches and irrigated area……..…..83
Figure 4.17 Measuring process of river cross section of Chirchik River …….……84
Figure 4.18 An example of the cross-section of the Chirchik River…….84
Figure 4.19 Daily discharge data of Ugam gauging station…….85
Figure 4.20 Daily discharge data of Charvak gauging station …….……..……..85
Figure 4.21 Location of gauging stations in Chirchik River Basin……...88
Figure 4.22 Calibration of simulated stream flow in Chinoz gauging station….....88
Figure 4.23 Validation of simulated stream flow in Chinoz gauging station ……..…88
Figure 4.24 Simulated and observed groundwater level for 2009-2011 …….…….90
Figure 4.25 Simulated and observed groundwater level for 2012-2013……..93
Figure 4.26 Estimated groundwater level during May, 2009….....96
Figure 4.27 Daily spatial distributed AET in irrigation period…….98
Figure 4.28 Daily spatial distributed AET in non-irrigation period……..98
Figure 4.29 Average water balance error in calibration period (2009-2011)…….……100

Figure 4.30 Average water balance error in calibration period (2011-2012)……..100
Figure 5.1 Location of Quyi Chirchik district in Tashkent Province, Uzbekistan……..106
Figure 5.2 Hydrogeological cross-section of Quyi Chirchik district…….....106
Figure 5.3 Soil types of Quyi Chirchik district……...109
Figure 5.4 Soil depth of Quyi Chirchik district……..109
Figure 5.5 Unconsolidated layer depth of Quyi Chirchik district…….....110
Figure 5.6 Initial groundwater depth of Quyi Chirchik district……..110
Figure 5.7 Land use map of Quyi Chirchik district……..…111
Figure 5.8 Potential evapotranspiration of Quyi Chirchik district…….....111
Figure 5.9 Daily precipitation of Quyi Chirchik district……..……...112
Figure 5.10 Irrigation channels and irrigation area of Quyi Chirchik district….……112
Figure 5.11 Incremental water balance results of Quyi Chirchik district……114
Figure 5.12 Daily spatial distributed AET in irrigation period …….....115
Figure 5.13 Daily spatial distributed AET in non-irrigation period …….……115
Figure 5.14 Average water balance error in calibration period (2009-2011)…….…116
Figure 5.15 Average water balance error in validation period (2012-2013)……..116
Figure 5.16 Accumulated average groundwater recharge map in calibration period (2009-2011)…….117
Figure 5.17 Accumulated average groundwater recharge map in validation period (2012-2013)…….117
Figure 5.18 Observed and simulated groundwater level in study period…….…….119
Figure 5.19 Groundwater depth of Quyi Chirchik district…….121
Figure 5.20 Geometrical model of groundwater height……..121
Figure 5.21 Comparison of groundwater table depth with government elaborated water table map in districts of Tashkent Province……122
Figure 5.22 Map of Quyi Chirchik district and location of groundwater samples……124
Figure 5.23 Correlation between groundwater table depth and WQI……130

Chapter 1: Introduction

1.1 Study area and climate

The Chirchik River Basin is located in the Tashkent province in the northeastern part of Uzbekistan and it covers almost one third territory of the province. Tashkent Province is one of the twelve provinces of Uzbekistan. As shown in **Figure 1.1** province consists of 16 districts: Bostonlik, Tashkent capital, Tashkent, Qibray, Parkent, Yuqori Chirchik, Orta Chirchik, Quyi Chirchik, Chinoz, Yangiyol, Oqqorgon, Piskent, Boka, Zangiota, Bekobod and Angren. The province has a border with Kazakistan in the north, Kyrgisistan in the east and Tajikistan in the south. The area of Tashkent province is 15, 260 km^2. Topography varies from 237 to 4,293 m above mean sea level. Climate is continental with mild wet winter and hot dry summer. Tashkent Province is located within Chirchik, Ahangaron and Syrdarya Rivers Basins.

The total area of the Chirchik River Basin is 5,626 km^2, of which 1,982 km^2 is agricultural land. The population of the basin is around 2.1 million people. As shown in **Figure 1.1**, the basin consists mainly of upper stream in the northeastern region, and downstream in southwestern part. The southwestern area is almost exclusively topographically plain. Therefore, the boundary of the basin in the upper stream is delineated according to watershed concepts, whereas the downstream is delineated according to the administrative boundaries of the districts of the Tashkent province. Basin boundary only covers 11 districts (part of Bostonlik, Tashkent capital, Tashkent, Qibray, Parkent, Yuqori Chirchik, Orta Chirchik, Quyi Chirchik, Chinoz, Yangiyol and Zangiota) of Tashkent province and 5 districts (Oqqorgon, Piskent, Boka, Bekobod and Angren) are outside basin boundary.

The climate of the basin is a mix of arid and semi-arid. The climate of the upstream is characterized by relatively high amounts of precipitation and lower average temperatures. The opposite climate characteristics can be seen in downstream site. The average annual temperature for the period of 1950 - 2000 is 11.5^0 C. The average monthly temperature in January, the coldest month is -9.9^0 C and in July, the hottest month is $+27.8^0$ C. Absolute maximum air temperature in summer reaches up to $+42.6^0$ C (1973), and the absolute minimum temperature in January falls to -30.30^0 C (1969). The wind direction within the study area is northeastern and speed is 2.8-3.3 m/s. The mean annual relative humidity is 60.3%.

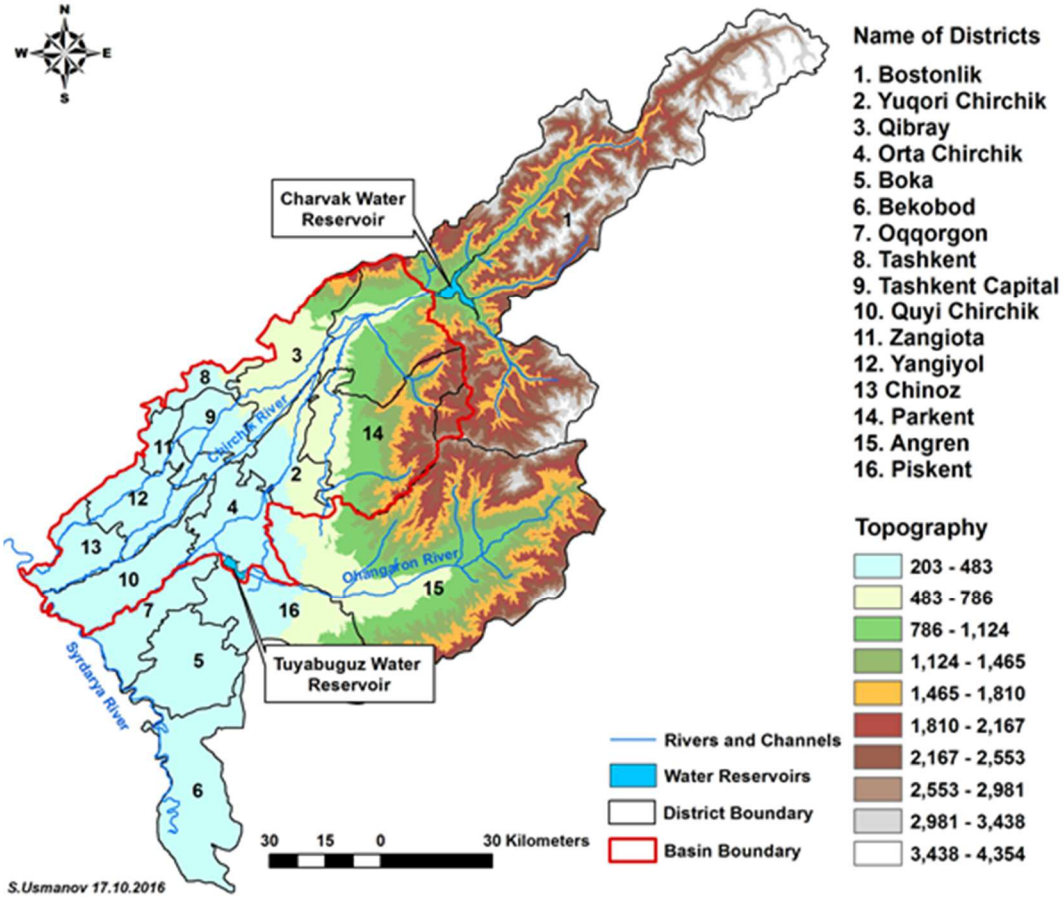

Figure 1.1 Map of Tashkent Province and districts

The dry season is typical for July-August, when the value of the relative humidity drops to 36-39%. The potential evapotranspiration decreases from the downstream (southwest) site to the upstream (northwest) site as altitude increases (Usmanov et al., 2015). **Figure 1.2** clearly shows spatial variation of potential evapotranspiration over the extent of Tashkent province. Precipitation is around 810 mm/year in upstream sites, and approximately 426 mm/year in downstream areas. The 38 % of the precipitation falls as a snow in winter months. The main part of the rainfall occurs during the March and April.

Figure 1.3 shows spatial distribution of annual precipitation over the extent of Tashkent province. Rainfall increases 60 mm/year for every 100-meter increase in elevation due to orographic effects. Maximum snow storage depth can reach 1200 mm/year in high mountainous areas (Chanisheva et al., 2011).

1.2 Demography and economic indicators

The total population of the province is more than 2.7 million people and 29 % of them work in agricultural sector. The average gross domestic product (GDP) of the province was 4712 billion Uzbek soms or 1.519 billion USD and 1271.1 billion soms or average 27 % (410 million USD) is came from agricultural sector. The total GDP of agriculture is mainly generated from two sub sectors. The irrigation agriculture and livestock sectors. **Table 1.1** shows the average GDP of each sub sectors (JICA. 2010).

Table 1.1 Average GDP of agricultural sub sectors

Subsectors	Billion som	%
Total GDP of Agricultural sector	1271.1	100
Irrigated agriculture	6.22.3	48.9
Livestock	648.8	51.1

As stated above, the total irrigated lands of the province is 395,872 ha and 111,100 ha is used for cotton and 124,300 ha is used for wheat growing. The cotton and wheat are planted about 60 % of irrigated field. The rest of irrigated fields are used for vegetables, orchards, grape yards and other vegetables. The information of average harvest of both plants are given in **Table 1.2**.

Table 1.2 Average harvest of the cotton and wheat

Plant type	Harvest (kg/ha)	Total harvest (ton/year)
Cotton	2590	258900
Wheat	4980	677400

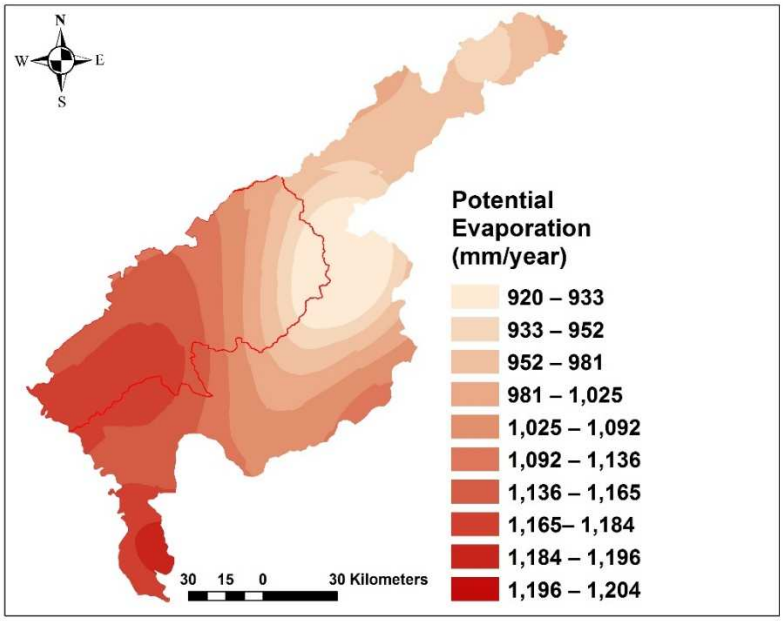

Figure 1.2 Potential evaporation of Tashkent Province

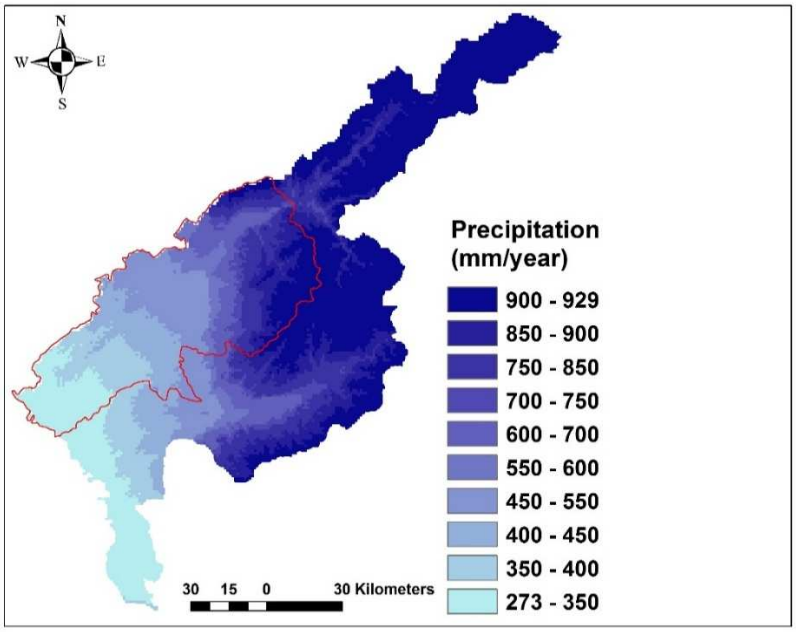

Figure 1.3 Precipitation of Tashkent Province

1.3 Water sources and hydrological characteristics

The total length of Chirchik River is 161 km and River is formed by discharges of the Chravak water reservoir **(Figure 1.4)**. Total capacity of reservoir is 2 km^3 and useful capacity is 1.58 km^3. The reservoir is used for seasonal streamflow control, mainly for irrigation and partially for power. The reservoir is mainly recharged by snow glaciers and precipitation.

The main tributaries of Chirchik River are Ugam (length – 68 km, source – snow glaciers) and Aksagatsay (length – 48 km, source – snow rain) Rivers. The Ugam River accounting for 9 % of the total runoff of the Chirchik River. The normal runoff of the Chirchik at the site of Charvak hydrostation is 6.5 km^3 and at the sites of the Gazalkent hydro station 7.2 km^3; 80 % of the annual runoff passes in the summer (April-September). **Figure 1.5** shows the major rivers and canals of Tashkent Province. The average winter natural discharges at the site of Charvak hydro station are 70-80 m^3/sec. The maximum observed discharge at the Charvak hydro station is 1,600 m^3/sec and at the Gazalkent hydro station 1,960 m^3/sec. The annual sediment discharge of the Chirchik under natural condition at the Charvak hydro station is 2.9 million tons, and of the Ugam River about 0.3 million tons, which determine the long period of silting of the dead storage of the reservoirs.

There are also the Syrdarya River and the Ahangaran River crossing the western and south-eastern parts of the study area, respectively. Each of these rivers has numerous tributaries, supplying the rivers, and off-takes in the form of irrigation canals and irrigation ditches. Akhangaran (Angren) River is the second major water source of Tashkent province. The length of the river is 236 km, water catchment area is 5,220 km^2 and inflow regime is snow – rain. The Syrdarya River originates in the Fergana Valley by melting snowfields and glaciers. The length of the river is 2,212 km formed by joining Norn and Karadarya Rivers. The flow of the river is fully regulated by Toktogul, Kairakum and Chardara reservoirs located in sequential order along the river channel. Maximum average monthly flow of the river is in May and June from 1,400-1,800 m^3/s. The salinity of the river flow has seasonal variations. Total dissolved solids vary from 900-1,300 mg/l in fall and winter and lower to 500 – 700 mg/l in summer.

Annually all economic sectors of Tashkent Province use average 4,897.9 mln.m^3 of water. **Table 1.3** shows utilization of total water resources by sectors. The irrigation purposes use average 3,187.9 mln.m^3 of water and rest of the water were used for industry, communal and other services (JICA. 2010). The main agricultural crops of the basin are cotton and wheat.

The largest expanse of irrigated land is located in the middle and downstream areas of the basin. Chirchik River water is distributed to agricultural lands and urban areas via the Bozsuv, the Qorasuv and Parkent's main canals. The remaining volume is mixed with returned water from agricultural lands and urban areas, and discharged into the Syrdarya River.

In present, Bozsuv, Parkent, Karasuv, Akhangaron and Dalverzin irrigation channels are functioning in Tashkent province. A Bozsuv irrigation channel serves to Kibray, Tashkent, Zangiota, Yangiyol, and Chinoz districts. Total irrigated area of the channel is 93.9 x 10^3 ha. Parkent-Karasuv irrigation channels serves to Oqqorgon, Ahangaron, Bostonlik, Kuyi Chirchik, Parkent, Orta Chirchik and Yuqori Chirchik districts. **Figure 1.6** shows the coverage area of these irrigation channels of Tashkent Province. Total irrigated area of the channels is 14.6 x 10^3 ha. Akhangaron-Dalverzin irrigation channels serve Oqqorgon only for 83.6 x 10^3 ha of lands, Ahangaron, Bekobod, Boka and Piskent districts of Tashkent province.

The Chirchik River is provided to all district of Tashkent Province. The districts and regions which have a remote distance with Chirchik River receive relatively low amount of water but these regions (Ohangaron, Bekobod, Boka and Piskent) mainly use Ohangaron and Syrdarya rivers.

Charvak and Ohangaron water reservoirs serve to regulate waters during the irrigation period. In the Tashkent province about 395,872 ha are irrigated and this is approximately 38 % of total agricultural land.

As stated above Chirchik River starts by water releasing from Charvak water reservoir and later join Ugam and Aksagatsay rivers. The water volume entering to Chichik River Basin via Chirchik River roughly can be estimated by sum of measurements of Charvak and Ugam gauging stations (UPCH).

In this research 4 gauging stations data were used. Locations of gauging stations are shown in **Figure 1.5.** Total water inflow (UPCH) to Chirchik basin via Chirchik River and total outflow from basin via Chinoz gauging station for 2009-2013 is given in **Figure 1.7**. **Figure 1.7** shows maximum utilization of Chirchik River water was observed in summer period when irrigation period starts. This means main part of water goes to atmosphere via evapotranspiration process. Another portion of water were spent to infiltration and outflow from basin boundary. The districts located outside of basin boundary also utilize the water of Chirchik River.

Figure 1.8 shows water sources of Tashkent province. The average water outflow from basin boundary to other districts is estimated annually 768.1 mln.m^3. **Table 1.4** shows water utilization by the districts of Chirchik River Basin territory.

Figure 1.4 Chravak water reservoir (www.travelpod.com)

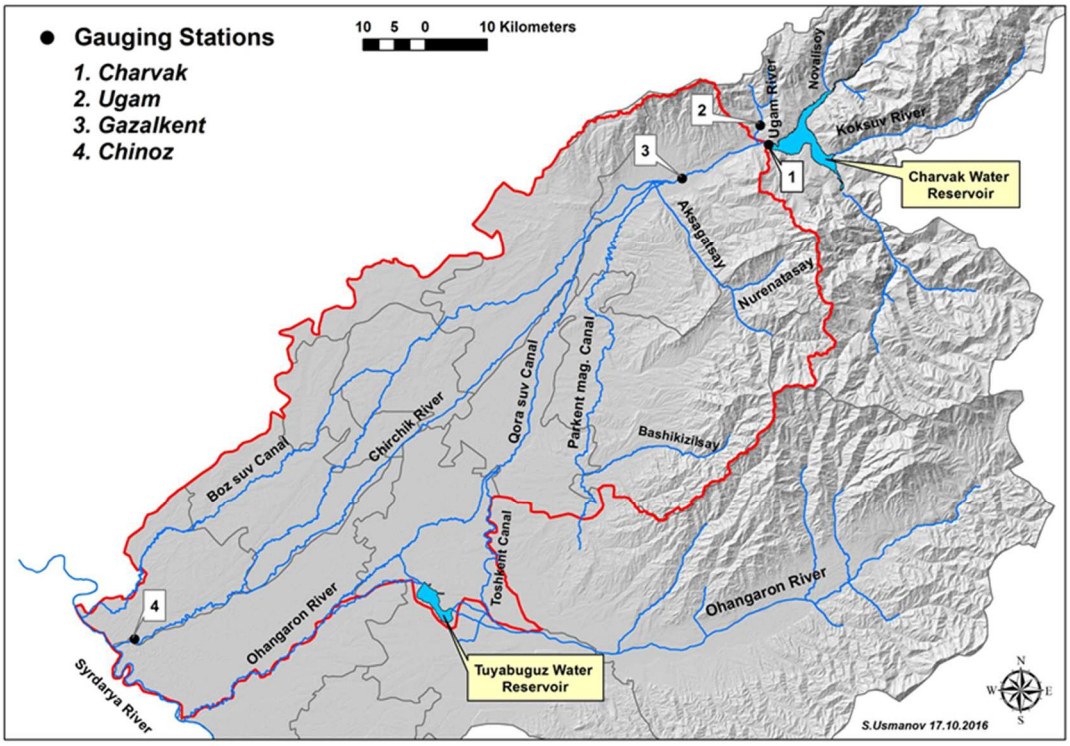

Figure 1.5 Main rivers and irrigation canals of Chirchik River Basin

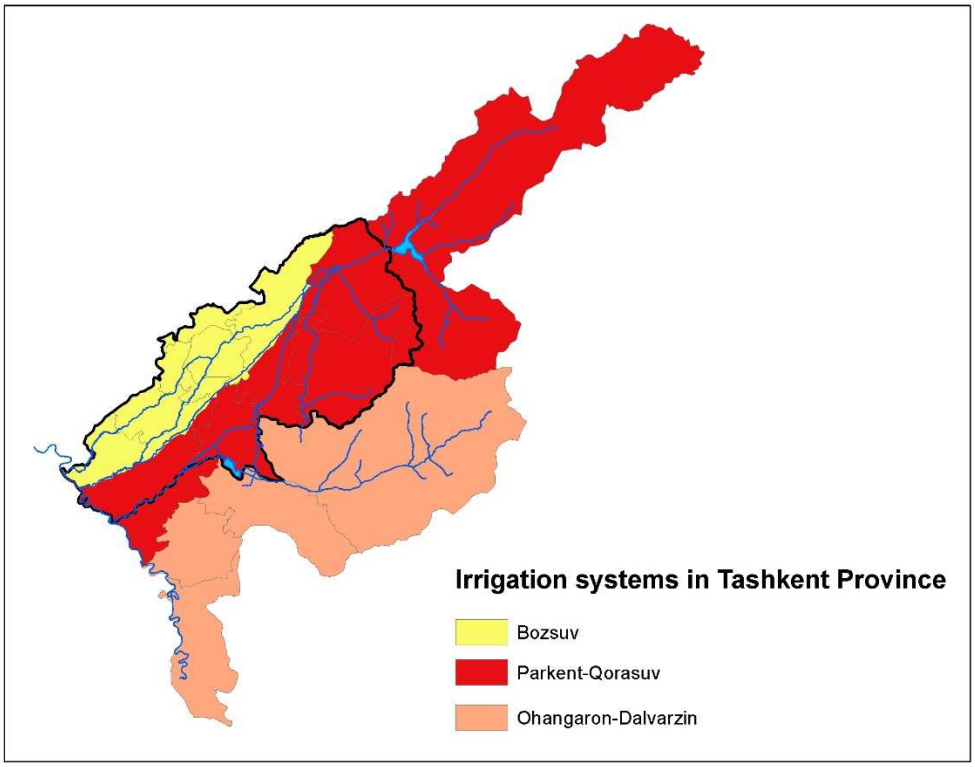

Figure 1.6 Coverage area of irrigation channels

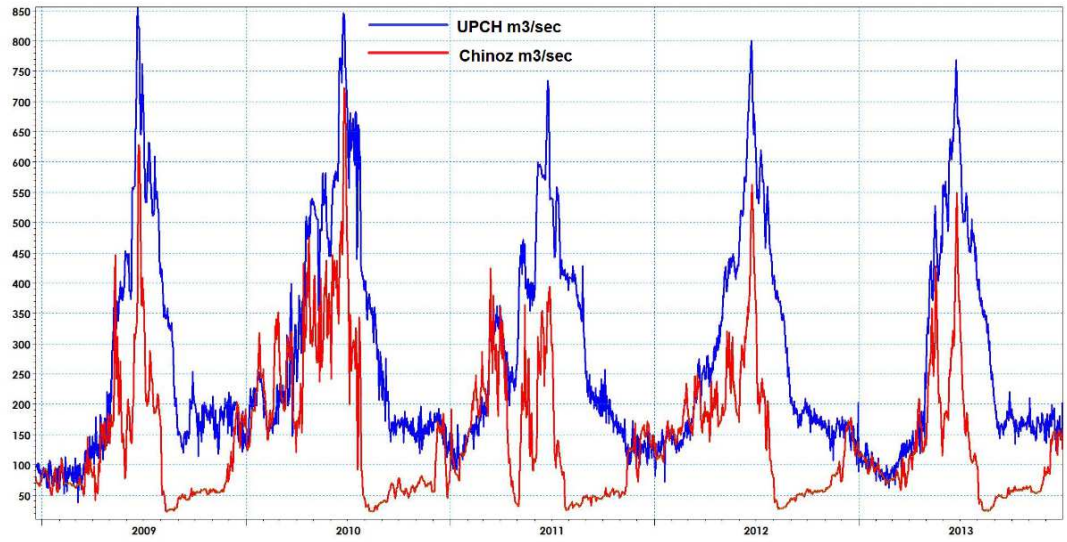

Figure 1.7 Discharge of UPCH (total discharge of Chirchik and Ugam Rivers) and Chinoz gauging station.

Table 1.3 Utilization of total water resources by sectors

Indicators	**Volume, mln. M^3**	**Percentage %**
Total	4897.9	100
Irrigation	3187.9	65.09
Power Industry	20	0.41
Industry	357	7.29
Communal services	890	18.17
Fisheries	355	7.25
Others	88	1.80

The Orta Chirchik and Quyi Chirchik districts are located Chirchik River basin territory but both districts use Chirchik and partly Ohangaron Rivers because Ohangaron River is located very close to both districts. Annually these two districts uses average 157 mln.m^3 water. During the construction of mass balance amount of water income to the Chirchik Basin from Ohangaron River should be take into account.

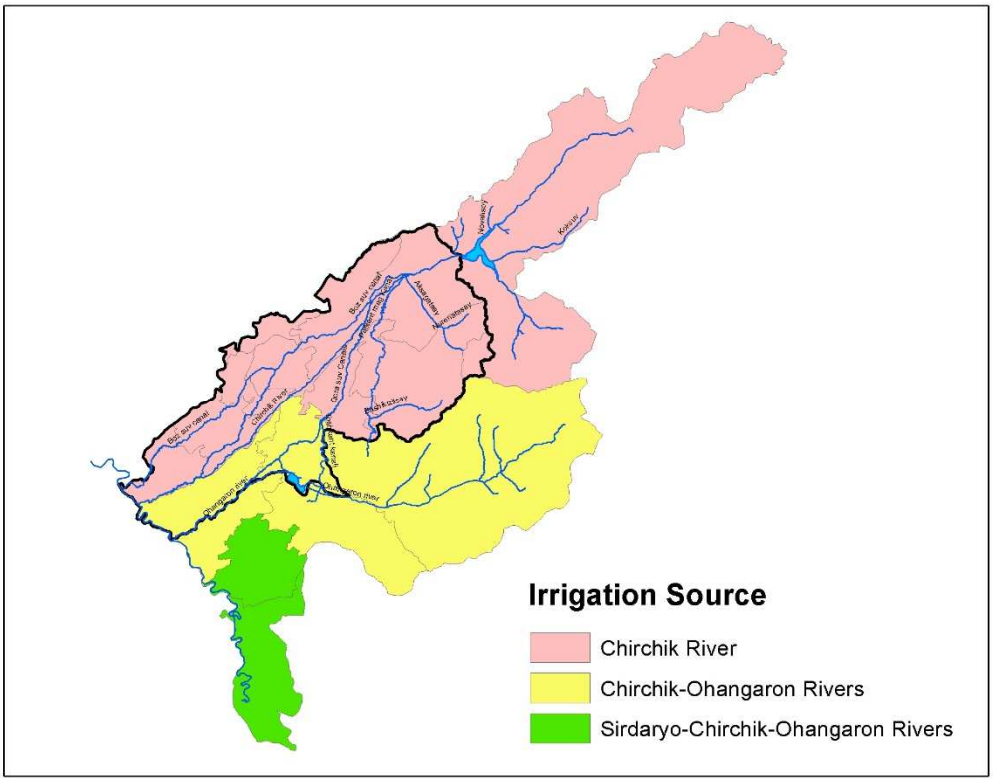

Figure 1.8 Irrigation sources of Tashkent Province.

Table 1.4 Water utilization of districts of Chirchik River Basin

N:	Districts	Total lands (km^2)	Total irrigated lands, km^2 (ha)	Utilized water for irrigation mln.m^3
1	Bostonlik	1004	20 (2000)	12
2	Kuyi Chirchik	560	399.67 (39967)	269
3	Zangi Ota	220	126.68 (12668)	125.5
4	Yuqori Chirchik	440	264.31 (26431)	185.8
5	Qibray	560	193.27 (19327)	179.24
6	Parkent	1080	160.22 (16022)	116.96
7	Orta Chirchik	510	341.75 (34175)	240.82
8	Tashkent Viloyat	158	107.24 (10724)	102.76
9	Chinoz	340	221.76 (22176)	176.82
10	Yangiyol	420	288.12 (28812)	236.94
11	Tashkent Capital	334	0	30.36
	Sum	**5626**	**2123.05 (212305.66)**	**1676.2**

1.4 Geology and soil

Chirchik River Basin is divided into three zones according to geomorphological aspects: the mountain zone, foothills and valleys. The mountain zone is characterized by high-billowy terrain. **Figure 1.9** shows topography of Tashkent province. It consists of the southern slopes of the foothill Beltau, Kazy-Kurt and ravines of the western Tien-Shan, including mountains ridges of Karzhantau, Ugam, Chatkal, Kuramin, mountains of Magol-Tau and Angren plateau. These ridges surround the study area from the north, northeast, east and south-east. The mountains characterized by: almost parallel spread with northeastern stretches; asymmetric structures with low slopes to the north and steep to the south; reducing absolute altitudes in south-western direction from 3,000-4,000 meter above sea level (masl) to 800-1,000 masl; represented by Paleozoic magmatic rocks.

The foothill areas represented by undulating plains, surrounding the mountains have the width varying from 0.5 to 5.7 km, and altitudes above 400 masl. The plains are formed by lateral cones of temporary watercourses, streaming down from the surrounding ridges. These cones gradually merge with the alluvial sediments of ancient terraces of the main watercourses. The surface of foothill plains has low slopes (up to 0.005) in the direction of flow of the rivers.

The valley including the lower reaches of the Angren River, Chirchik River, Keles River,Kuruk-Keles River and right bank of the Syrdarya River has altitudes at 400 masl or less. This zone has smooth relief, except river channels forming depressions of 80-100 m wide and 10-25 m deep.

The geological structure on the territory of Uzbekistan consists of geological formations of sedimentary, magmatic and metamorphic genesis from Proterozoic to Quaternary deposits. In mountainous areas, Proterozoic and Paleozoic rocks appear on the surface, and in the vast plains and intermountain hollows they lay below Mesozoic and the Cenozoic rocks. Underground mineral water in Uzbekistan is exploited from Neogene-Quaternary, Paleocene and Cretaceous deposits. Earlier studies of the Institute of Hydrogeology and Engineering Geology show that mineral water is mainly associated with the Cretaceous-Neogene sediments, Quaternary and Palaeozoic formations. The Pretashkent Aquifer is associated with Paleozoic floor, which is made of thick Cenozoic deposits containing the mineral water. The formations are represented by sand-clay differences of Cretaceous deposits (Cenomanian layer). **Figure 1.10** shows geological profiles of Chirchik River Basin from mountain zone to foothill area.

The foundation of the Gazalkent hydrostation are composed of soft silty-clay and silty-sand carbonate rocks with rare inter layers of gravel stone covered by alluvial

conglomerate-gravel deposits and a small layer of loamy sand and loam material. The thickness of the alluvial deposits in the river channel is small up to 7 m.

Geological layers of Chirchik River Basin mainly consist of Alluvium and Proluvium quaternary unconsolidated and consolidated sediments (Kholmatov et all. 2010). These sediments mainly composed by bench gravels and conglomerates composing a series of terraces. The structure of bench gravels is identical everywhere: well-rounded pebble with gray quartz sand; the cementation of conglomerates is usually calcareous. Proluvium includes loess and loess-like breeds overlapping bench gravels and conglomerates of ancient terraces.

It is advanced in valleys of the rivers of Chirchik, Akhangaran and Dalvarzin steppes. Water horizon in the top part of a valley of Chirchik river from Gazalkent city up to Chirchik city is supervised by flood plain area are I and II terraces that frequently on width makes 1-2 km. In the top part of a valley are pebbles with boulders with sand-gravel filler of modern age. Sometimes they are spread with conglomerates and gravels of Q IV. The thickness of water horizon is up to 20 m.

In the middle part of Chirchik city up to Yangiyol city also covers and the area of III up-flood plain terraces. Due to expansion of a valley its width increases up to 6-20 km. In middle part of valley are modern pebbles with boulders with sand-gravel.

Filler with boulders with sand-gravel and sandy filler are with layers of conglomerates of QIV age. Total thickness of horizon is 50-80m. Top and middle part of valley have factor modern pebbles with boulders with sand-gravel filler and factor of a filtration (permeability) of 100-150 m/day and 150-250 m/day respectively. Less permeable QIV alluvial pebbles with layers of conglomerates (permeability) <25 m/day and pebbles with boulders with sand gravel and sandy filler with layers of conglomerates (permeability 25-50 m/day) which are covered by very friable pebbles with thickness 5-10 m having permeability more than 250 m/day.

In the bottom part of the valley from Yangiyol city up to Syr-Darya river the water horizon is traced not only in limits actually valley of chirchik river but also due to development of alluvial sediments in limits of Chirchik Keles watershed in upper Pliocene, bottom and middle Pleistocene borrows a part of the area of watershed.

In the bottom part of valley the pebbles with sandy thin and fine-grained filler characterized by permeability 10-21 m/day and 35-160 m/day respectively.

Figure 1.11 shows geological map of Chirchik River Basin. Description of grid codes are described below:

- **Code 10:** QII-III age, Proluvium includes loess and loess-like breeds overlapping bench gravels and conglomerates of ancient terraces.

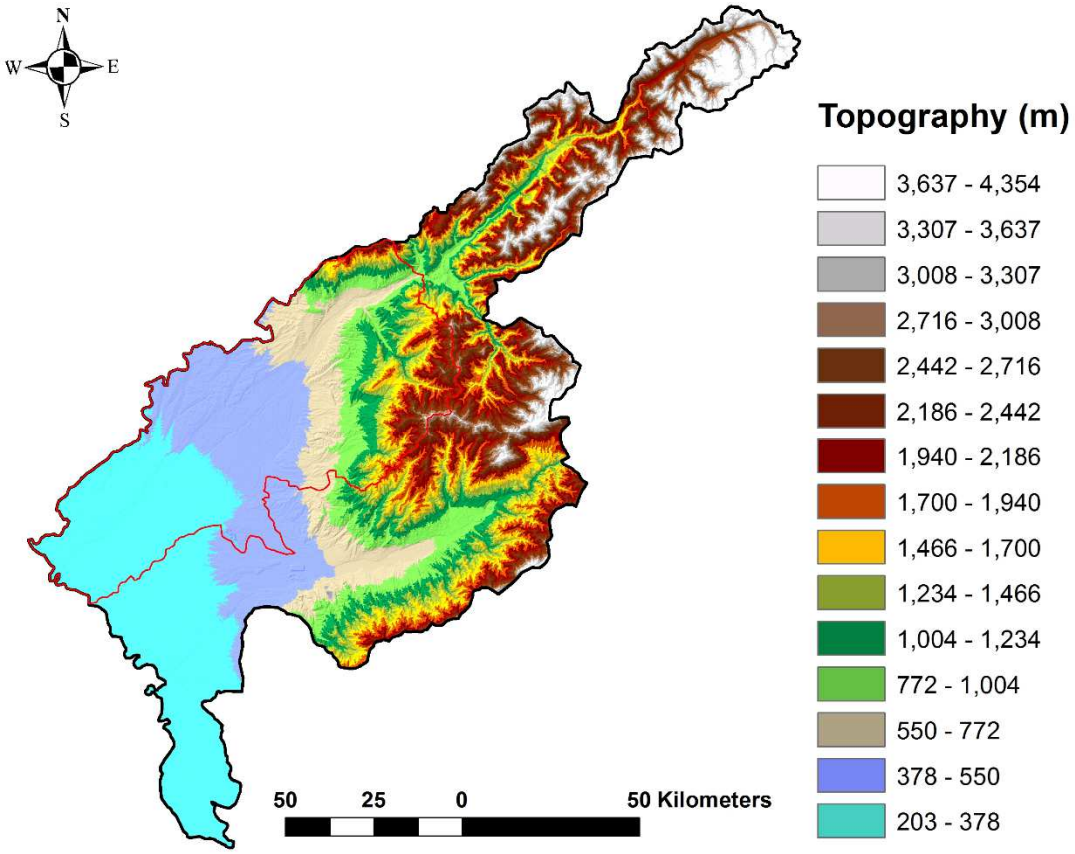

Figure 1.9 Topography of Tashkent Province

- **Code 20:** lightly rubbly on loess-like skeleton-melkozem sediment.
- **Code 30:** Modern QIV age, alluvium. Alluvium includes bench gravels and conglomerates composing a series of terraces. The structure of bench gravels is identical everywhere: well-rounded pebble with gray quartz sand; the cementation of conglomerates is usually calcareous.
- **Code 40:** Highly rubbly on stony-rubbly sediments, Skeleton-loam sediments, pebbles and sands.

According to soil climatic zoning of Eurasian continent, northern and northwestern parts of Uzbekistan is attributed as an arid and semiarid zone. Geomorphologic zoning of Chirchik basin reflects geographic distribution of soils according to relief and depending on types of soil-forming rocks. Soil type of Chirchik basin is strongly depends on geographic location. Then basin territory is classified to soil-geomorphologic areas. Following soil types are determined on the territory of the Chirchik basin: Light-brown grassland-steppe soils, Mountain brown soils and dark and typical Sierozem. In addition, transient soils are identified: grassland-sierozem and sierozem-grassland soils. In terms of hydro-morphologic series there are: grassland dark, grassland light, grassland-marsh and marsh soils. Soils of the basin have been formed in various soil-climatic zones: Subnival (high mountainous light-brown soils); Humid-climate-formed type (mountainous brown woodland and mountainous brown soils); Sub-arid (dark sierozem soils); Semi-arid (typical sierozem soils).

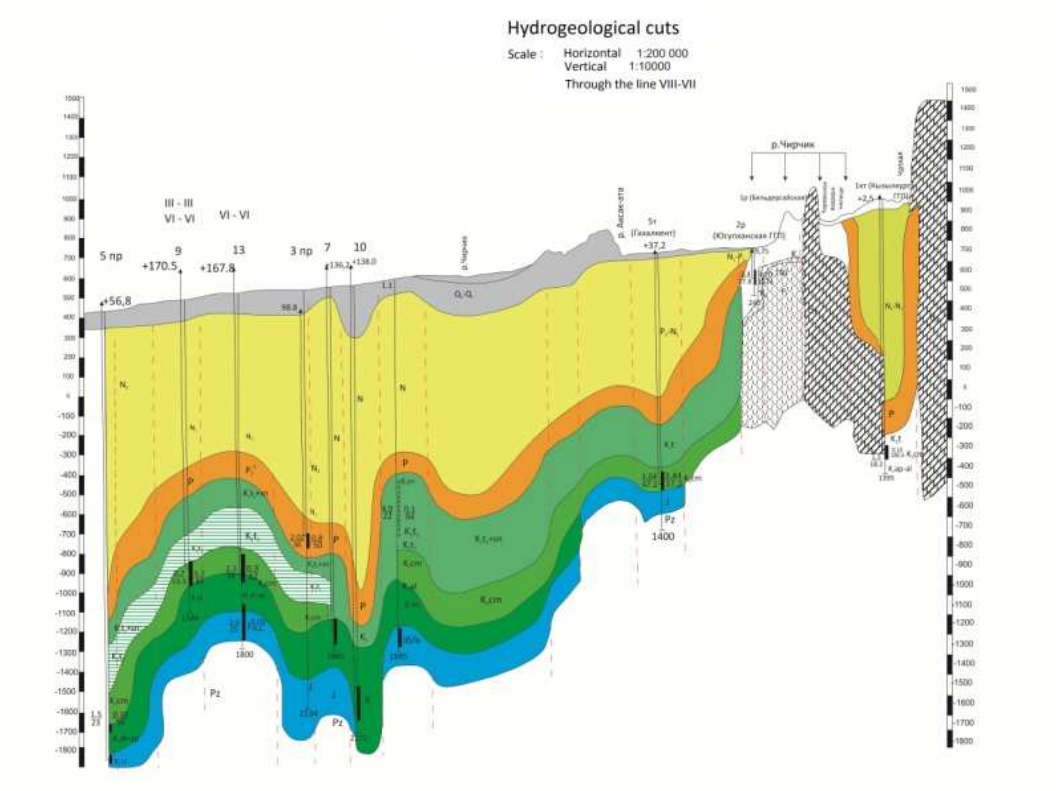

Figure 1.10 Geological profile of Chirchik River Basin from mountain zone to foothill area

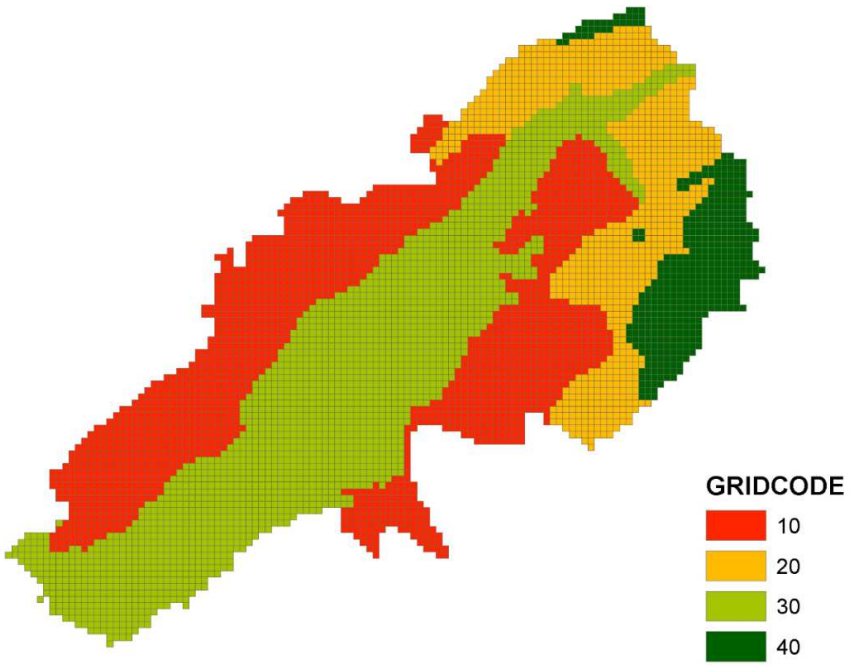

Figure 1.11 Geological map of Chirchik River Basin

1.5 Problems of water resources management

The Republic of Uzbekistan is a doubly land locked country in central Asia. Therefore, most water resources are supplied from neighboring countries. In the last decades, water supply into to the country has significantly decreased due to the mismanagement of trans-boundary water resources by Central Asian countries (Saifulin et al., 1998; United Nations., 2011; GIZ, 2013). This is happened because during the Soviet period a regional water-sharing agreement between the Syrdarya riparian states provided that the Tajik and Kyrgyz republics restrict power generation during winter in return for receiving energy resources from their downstream neighbors. After the collapse of the Soviet Union, this water-sharing agreement is no longer functioned efficiently. Tajikistan is sees the solution of energy crisis and also economic growth by construction of Rogun dam on the Vakhsh River using one of the main tributaries of Amu Daria River. The dam's reservoir could take as long as 18 years to fill and during this period, water flow downstream would be reduced. Therefore, Uzbekistan argues the Rogun dam would significantly reduce the amount of water reaching to Uzbekistan. The water shortage will result in decrease of GDP of Uzbekistan and some 300,000 people will lose their jobs. The water demand is increasing in Tashkent Province in all economic sectors as increase population. **Figure 1.12** shows population increase since 1979 in Tashkent Province. Apart from this Rogun dam will bring big environmental impacts; further desertification of the region and as well as risk of flooding and accident.

Consequently, most river basins in the region suffer from water shortages and increased aridity. Global climate change threatens to worsen these life-threatening problems (Rakhmatullaev et al., 2013). The development of plans for the sustainable usage of water resources, and mitigation and adaptation strategies is a key concern for all stakeholders across Uzbekistan (Makhmudov et al., 2014). The Chirchik River Basin is considered one of the country's largest and most important basins. It is located in the northeastern province of Tashkent (**Figure 1.1**), and its economy relies heavily on agricultural production; employing most of the region's population and consuming the lionshare of available water through irrigation practices (Dukhovny et al., 2006).

In present, the Chirchik River Basin is facing several potentially severe water related problems, including increased aridity and, land salinization, and has been declining in agricultural production. Continuously rising groundwater level and the inefficient use of river waters are assumed to further cause these problems. (Makhmudov et al., 2014). Total groundwater impacted areas in Tashkent Province are highlighted in **Figure 1.13** with green, red and yellow colors. From the total, highlighted area with red

and yellow shows rehabilitated area in 2008 and 2009 respectively. Rehabilitation is hydrologic procedure aiming to minimize groundwater level trough creating additional drainage systems or other conventional methods.

The figure shows that main groundwater impacted irrigated lands are located in downstream districts. **Figure 1.14** shows high groundwater exposed area by hectares. The total impacted area was classified by the two impacted level. The first level is the most critical situation, when the groundwater table is less than 2 meters from the soil surface. The second level is groundwater depth is less than 3 meters from soil surface. **Figure 1.14** tells us, the most groundwater impacted irrigated lands are located in Quyi Chirchik district, which almost 65 % area of total irrigated lands are in first critical level.

Poor management of water resources due to limited knowledge of hydrological processes has been identified as a root cause of water resource problems in the basin (Iskandar et al., 2008 and Kai et al., 2001).

Efficient management requires accurate estimation and modeling of water balance and main hydrological parameters. In order to obtain reliable and useful results, irrigation processes, which play an important role in the hydrological cycle, should be included in the modelling process. The accounting the contribution of irrigation water to other hydrological parameters gives the accurate results. However, few studies (Demetriou and Punthakey, 1998) have investigated the hydrologic impacts of agricultural water use in the context of integrated SW-GW (surface water – ground water) modeling, especially for large river basin. Understanding the complex behavior of the integrated SW-GW system is very important to the regional water resources management (Rassam et al., 2013), and integrated modeling is a highly desired approach.

Integrated and fully distributed hydrological models have been used widely and effectively by many researchers in producing detailed water balance estimations, examining hydrological responses to land use and cover change, and in groundwater and irrigation management (Bahaa-eldin et al., 2012; Spyridon et al., 2015; Sing et al., 1998; Foster S. and Allen D. 2015). Compared with other conventional methods, the model used in this study has the advantage of fully integrating the surface, subsurface, channel flow and their interactions in hydrological process simulation. Moreover, this model also has an integrated system to calculate irrigation processes (DHI, 2012). Further evaluation and comparison of the integrated hydrological model and other hydrological models are provided by Im et al (2008), Fate-ma et al (2012), Golmar et al (2014), and Jiao et al (2016). Integrated hydrological models have rarely been used in Chirchik River Basin studies, and there is a paucity of literature estimating water balance and hydrological parameters.

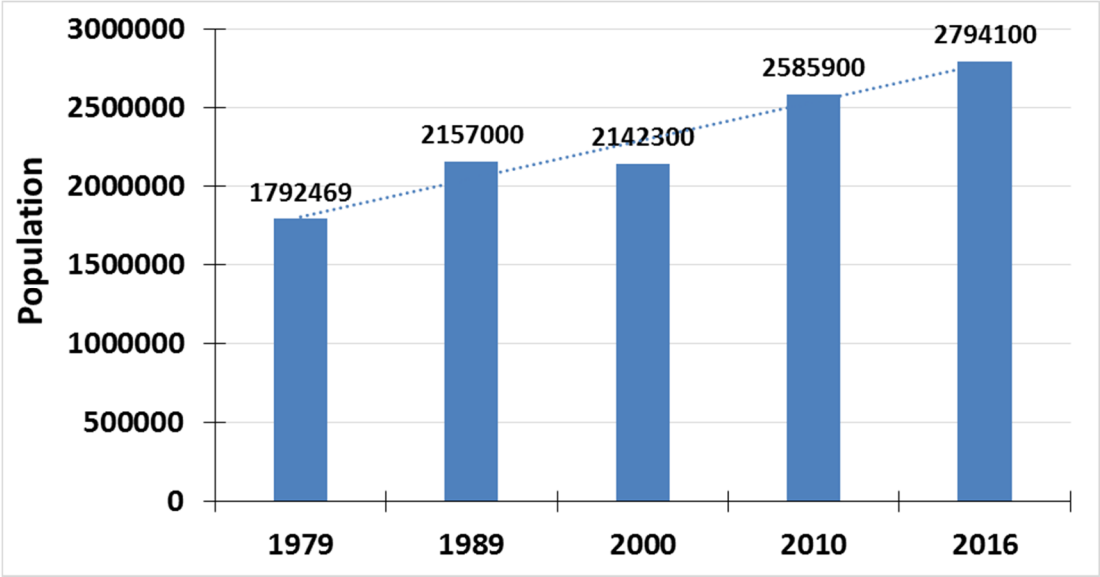

Figure 1.12 Demographic changes of Tashkent Province

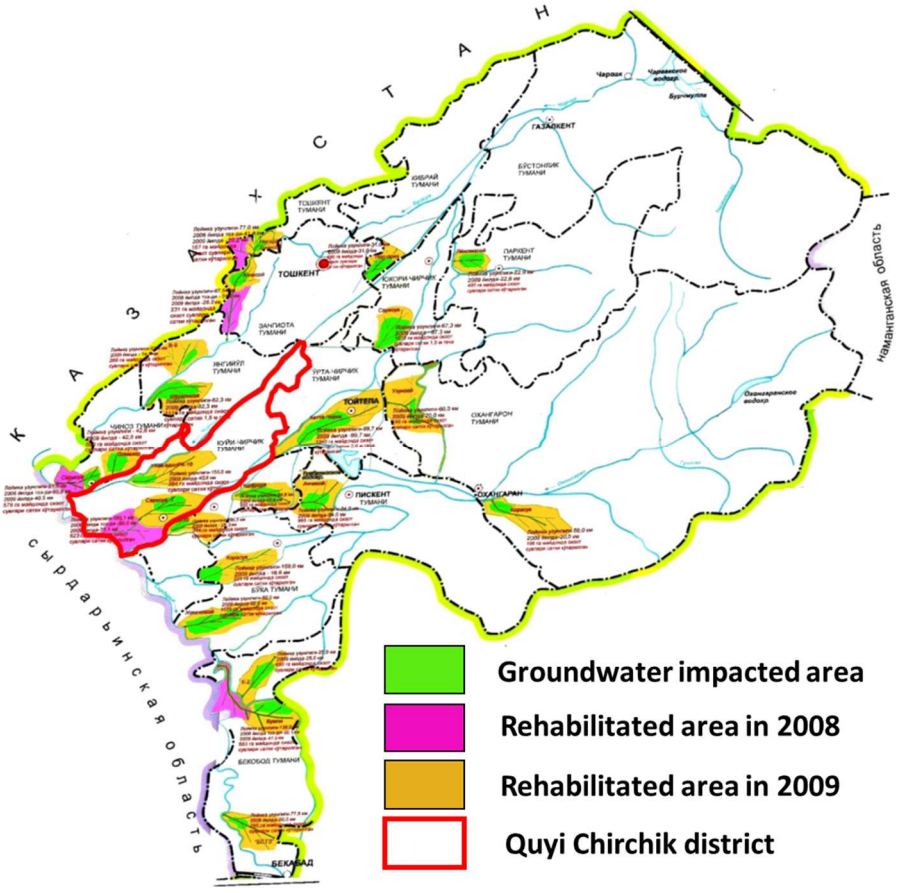

Figure 1.13 Groundwater impacted map of Tashkent Province

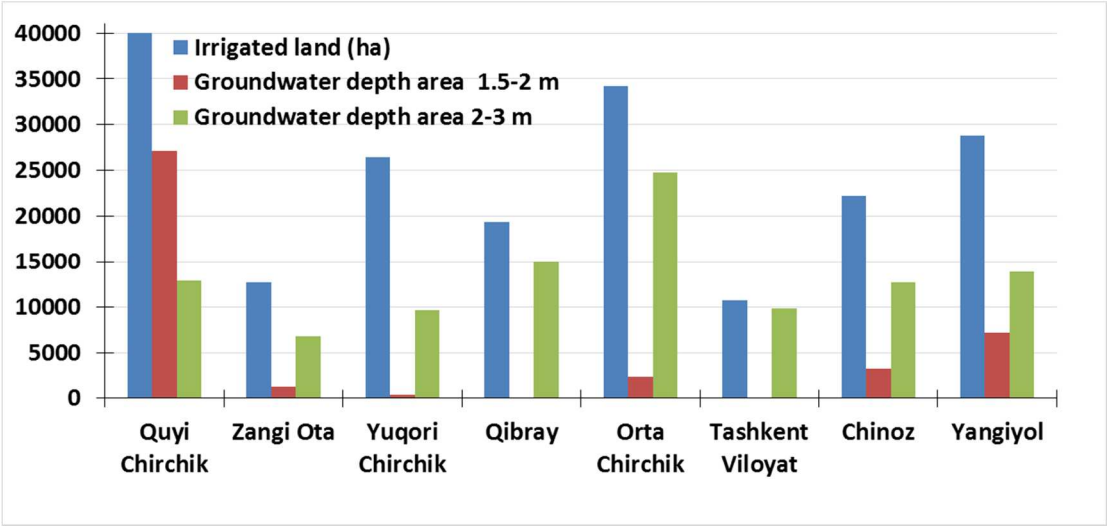

Figure 1.14 Groundwater impacted areas in districts of Tashkent Province

1.6 Research objectives

In this concern, a main aim of this investigation is to study hydrological processes in the basin territory through detailed water balance estimation using an integrated hydrological model and establish GIS based coupled model for detail estimate spatial and temporal variation of groundwater dynamics. This research aims to contribute to the knowledge of groundwater and surface water interaction and spatial variability of hydrological parameters. This research also aims to demonstrate how the integrated modeling would benefit the water resources management at large basins in arid and semi-arid environments.

1.7 Dissertation arrangements

This thesis is consist of seven chapters and contents of each the chapter is described as follows:

Chapter 1 introduce general information of Tashkent Province and Chirchik River Basin, including climate, soil, geology, water sources and hydrological characteristics. The chapter also describe existing water related issues and research objectives.

Chapter 2 describes integrated hydrological modeling system and simulation specification. The chapter then introduce governing equations of hydrological process and its solution methods.

Chapter 3 analyses the evaluation of interpolation methods for spatial modeling of reference evapotranspiration and modifying Hargreaves method. Secondly, this chapter describes the geostatitical interpolation methods and its advantages during the data limited condition.

Chapter 4 presents generation process of spatial distributed hydrological parameters of Chirchik River Basin for integrated hydrological modeling. Secondly, the calibration and validation of hydrological parameters and simulation performances are introduced. Secondly, the spatial-temporal analyses of stream flow and groundwater dynamics are introduced. Finally, model estimated water balance results and its benefits to water resources managements are described.

Chapter 5 introduce new GIS based method to study spatial-temporal variation of groundwater level and water balance analyses of Quyi Chirchik districts of Tashkent province. Then relationship between spatial and temporal variation of groundwater level and salinity are introduced. Finally, groundwater quality status and its physico-chemicals properties were analyzed.

1.8 References

Bahaa-eldin, R., Ismail, Y., Azmi, J., Zainudin, O. and Azman, G. Application of MIKE SHE Modelling System to set up a Detailed Water Balance Computation. *Water and Environment,* 26, 490–503 (2012).

Chanisheva, S. and Smirnova, E. Climate Characteristics of Tashkent Province. Hydro meteorological Bureau Press., Tashkent, Uzbekistan (2011).

Dukhovny, V., Sorokin A., Tuchin A., Rysbekov U., Stulina G., Nerosin S., Rusiev I., Sorokin D., Katz A., Shahov V. and Solodky G. D 34 - Final Report on Alternative Scenarios of Sustainable Development of Water Management for the Chirchik Basin. RiverTwin Project (2002-2006), Germany (2007).

DHI, MIKE SHE User's Manual, Volume 1 and 2 of An Integrated Hydrological Modelling Framework (2012).

Demetriou, C., Punthakey, J.F. Evaluating sustainable groundwater management options using the MIKE SHE integrated hydrogeological modelling package. Environ. Model. Software. 14 (2-3), 129-140 (1998).

Foster S. and Allen D. Groundwater-Surface Water Interaction in a Mountain-to-Coast Watershed: Effects of Climate Change and Human stressors. *Advances in Meteorology,* 22 (2015). http://dx.doi.org/10.1155/2015/861805

Fatema, A., Rasul, M., Khan. M and Amir M. A Comparative View of Groundwater Flow Simulation Using Two Modelling Software - MODFLOW and MIKE SHE. *Proceedings of the 18th Australasian Fluid Mechanics Conference*, Launceston, Australia, 3-7 December 2012.

Golmar, G., Shiv, P., Ali, M. and Ramesh, R. Evaluating Three Hydrological Distributed Watershed Models: MIKE-SHE, APEX, and SWAT. *Hydrology*, 1, 20-39 (2014). http://dx.doi.org/10.3390/hydrology1010020

Im, S., Kim, H. and Kim C. Assessing the Impacts of Land Use Changes on Watershed Hydrology Using MIKE SHE. Environmental Geology, 57, 231–239 (2008).

Iskandar, A., Fatima, N., Farida, A and John L. (2008) Socio-technical Aspects of Water Management in Uzbekistan: Emerging Water Governance Issues at the Grass Root Level. Water & Development Publications - Helsinki University of Technology. http://www.zef.de/module/register/media/b450_09_Central_Asian_Waters.pdf

JICA report on "Water Resources Utilization in Tashkent Province, Uzbekistan", (2010).

Jiao, L., Tie, L. and Anming, B. Assessment of Different Modelling Studies on the Spatial Hydrological Process in an Arid Alpine Catchment. *Water Resources Management*, 30**,** 1757–1770 (2016).

Kai, W. The Potentials for Success: Uzbek Local Water Management. Occasional Paper No. 29 Water Issues Study Group School of Oriental and African Studies (SOAS) University of London (2001).

Makhmudov, E. Rahimov, Sh., Chen, S. and Tzilili, A. Water Resources and Its Utilization in Uzbekistan. Pliograf Group Press., Tashkent, Uzbekistan (2013).

Rakhmatullaev, S., Frederic, H., Kazbekov, J., Helene, C. J., Mikael, M. H., Philippe, Le C. and Jumanov, J. Groundwater Resources of Uzbekistan: An Environmental and Operational Overview (2013).

Rassam, D.W., Peeters, L., Pickett, T., Jolly, I., Holz, L. Accounting for surface groundwater interactions and their uncertainty in river and groundwater models: a case study in the Namoi River, Australia. Environ. Model. Software. 50 (0), 108-119 (2013).

Saifulin, R., Russ, S., Fazylova, M., Fakhrutdinova, N., Petrenko, Y. (1998) Management of Water Resources in Uzbekistan and Way of Raising its Efficiency. Prepared for Central Asia Mission of United States. http://pdf.usaid.gov/pdf_docs/Pnacf072.pdf

Spyridon, P. and Fotios, M. Hydrological Simulation of Sperchios River Basin in Central Greece Using the MIKE SHE Model and Geographic Information Systems. *Applied Water Science,* 1-9 (2015).

Singh, R., Subramaniana, K. and Refsgaard, C. Hydrological Modelling of a Small Watershed Using MIKE SHE for Irrigation Planning. *Agricultural Water Management,* 41, 149-166 (1998).

Usmanov, S., Yasuhiro, M. and Tetsuya, K. Evaluation of Interpolation Methods for Spatial Modelling of Refer-ence Evapotranspiration Using Modified Hargreaves Equation. Journal of Arid land Studies, 25, 141-144 (2015).

Kholmatov, K., Khashimova, Diana. and Musaev, M. Geotechnical Site Charakterisation of Municipal Solid Waste Landfillin Uzbekistan. Advances in Environmental Geotechnics, pp 571-577 (2010).

Chapter 2: Integrated hydrological modeling system

2.1 Hydrological model selection

Hydrological models are classified as either theoretical or empirical models. A theoretical model is based on physical principles. If all the governing physical process are described by mathematical functions, a model containing those functions is a physical based model. However, most existing hydrological models simplify the physics and often include empirical components. Depending on the character of the results obtained, hydrological models can also be classified as deterministic or stochastic **(Figure 2.1)**. If all the variables are considered to be free from random variation, the model is deterministic. The some deterministic models may include stochastic process that capture some of the spatial and temporal variability of some of the sub-process, such as infiltration. Hydrological models can also be classified as event-based models or as continuous-times models. An event-based model simulates a single runoff event, such as a single storm, usually occurring over a period of time ranging from about an hour to several days. Continuous-times watershed model includes a sequence of time periods and for each period determines the state of watershed, whether or not any events take place that will produce surface runoff. The model keeps a continuous account of the watershed surface and groundwater conditions. Most continuous watershed models include three water balances – one for the surface water, another for unsaturated zone moisture content, and a third for groundwater. An event model may omit one or both of the subsurface components and also evapotranspiration when those losses are small in relation to the surface runoff. Finally, models that have been developed to simulate hydrological process can be classified as either limped or distributed or a mix of both. Lumped models assume homogenous or average conditions over all or portions of a watershed. Lumped models are not sensitive to the actual locations of the varying features in the watershed. Distributed models take into account the locations of various watershed conditions such as land covers, soil types and topography when estimating the total runoff. Both types of models are useful. Distributed models require more detailed data. Some models are mixes of the two types of models, in other words, quasi- or semi-distributed models made up of multiple connected lumped models representing different parts of watershed. Proper selection of hydrological models is important to achieve research objectives.

Considering the characteristics all above mentioned hydrological models, the

most suitable model in our study is distributed and fully integrated deterministic model. Because the integrated hydrological model is perquisite for integrated river basin management. **Figure 2.2** shows a schematic view of the integrated hydrological model.

Moreover river basin management requires the integration of surface water-groundwater interaction and quantity-quality and the upstream and downstream water-related demands or interests. Irrigation process is dominant in the Chirchik River basin therefore selected modeling structure should consider an irrigation process to simulate the hydrological balance accurately.

A number of integrated models have been developed, such as GSFLOW (Markstrom et al., 2008), HydroGeoSphere (Brunner and Simmons, 2012; Therrien et al., 2010), ParFlow (VanderKwaak and Loague, 2001), MIKE SHE (Graham and Butts, 2005), MODHMS (Panday and Huyakorn, 2004) and SWATMOD (Sophocleous et al., 1999). Some of these models incorporate MODFLOW (Harbaug, 2005), a classic 3-D groundwater simulator, as their subsurface module. However, the MIKE SHE hydrological model has been used widely and effectively in hydrological modeling in the river basin. Moreover, the MIKE SHE model is capable to integrate and simulate the irrigation process. Therefore, in this study MIKE SHE model was selected to develop a hydrological model for the Chirchik River Basin. In below sections were described structures and governing equations of the MIKE SHE model.

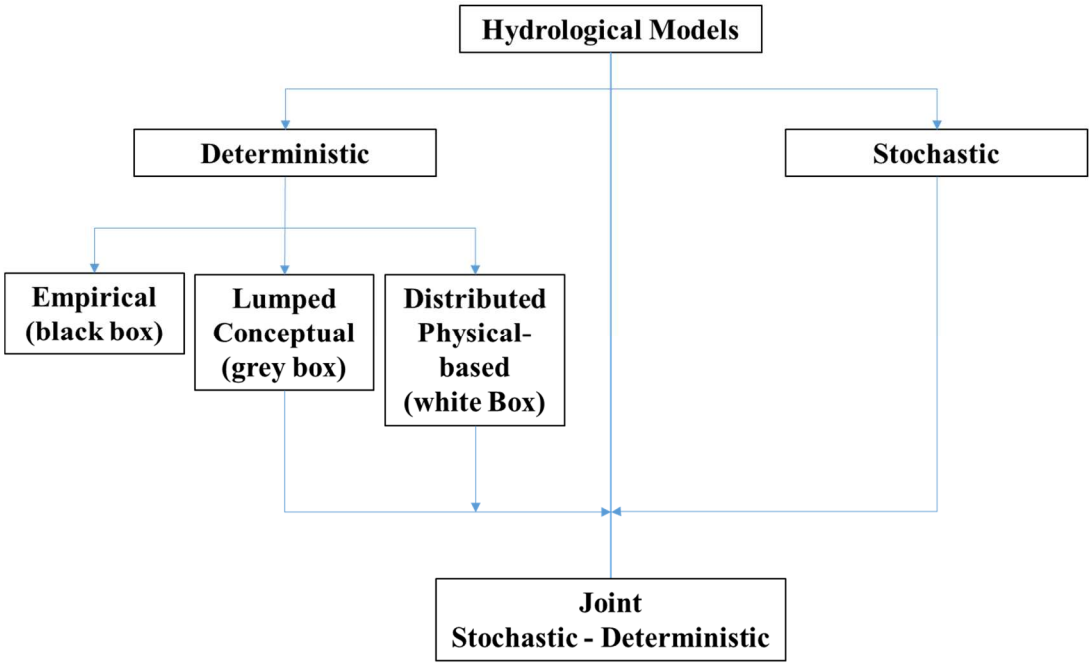

Figure 2.1 Classification of hydrological models

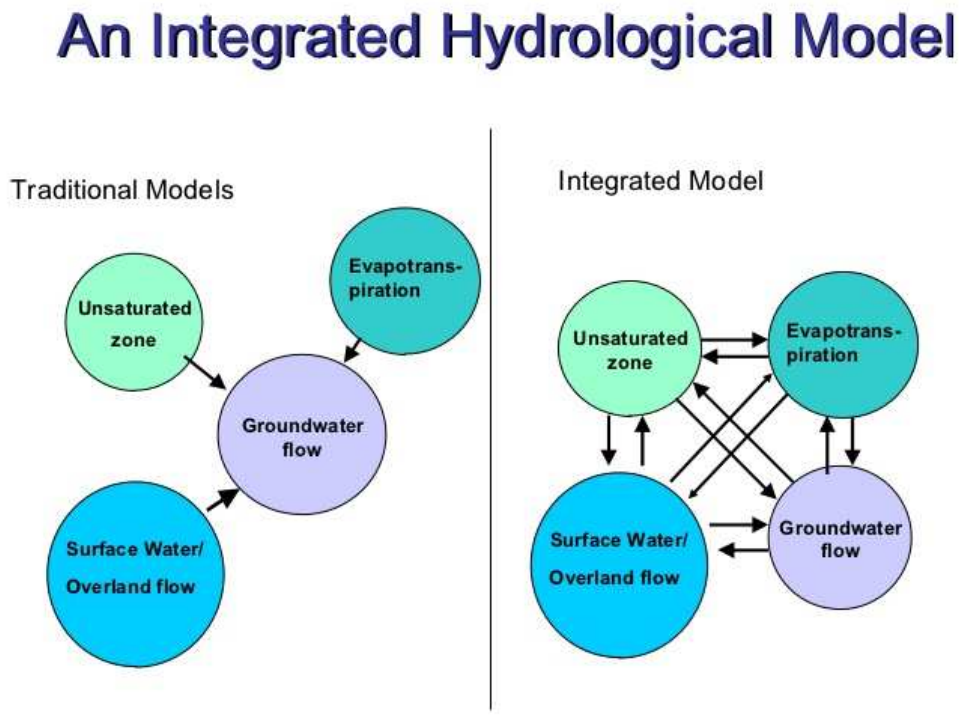

Figure 2.2 Schematic view of the integrated hydrological model.

2.2 Modeling structures

MIKE SHE is a deterministic, fully distributed and physically based modelling system (Jain et al., 1992; Christianens and Feyen, 2001; Thompson et al., 2004; Graham and Butts, 2005). It is based on the Systeme Hydrologique Europeen (SHE) model (Abbott et al., 1986a, b), which integrated the unsaturated and saturated zone together with the overland flow into a complete dynamic system with interaction among the various components. The original system had a relatively simple river model but this has been coupled to MIKE 11, a one-dimensional hydraulic model (Havnø et al., 1995; Thompson et al., 2004). It allows components to be used independently and customized to local needs. As shown in **Figure 2.3**, the model calculates following major hydrologic process in the hydrological cycle by fully integrated basis: Evapotranspiration, overland flow, unsaturated flow, saturated flow, and stream flow.

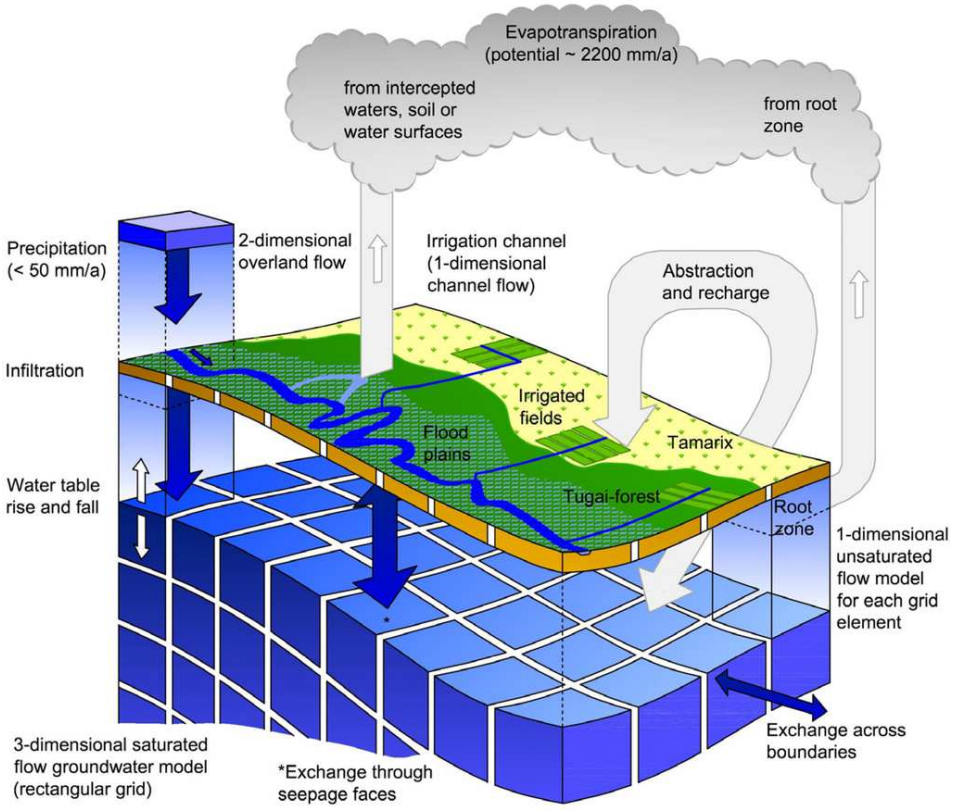

Figure 2.3 Hydrological processes simulated by MIKE SHE. Source: Refsgaard and Storm (1995).

MIKE SHE uses the MIKE 11 model to simulate stream flow, lakes, and channels in 1D. Finite element methods are used to solve these partial differential equations. MIKE SHE uses a network of regular grids to discretize the horizontal plane of a watershed, and represent the spatial variability of the calculated hydrological process. The model also simulates irrigation processes, pumping wells and various water control structures.

2.3 Actual evapotranspiration

MIKE SHE uses the Kristensen-Jensen model (Kristensen and Jensen, 1975) to calculate actual ET. The Kristensen-Jensen model (Kristensen and Jensen, 1975) is based on empirically derived equations. The calculation of evapotranspiration uses meteorological and vegetative data to predict the total evapotranspiration and net rainfall due to:

- Uptake of water by plants roots and its transpiration, based on soil moisture in the unsaturated root zone,
- Interception of rainfall by the canopy,
- Drainage from the canopy to the soil surface,
- Evaporation from canopy surface,
- Evaporation from soil surface.

The plant transpiration is given by the following **Equation (2.1)**:

$$ET_a = f_1(LAI) \cdot f_2(\theta) \cdot RDF \cdot ET_{ref} \quad \textbf{(2.1)}$$

Where ET_a - actual transpiration; $f_1(LAI)$ - leaf area index function; $f_2(\theta)$ - soil moisture function; RDF – root depth distribution function; and ET_{ref} - reference evapotranspiration.

The function, $f_1(LAI)$ express the dependency of the transpiration on the leaf area of the plant by **Equation (2.2):**

$$f_1(LAI) = C_2 + C_1 LAI \quad \textbf{(2.2)}$$

Where *C1* and *C2* are empirical parameters that influence the ratio of soil evaporation and transpiration (Kristensen and Jensen, 1975). The estimated value of *C1* for agricultural crops and grass is approximately 0.3. *C2* has an approximate value between 0 and 0.5.

The soil moisture function is mathematically expressed as **Equation (2.3)**:

$$f_2(\theta) = 1 - \left\{ \frac{\theta_f - \theta}{\theta_f - \theta_w} \right\}^{C_3 / E_p} \quad \textbf{(2.3)}$$

Where θ_f - volumetric moisture content at field capacity; θ_w - volumetric moisture content at wilting point; θ - volumetric moisture content; and C_3 - empirical parameter, mm/d.

The evaporation from the soil surface is given by **Equation (2.4)**:

$$E_s = ET_{ref} \cdot f_3(\theta) + \left(ET_{ref} - E_{at} - ET_{ref} \cdot f_3(\theta)\right) \cdot f_4(\theta) \cdot \left(1 - f_1(LAI)\right) \quad \textbf{(2.4)}$$

Where E_s- soil evaporation; functions $f_3(\theta)$ and $f_4(\theta)$ are expressed as **Equation (2.5):**

$$f_3(\theta) = \begin{Bmatrix} C_2 & for & \theta \geq \theta_w \\ C_2 \dfrac{\theta}{\theta_w} & for & \theta_r \leq \theta \leq \theta_w \\ 0 & for & \theta \leq \theta_r \end{Bmatrix} \quad \textbf{(2.5)}$$

Where θ_r - residual soil moisture content is given by **Equation (2.6):**

$$f_4(\theta) = \begin{cases} \dfrac{\theta - 0.5 \cdot (\theta_w + \theta_f)}{\theta_f - 0.5 \cdot (\theta_w + \theta_f)} & for \quad \theta \geq 0.5 \cdot (\theta_w + \theta_f) \\ 0 & for \quad \theta \prec 0.5 \cdot (\theta_w + \theta_f) \end{cases} \qquad \textbf{(2.6)}$$

Reference evapotranspiration is given by **Equation (2.7):**

$$ET_O^{FAO} = \frac{0.408\Delta(R_n - G) + \gamma \dfrac{900}{T_m + 273} u_2 (e_s - e_a)}{\Delta + \gamma(1 + 0.34u_2)} \qquad \textbf{(2.7)}$$

Where ET_0 - reference evapotranspiration (mm/day); Δ - slope vapour pressure curve *(kPa/C^0); R_n* - daily net solar radiation *(MJ/m^2 day); G- soil heat flux density (MJ/m^2 day);* γ - psychrometric constant *(kPa/C^0); T_m*- mean daily air temperature at 2 m height *(C^0); u_2*- daily mean wind speed at 2 m height *(m/s); e_s*- saturation vapor pressure *(kPa); e_a:* actual vapor pressure *(kPa), and G:* soil heat flux density *(MJ/m2 day).*

2.4 Snow melting and freezing

The snow melting and freezing processes are simulated using a degree-day empirical approach, which requires a degree-day coefficient of the study area. If the air temperature is above the Threshold melting temperature (see Snowmelt Constants) then the snow will begin to melt. The snow storage will be reduced by following **Equation (2.8):**

$$M = C_M (T_a - T_t) \qquad \textbf{(2.8)}$$

Where M – snowmelt (mm/day); C_M – the degree-day coefficient *(mm/degree day C^0); T_a* – mean daily air temperature (C^0); T_t – threshold melting temperature (C^0).

If the air temperature is below the threshold melting temperature, then the *ET* module will remove water from the snow storage as sublimation before any other *ET* is removed using following **Equation (2.9)**:

$$ET_{snow} = ET_o * t \quad \textbf{(2.9)}$$

Where Reference *ET* refers to the Reference Evapotranspiration before being reduce by the Crop Coefficient (k_c), which is specified in the Vegetation Development Table. If there is not enough snow storage then E_{snow} will reduce the snow storage to zero.

The coefficient C_M varies seasonally and by location. Typically values range from 1.6 to 6 mm/degree day C^0. C_M has also been related to snow density and wind speed and elevation.

2.5 Unsaturated zone components

In MIKE SHE model, three options are available for calculate vertical flow in the unsaturated zone:

- The full Richards equation, which requires relationships for both the moisture-retention curve and the effective conductivity,
- A simplified gravity flow procedure, which assumes a uniform, vertical unit-gradient and ignores capillarity force, and
- A simple two-layer water balance method for shallow water tables.

The full Richards method options is require comprehensive calculations but most accurate when the unsaturated flow is dynamic.

The full Richards equation is only consider vertical flow since gravity plays the major role during infiltration. Therefore, unsaturated flow in MIKE SHE is calculated only vertically in one-dimension, which is sufficient for most applications.

Generally the full Richards equation is derived from mass conservation principles which is considering only Z direction, vertical flow (Roger Beckie. 2005). The method is function of two variables the moisture retention curve and the effective conductivity. The full Richards equation is given by **Equation (2.10)**:

$$C\frac{\partial \psi}{\partial t} = \frac{\partial}{\partial z}\left(K(\theta)\frac{\partial \psi}{\partial z}\right) + \frac{\partial K(\theta)}{\partial z} - S \quad \textbf{(2.10)}$$

Where $K(\theta)$ – unsaturated hydraulic conductivity; $\psi(\theta)$ – soil moisture retention curve;

The sink terms in **Equation (2.10)** are estimated by root extraction for the transpiration in the top part of unsaturated zone. The sum of the all root extraction entire rot zone equals the total actual evapotranspiration.

2.6 Saturated zone components

MIKE SHE model use 3-dimensional Darcy equation to simulate the spatial and temporal variations of the hydraulic head solved numerically by an iterative implicit finite difference method. The governing flow **Equation (2.11)** for three-dimensional saturated flow in saturated porous media is (Roger Beckie. 2005 and Fetter. 2001):

$$\frac{\partial}{\partial x}\left(K_{xx}\frac{\partial h}{\partial x}\right)+\frac{\partial}{\partial y}\left(K_{yy}\frac{\partial h}{\partial y}\right)+\frac{\partial}{\partial z}\left(K_{zz}\frac{\partial h}{\partial z}\right)-Q=S\frac{\partial h}{\partial t} \qquad \textbf{(2.11)}$$

Where K_{xx}, K_{yy}, K_{zz} the hydraulic conductivity along the x, y and z axes of the model, which are assumed to be parallel to the principle axes of hydraulic conductivity tensor, h is the hydraulic head, Q represents the source/sink terms, and S_s is the specific storage coefficient.

MIKE SHE has a two options to solve this equation: the SOR groundwater solver based on a successive over-relaxation solution method and the PCG groundwater solver based on a preconditioned conjugate gradient solution method. Two special features of this apparently straightforward elliptic equation should be noted. First, the equations are non-linear when flow is unconfined and, second, the storage coefficient is not constant but switches between the specific storage coefficient for confined conditions and the specific yield for unconfined conditions.

2.7 Overland flow components

Overland flow or runoff process is calculated using the diffusive wave approximation of the Saint Venant equations, or using a semi-distributed approach based on the Mannings equation. The overland flow occurs when the net rainfall rate exceeds the infiltration capacity of the soil, water is ponded on the ground surface. The runoff water flow against topographical gradient towards the river system. The some portions of overland water losses due to evaporation and infiltration along the flow path.

Considering only flow in the x-direction the diffusive wave approximation is given by **Equation 2.12** (Mehdi et al., 2010; Fan et al 2005).

$$S_{fx} = S_{ox} - \frac{\partial h}{\partial x} = -\frac{\partial Z_g}{\partial x} - \frac{\partial h}{\partial x} \quad \textbf{(2.12)}$$

Where S_{fx} - is the friction slopes in the x- and y-directions and S_O is the slope of the ground surface. The h - flow depth (above the ground surface). If we further simplify **Equation (2.12)** using the relationship $z = zg + h$ it reduces to **Equation (2.13)**:

$$S_{fx} = -\frac{\partial}{\partial x}\left(Z_g + h\right) = -\frac{\partial Z}{\partial x} \quad \textbf{(2.13)}$$

In the x-direction. In the y-direction **Equation (2.12)** becomes as **Equation (2.14)**:

$$S_{fy} = -\frac{\partial}{\partial y}\left(Z_g + h\right) = -\frac{\partial Z}{\partial x} \quad \textbf{(2.14)}$$

Use of the diffusive wave approximation allows the depth of flow to vary significantly between neighboring cells and backwater conditions to be simulated.

2.8 MIKE 11 model for river flow simulation

MIKE SHE uses the MIKE 11 model to simulate stream flow and model uses a 1 dimensional Saint-Venant equation to compute stream flow modeling. The Saint-Venant equation expresses the conservation of mass and momentum for one-dimensional open channel flow. Therefore it consists of two coupled partial derivative equations (Roger Beckie. 2005). The schematic view of open river flow along with axis indexed by the abscissa x is given in **Figure 2.4.**

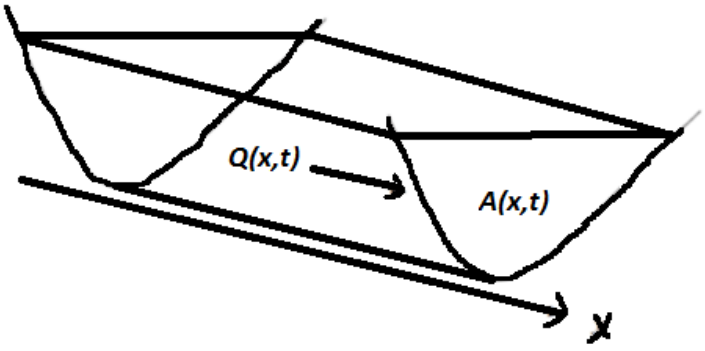

Figure 2.4 Open channel flow along a longitudinal axis indexed by the abscissa x.

The Saint-Venant method can be described by the mass conservation equation (Sleigh, P. and Goodwill, I. 2000), which stated as **Equation (2.15)**:

$$\frac{\partial A(x,t)}{\partial t}+\frac{\partial Q(x,t)}{\partial x}=0 \qquad \textbf{(2.15)}$$

And the second one is the momentum conservation **Equation (2.16)**:

$$\frac{\partial Q(x,t)}{\partial t}+\frac{\partial}{\partial x}\left[\frac{Q^2(x,t)}{A(x,t)}\right]+gA(x,t)\left(\frac{\partial Y(x,t)}{\partial x}+S_f(x,t)-S_b(x)\right)=0 \qquad \textbf{(2.16)}$$

Where A*(x, t)* represents the wetted area (m^2), *Q(x, t)* the discharge (m^3/s) across-section *A*, *V(x,t)* the average velocity (m/s) in section *A*, *Y(x,t)* the water depth (m), $S_f(x,t)$ the friction slope (m/m), $S_b(x)$ the bed slope (m/m), and g the gravitational acceleration (m/s^2).

2.9 Geostatistical interpolation methods

Geostatistical interpolation techniques utilize spatial autocorrelation among the measured points and account for the spatial configuration of the sample points around the predicted location. The basic tool of geostatistics and kriging is the semivariogram. The semivariogram captures the spatial dependence between samples by plotting semivariance against separation distance. The premise of any spatial interpolation is that close samples tend to be more similar than distant samples (this is also called spatial autocorrelation). The semivariance (γ) of can be estimated from the sample data using the **Equation (2.17):**

$$\gamma(x_i,x_0)=\gamma(h)=\frac{1}{2}var[Z(x_i)-Z(x_0)] \qquad \textbf{(2.17)}$$

Where h is the distance between point x_i and x_0 and $\gamma(h)$ is the semivariogram (commonly referred to as variogram) (Webster and Oliver, 2001).

The variogram models may consist of simple models, including: Nugget, Exponential,

Spherical, Gaussian, Linear, and Power model or the nested sum of one or more simple models (Burrough and McDonnell, 1998; Pebesma, 2004; Webster and Oliver, 2001).

For ordinary kriging, rather than assuming that the mean is constant over the entire domain, we assume that it is constant in the local neighborhood of each estimation point. In this case, the kriging estimator can be written as an **Equation (2.18):**

$$Z(\mathrm{x}_0) - \mu = \sum_{i=1}^{n} \lambda[\mathrm{Z(xi)} - \mu(\mathrm{x}_0)] \qquad \sum_{\mathrm{i}=1}^{n} \lambda_{\mathrm{i}} = 1 \qquad \textbf{(2.18)}$$

Where Z is the estimated value of an attribute at the point of interest x_0, Z is the observed value at the sampled point x_i, λ is the weight assigned to the sampled point, and n represents the number of sampled points used for the estimation (Webster and Oliver, 2001).

Co-kriging System of Equations for two-variable given in **Equation (2.19):**

$$Z(x_o) = \sum_{i=1}^{n} \lambda_i Z_i + \sum_{j=1}^{n} \beta_j t_j \qquad \textbf{(2.19)}$$

Where λ_i is the undetermined weight assigned to the primary sample z_i and varies between 0 and 100%; z_i is the the regionalized variable at a given location, with the same units as for the regionalized variable; tj is the the secondary regionalized variable that is co-located with the primary regionalized variable z_i, with the same units as for the secondary regionalized variable; and βj is the the undetermined weight assigned to tj and varies between 0 and 100%.

The unknown value $Z(x_o)$ is a linear combination of N values of two or more regionalized variables. Co-kriging's advantage comes from its use of a secondary variable that is sampled at many locations, but is not necessarily coincident with the primary variable.

2.9 References

Abbott, M.B., Bathurst, J.C., Cunge, J.A., O'Connell, P.E. and Rasmussen, J., An introduction to the European Hydrological System—Systeme Hydrologique Europeen, SHE. 1 History and philosophy of a physically-based distributed modelling system. Journal of Hydrology v87, p45–59 (1986).

Brunner, P., Simmons, C.T., HydroGeoSphere: a fully integrated, physically based hydrological model. Ground Water 50 (2), p170-176 (2012).

Therrien, R., McLaren, R.G., Sudicky, E.A., Panday, S.M., HydroGeoSphere A 3D Numerical Model Describing Fully integrated Subsurface and Surface Flow and Solute Transport. Technical report (2010).

Burrough, P.A. and McDonnell, R.A. Principles of Geographical Information Systems. Oxford University Press, Oxford, p333 (1998).

Christiaens, K. and Feyen, J., Analysis of uncertainties associated with different methods to determine soil hydraulic properties and their propagation in the distributed hydrological MIKE SHE model, in Journal of Hydrology, v246, p63-81 (2001).

Fetter, C., Applied Hydrogeology, Fourth edition by Prentice-Hall, Inc, p125-129 (2001).

Fan, P. and Li, J., Diffusive wave solutions for open channel flows with uniform and concentrated lateral inflow, Advances in Water Resources 29, p1000–1019 (2006).

Graham, D. and Butt, M. Watershed Models: Flexible integrated watershed modelling with MIKE SHE. Taylor and Francis Group Press, Boca Raton, Florida (2005).

Havnø, K., Madsen, M.N. and Dørge, J., MIKE 11 - A generalized river modelling package, in Computer Models of Watershed Hydrology, Singh, V.P., Ed., Water Resources Publications, Colorado, USA, p809-846 (1995).

Harbaug, A.W., MODFLOW-2005. The U.S. Geological Survey modular groundwater model-the ground-water flow process. USGS Techniques and Methods: 6-A16 (2005).

Jain, S.K., Storm, B., Bathurst, J.C., Refsgaard, J.C., and Singh, R.D., Application of the SHE to Catchments in India - Part 2: Field Experiments and Simulation Studies with the SHE on the Kolar Sub catchment of the Narmada River, in Journal of Hydrology, v140, p25-47 (1992).

Mehdi, D., Mohammad, M. and Houshang, H., Application of Diffusion Wave Method for Flood Routing in Karun River, International Journal of Environmental Science and Development, Vol.1, No.5, ISSN: 2010-0264 (2010).

Markstrom, S.L., Integrated Watershedescale Response to Climate Change for Selected Basins across the United States. U.S. Geological Survey Scientific Investigations Report 2011e5077, p143 (2012).

Panday, S., Huyakorn, P.S., A fully coupled physically-based spatially-distributed model for evaluating surface/subsurface flow. Adv. Water Resource. 27 (4), p361-382 (2004).

Roger, B., Fundamental Hydrological Equations, John Wiley and Sons, Ltd, (2005).

Pebesma, E.J., Duin, R.N.M. and Burrough, P.A. Mapping sea bird densities over the North Sea: spatially aggregated estimates and temporal changes. Environmetrics, 16(6): p573-587 (2005).

Sleigh, P. and Goodwill, I., The St Venant Equations, School of Civil Engineering, University of Leeds March (2000).

Sophocleous, M.A., Koelliker, J.K., Govindaraju, R.S., Birdie, T., Ramireddygari, S.R., Perkins, S.P., Integrated numerical modeling for basin-wide water management: the case of the Rattlesnake Creek basin in south-central Kansas.J. Hydrol. 214 (1-4), p179-196 (1999).

Thompson, J.R. Sørensen, H.R., Gavin, H., and Refsgaard, A., Application of the coupled MIKE SHE/MIKE 11 modelling system to a lowland wet grassland in southeast England, in Journal of Hydrology, v293(1-4), p151-179 (2004).

VanderKwaak, J.E., Loague, K., Hydrologic-Response simulations for the R-5 catchment with a comprehensive physics-based model. Water Resource. Res. 37 (4), p999-1013 (2001).

Webster, R. and Oliver, M. Geostatistics for Environmental Scientists. John Wiley & Sons, Ltd, Chichester, p271 (2001).

Chapter 3: Evaluation of Interpolation Methods for Spatial Modeling of Reference Evapotranspiration Using Modified Hargreaves Equation

3.1 Introduction

This chapter introduces spatial prediction of reference evapotranspiration (ETo) using a modified Hargreaves empirical model for Tashkent province, Uzbekistan. Previously, the empirical coefficient (0.0023) of Hargreaves model (HM) was modified under local climatic conditions of Tashkent province using standard Penman Monteih FAO 56 (FAO-56 PM) model estimates for every month of the years. The monthly climate data were provided by Uzhydrometeorological authority of Uzbekistan. Statistical comparison has been conducted in ArcGIS platform (ver. 10. 2 ESRI) among deterministic and geostatistical methods to evaluate the performance of interpolation methods, concerning suitability for spatial prediction of monthly average ETo.

3.2 Spatial distributed reference evapotranspiration

Accurate estimation of spatially distributed ETo is very important in arid and semi-arid environment. This is often problematic reasoning insufficient of full climate data sets and scarce of meteorological stations especially in Tashkent province (**Figure 3.1**). Reliable ETo is required for sustainable water management, improving crop-water productivity and arid land studies. The ETo represents the rate of evapotranspiration from a hypothetical reference crop with an assumed crop height of 0.12 m, a fixed surface resistance of 70 sec/m and an albedo of 0.23. The hypothetical reference crop is defined as green grass of assumed uniform height, actively growing, free of water stress and disease and completely shading the ground (Allen et al., 1998). ETo represents the evaporative power of the atmosphere at a specific location and time of the year independently of crop type, condition and soil parameters. **Table 3.1** shows the estimated average ETo of all 16 meteorological stations for the observation period 2009-2011 across Tashkent province. Many methods have been developed to estimate ETo, and FAO-56 Penman-Monteith (FAO-56 PM) is accepted as the most reliable method because it is a theoretically structured model. However, this model uses five climatic parameters. The HM (Hargreaves and Samani, 1985) is a simpler model that requires only temperature data and extraterrestrial radiation.

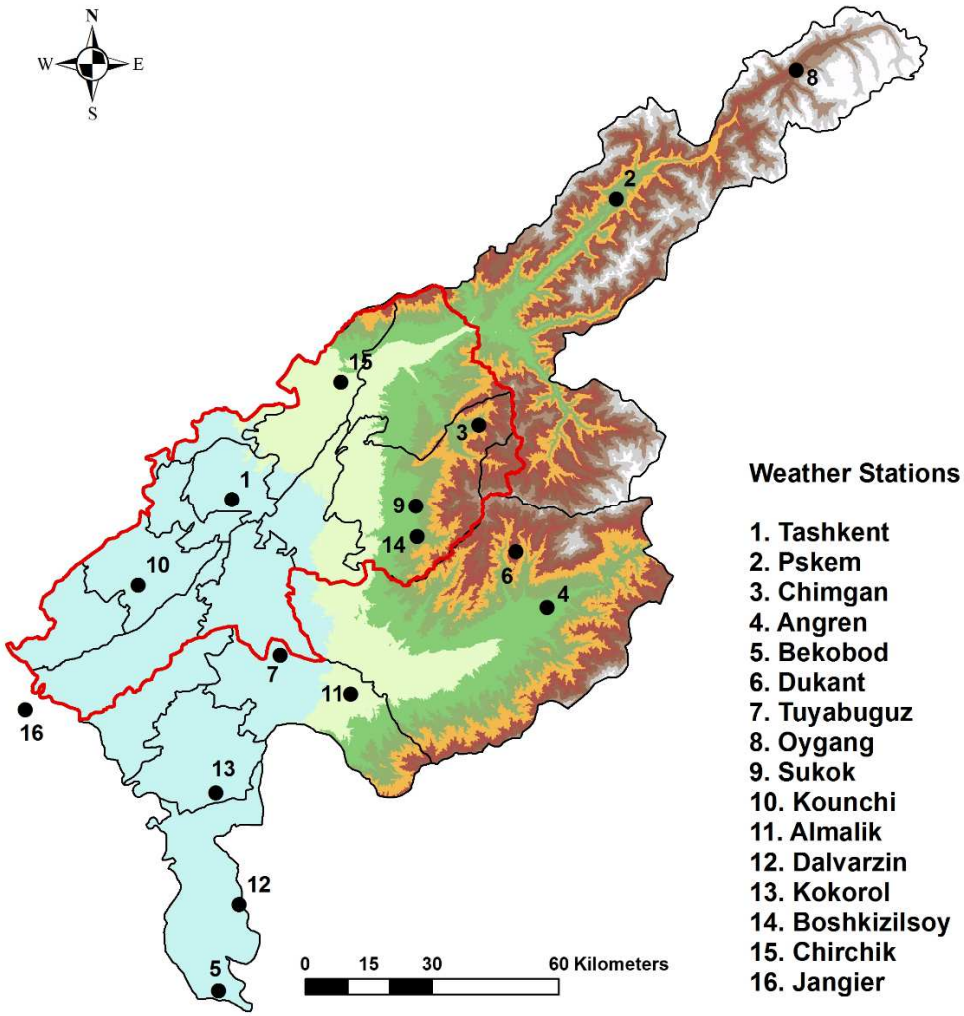

Figure 3.1 Location of meteorological stations and Digital Elevation Model (DEM) of Tashkent Province, Uzbekistan.

Nevertheless, HM requires regional and temporal adjustment to local climatic conditions to obtain accurate results (Gavilan et al., 2006). Apart from this, the meteorological stations are not enough to accurately represent the ETo in the Tashkent province. Hence the determination of a suitable interpolation method is important to spatial prediction of ETo in the agricultural lands in Tashkent province that are far from weather station (Dukhovny et all.). Therefore, the purposes of this study are to calibrate HM in the local climate of Tashkent province and to determine of suitable interpolation methods to spatial modeling of ETo over Tashkent province using modified HM estimates. In this study, monthly average (temperature, relative humidity, wind, vapor pressure and net solar radiation) climate data were obtained from 16 weather stations of Tashkent province for 2009-2013.

3.3 Materials and methods

The FAO-56 PM model is considered to be the most accurate to estimate ETo under the variety of climatic conditions (Allen et al., 1998). For that reason the FAO –56 PM model was selected to calibrate the HM in this study. The FAO-56 PM model is written as following **Equation (3.1)**:

$$ET_O = \frac{0.408\Delta(R_n - G) + \gamma \frac{900}{T_m + 273} u_2 (e_s - e_a)}{\Delta + \gamma(1 + 0.34u_2)} \quad \textbf{(3.1)}$$

Where ETo is the reference evapotranspiration (mm/day), Δ is the slope vapour pressure curve (kPa/C^o), R_n is the daily net solar radiation (MJ/m^{2}day), G is the soil heat flux density (MJ/m^2 day), γ is the psychrometric constant (kPa/C^o), T_m is the mean daily air temperature at 2 m height (C^o), u_2 is the daily mean wind speed at 2 m height (m/s), e_s is the saturation vapor pressure (kPa), and e_a is the actual vapor pressure (kPa).
The Hargreaves **Equation (3.2)** is written as:

$$ET_O = C_{org} R_a (T_{mean} + 17.8)\sqrt{T_{\max} - T_{\min}} \quad \textbf{(3.2)}$$

Where ET_o is the reference evapotranspiration (mm/day), R_a is the water equivalent of the extraterrestrial radiation (mm/day), T_{mean} is the monthly mean air temperature (C^o),

T_{max} is the mean monthly maximum temperature (C°), T_{min} is the mean monthly minimum temperature (C°), and C_{org} is the empirical coefficient (0.0023).

Table 3.1 Statistics for mean monthly, vegetation period (VP), and annual ETo (mm) of all 16 meteorological stations for the observation period 2009-2011 across Tashkent province (*SD* = standard deviation). The last column give the linear correlation coefficient between ETo and elevation.

Period	Reference Evapotranspiration (ETo, mm)				
	Mean	**Max.**	**Min.**	**SD**	**Correlation**
January	19.91	28.37	13.82	4.25	0.07
February	25.50	34.78	19.81	4.31	0.28
March	57.88	73.03	42.31	8.23	0.66
April	88.90	104.43	70.15	9.69	0.80
May	131.05	150.76	106.56	16.68	0.83
Jun	160.02	191.85	124.99	24.16	0.74
July	181.95	208.06	156.33	17.88	0.70
August	160.31	178.98	134.07	13.97	0.36
September	115.44	129.77	100.38	8.64	0.56
October	71.59	81.97	57.19	7.41	0.70
November	33.03	40.21	26.34	3.34	0.10
December	20.39	32.29	14.41	4.05	0.02
VP	**895.55**	**1013.96**	**769.35**	**91.44**	**0.79**
Annual	**1065.97**	**1204.18**	**920.72**	**102.39**	**0.82**

The FAO 56 PM model was used to calculate ETo with monthly average climate data of 16 weather stations then these results were used to local calibration of HM at each station. After calibration monthly coefficients of HM were determined for each weather stations of Tashkent province.

The validation of the new coefficients of HM was conducted with data recorded from 2012 to 2013. The performance of validation were assessed using a cross validation regression coefficient and root mean square errors (RMSE).

Statistical comparison was made in ArcGIS platform (ver. 10. 2 ESRI) among deterministic (inverse distance weighting, polynomial and spline), geostatistical (kriging and ordinary co-kriging) and regression (Ordinary Least Square) methods to evaluate the performance of interpolation methods (Sluiter R. 2008; Lixin L. and Peter R. 2002) for spatial prediction of average monthly, vegetation period (Mar-Sep) and annual of ETo.

The performance of interpolation methods was assessed with RMSE. The general **Equation (3.3)** for spatial interpolation is as follows:

$$S(x,y) = \sum_{j=1}^{N} \lambda_j R(r_j) \qquad \textbf{(3.3)}$$

Where *S*: interpolated value at point (*x, y*); *N*: total number of observed points (meteorological stations); *R(rj)*: observed value at point *j* and λ is the weight contributing to the interpolation.

On the basis that how weights are chosen, methods are divided to deterministic and geostatistical. Deterministic interpolation techniques create surfaces from measured points, based on either the extent of similarity or the degree of smoothing. Geostatistical interpolation techniques utilize spatial autocorrelation among measured points and account for the spatial configuration of the sample points around the prediction location. The detailed explanation of deterministic and geostatistical methods can be found in Goovaerts (1997).

3.4 Results and discussions

Three year (2009-2011) monthly ETo were estimated using HM and FAO-56 PM models and estimation of *ETo* with HM was mathematically adjusted to the estimates of FAO 56 PM model as a reference. As a result, locally adjusted monthly new coefficients were generated for HM. Then, these three years monthly coefficients were averaged and validated with climate data recorded during 2012 – 2013, from 16 meteorological stations of Tashkent province. **Table 3.2** shows average of new coefficient of HM for all weather stations. The coefficient of determination (R^2) and RMSE were used to estimate difference of ETo estimated using FAO-56 PM and the estimates using original HM with 0.0023 coefficient and the adjusted coefficients.

The average RMSE were relatively higher ranging from 21.40 – 6.99 mm/annual. Use of new empirical coefficients for all 16 weather stations improved the accuracy of ETo estimations and average RMSE were decreased by 65% off all weather stations **(Figure 3.2)**.

In result, the over and under estimation of ETo with original HM in the studied metrological weather stations were significantly minimized. The over estimation of ETo would cause over use of water resources for irrigation of agricultural crops.

Table 3.2 Average of new coefficient of HM for all weather stations (values in the table are multiples of 0.001). The first column shows ID of weather stations.

ID	Jan	Feb	Mar	Apr	May	Jun	Jul	Aug	Sep	Oct	Nov	Dec
1	2.13	2.05	2.03	2.03	2.00	2.05	2.05	2.07	2.19	2.23	2.19	2.15
2	2.35	2.09	2.03	2.13	2.11	2.12	2.19	2.36	2.51	2.27	2.20	2.41
3	2.89	2.74	2.53	2.24	2.22	2.12	2.29	2.18	2.55	2.35	2.59	2.81
4	2.18	2.27	2.07	2.01	2.03	2.04	2.09	2.10	2.20	2.19	2.16	2.28
5	3.30	2.84	2.19	2.01	2.13	2.21	2.22	2.15	2.22	2.50	2.94	4.02
6	1.71	2.41	2.07	2.11	2.12	2.21	2.37	2.44	2.64	2.33	2.55	2.43
7	1.93	1.97	2.03	2.03	2.08	2.23	2.29	2.31	2.41	2.46	2.44	2.36
8	2.70	2.68	2.70	2.29	2.20	2.18	2.38	2.66	2.78	2.91	3.32	3.48
9	2.68	2.06	1.97	2.08	2.09	2.13	2.23	2.28	2.39	2.47	2.49	2.57
10	1.38	1.57	1.87	2.00	2.05	2.16	2.12	2.11	2.16	2.09	1.85	1.58
11	1.62	1.73	1.85	1.80	1.99	2.25	2.16	2.05	2.19	2.12	2.27	1.94
12	2.11	2.22	2.13	2.05	2.06	2.20	2.19	2.11	2.12	2.22	2.24	2.44
13	1.94	2.24	1.94	2.01	1.99	2.01	2.01	1.99	2.30	2.07	2.12	2.28
14	2.15	2.02	2.03	2.02	2.03	2.05	2.07	2.09	2.26	2.36	2.37	2.45
15	1.85	1.85	1.96	2.05	2.07	1.79	1.91	2.09	2.07	2.06	1.76	1.89
16	1.56	1.53	1.85	1.98	2.04	2.15	2.11	2.11	2.16	2.08	1.83	1.56

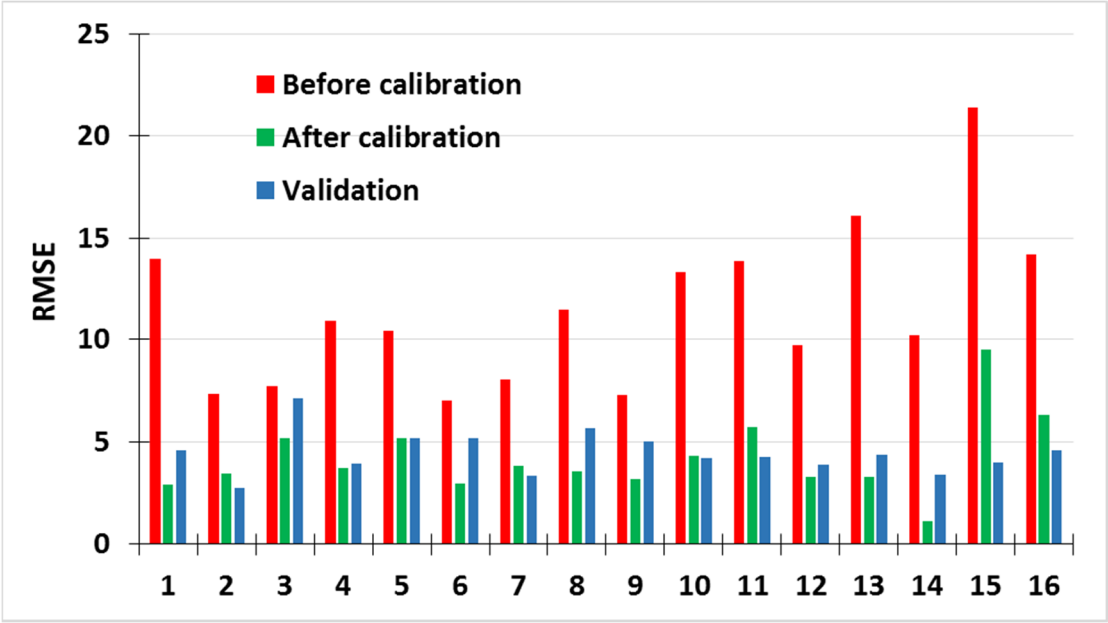

Figure 3.2 Comparison of estimated ETo by two methods (values in the table are multiples of 0.001). The x axes has labeled with ID of weather stations.

Underestimation of ETo would increase plant water stress and lead to a decrease in the quantity and quality of the yields.

Annual variation of new coefficients was very sensitive depending on topographical and temporal changes of the study area. Coefficients of variation were estimated to be very low for almost all weather stations particularly in vegetation periods. **Figure 3.3** shows a variation of new average coefficients of HM over the year.

From this research it was observed that estimated ETo was inversely proportional to elevation in Tashkent province and relatively high solar radiation, low relative humidity and low precipitation that created higher vapor pressure deficits were the main causes of the high ETo in low elevation sites of Tashkent province. Therefore, the influence of elevation to spatial prediction of ETo should be taken into account in complex topographical areas.

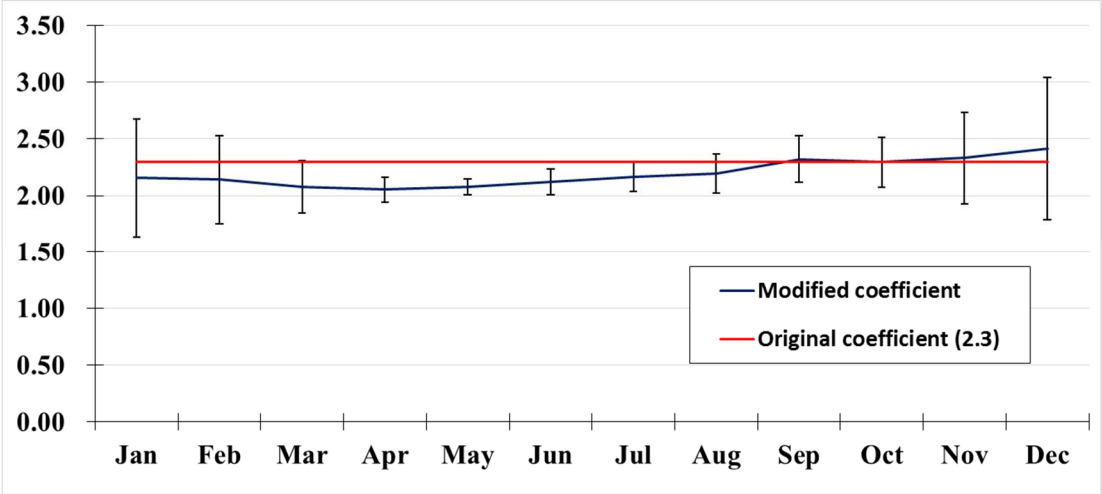

Figure 3.3 Variation of new average coefficients of HM

3.5 Evaluation of interpolation methods

Table 3.3 shows RMSE of predictions calculated by each of the six interpolators (inverse distance weighting, polynomial, spline, kriging, ordinary co-kriging and Ordinary Least Square) for the monthly (Jan–Dec), VP and annual. The lower RMSE values were obtained from ordinary co-kriging (OCK) methods. The OCK method is developed to improve the estimation of a variable using secondary spatial correlated variable and it uses the cross semi-variograms of primary and secondary variable. And success of prediction of this method strongly depends on the degree of correlation between primary and secondary variables. And selection of an appropriate cross semi-variogram model among exponential, Gaussian, spherical, cir cular and rational quadratic models. In this study, OCK used elevation data of weather stations as a secondary variable for spatial prediction of ETo. The Gaussian cross semi-variogram model was best fitted in February, September, November and December. The circular model was appropriate to January, June, July, August and VP. The spherical model was selected to May, October and annual. And the exponential model was optimal for March and April. The values of R^2 between ETo and elevation data ranged from 0.02 (in Dec) to 0.83 (in May). The highest R^2 were observed during the hot months (Mar, Apr, May, Jun, Jul and Oct), VP and annual when ETo rate is high. For that reason, the prediction accuracy of co-kriging method is relatively higher in these periods rather than other methods. The spatial distribution of ETo for VP and annual of Tashkent province is presented in **Figure 3.4.** These maps shows, ETo showed stable decrease toward to northeast at increased elevation. **Figure 3.5** shows spatial predictions of average monthly (2009-2011) ETo (mm) using the OCK method. Therefore, OCK is best method to spatial prediction of ETo in Tashkent province, particularly periods which have a good correlation between ETo and elevation.

Table 3.3 RMSE of prediction produced by each of the interpolation methods for monthly (Jan-Dec), vegetation period (VP) and annual ETo.

Month	Co-Kriking	Kriking	IDW	Spline	Local Poly.	OLS
Jan	4.3	4.33	4.623	4.61	4.46	4.09
Feb	2.77	2.62	2.933	2.86	3.22	3.65
Mar	5.48	5.67	6.189	5.82	6.78	4.74
Apr	4.13	5.65	6.44	6.09	6.08	4.3
May	5.78	7.73	9.316	7.59	9.73	6.84
Jun	8.23	8.69	8.42	9.14	11.86	12.16
Jul	7.24	7.63	9.519	8.43	9.47	9.64
Aug	8.14	10.06	10.93	10.07	9.72	11.12
Sep	4.23	5.06	6.165	5.64	6.21	5.71
Oct	4.3	4.52	5.26	4.92	6.03	4
Nov	3.23	3.2	3.27	3.31	3.61	3.17
Dec	3.56	3.65	3.78	3.94	3.57	3.99
VP	**26.73**	**35.83**	**45.107**	**37.86**	**50.23**	**41.45**
Annual	**29.72**	**39.85**	**51.51**	**42.29**	**57.87**	**43.02**

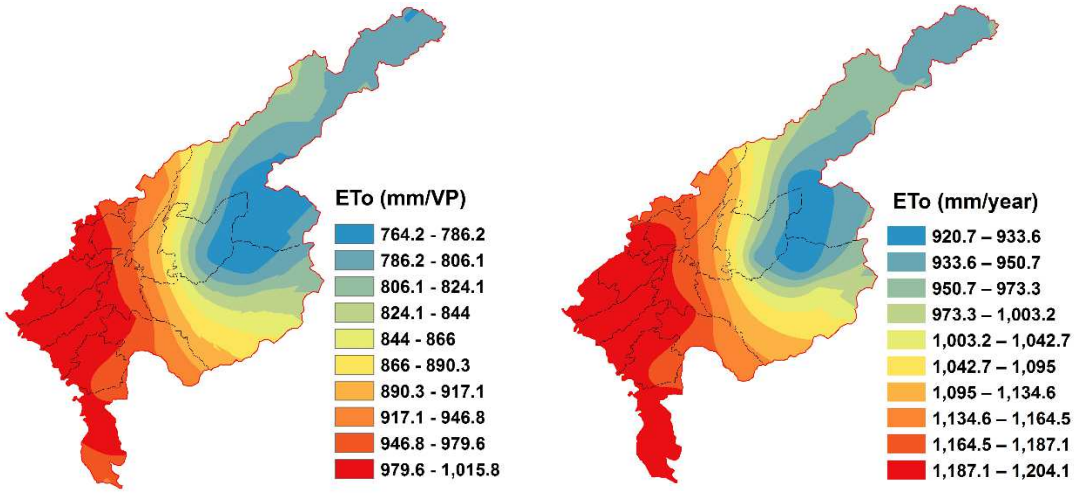

Figure 3.4 Spatial prediction of average (2009-2011) annual and vegetation period (VP) ETo (mm) across Tashkent Province.

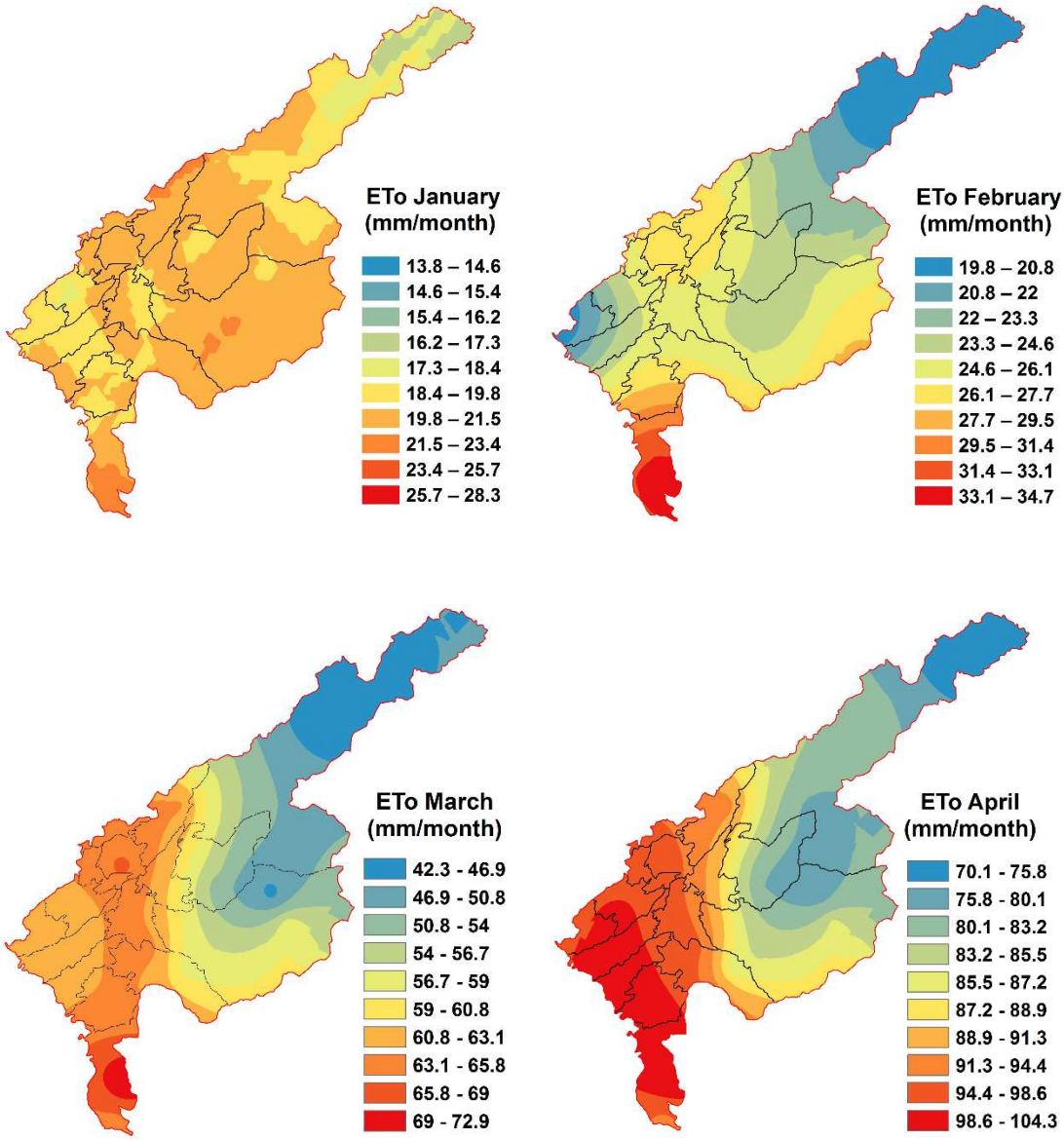

Figure 3.5 Spatial prediction of average monthly (2009-2011) ETo (mm) across Tashkent Province (*cont*.).

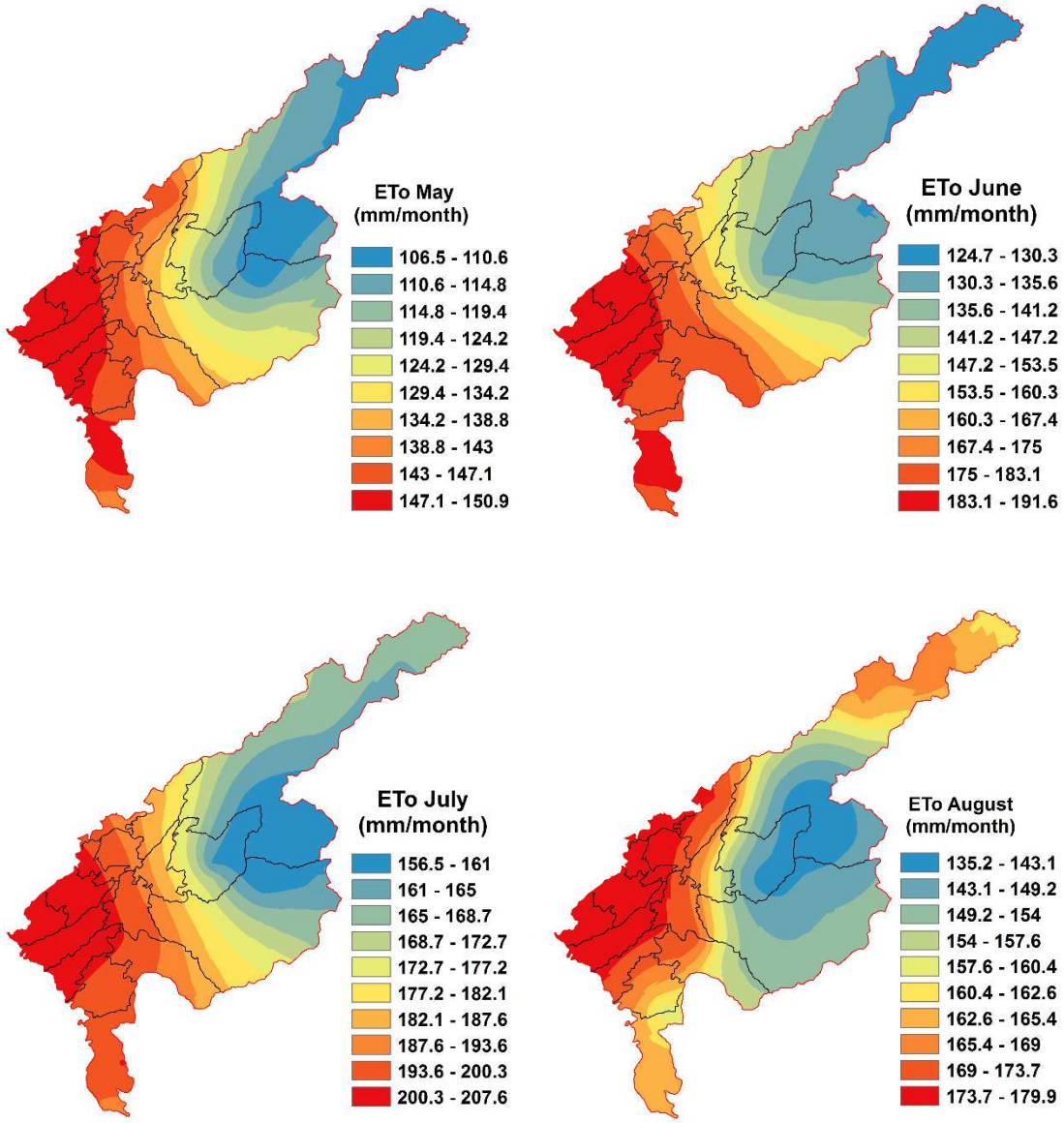

Figure 3.5 Spatial prediction of average monthly (2009-2011) ETo (mm) across Tashkent Province (*cont*.).

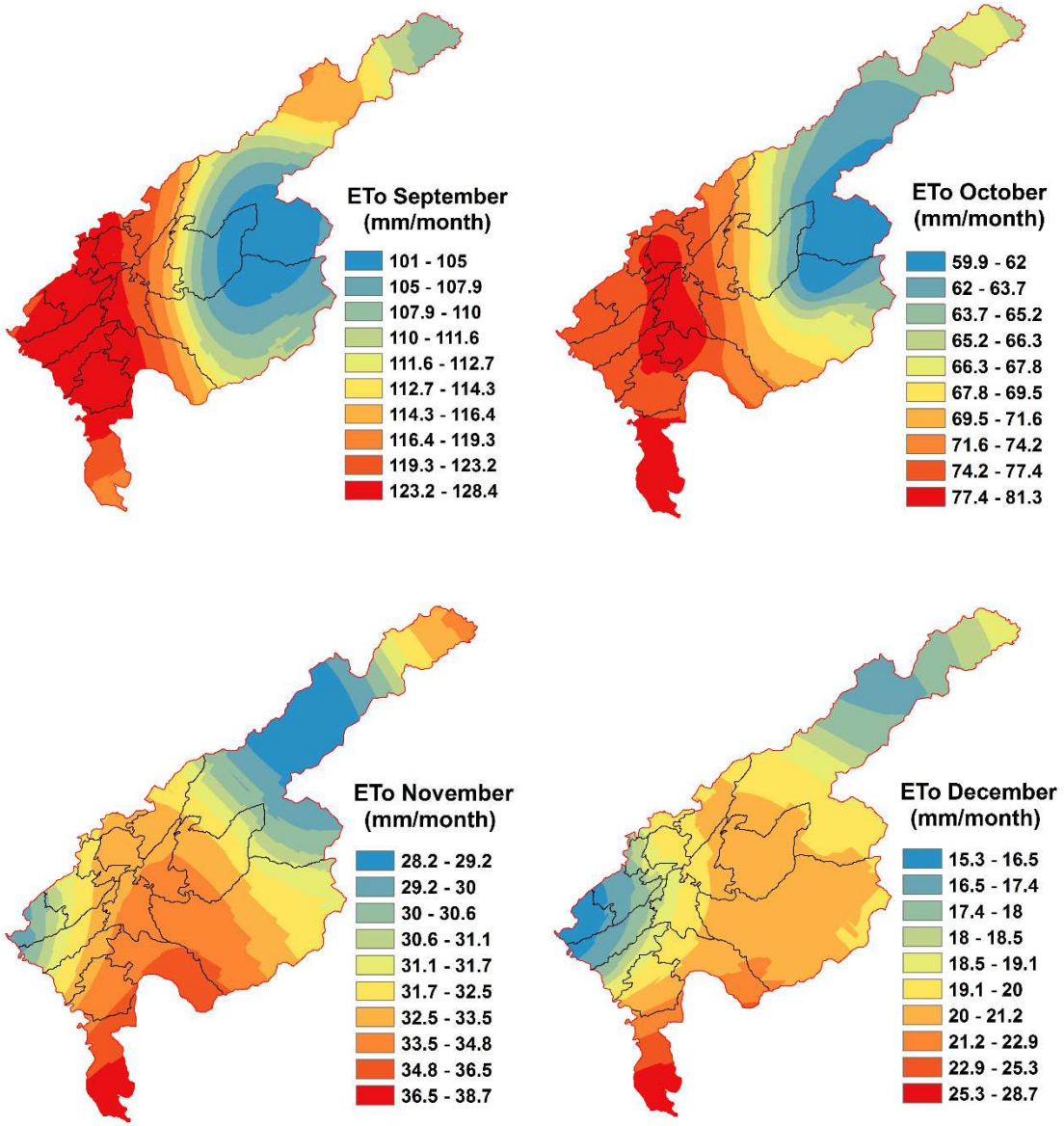

Figure 3.5 Spatial prediction of average monthly (2009-2011) ETo (mm) across Tashkent Province.

3.6 Conclusion

The HM showed a good performance with locally calibrated empirical coefficients in Tashkent province as an arid and semi-arid region. Over and under estimations of ETo with the original HM were reduced by 65 % as an average using new empirical coefficients for all 16 weather stations.

The study revealed that estimated ETo value decreased from southwest to northeast as the altitude increased. Using calibrated empirical coefficient, HM model can be an acceptable alternative method instead of FAO 56 PM model to estimate local ETo, when full a climate data set is not available. More weather stations would have to be installed to improve the prediction accuracy of calibrated HM estimates.

This research confirm that for low density network of weather stations geostatistical methods outperforms deterministic interpolation methods. The OCK method is better predicted estimated ETo in Tashkent province using elevation data as a covariance. The results revealed that the incorporation of elevation data improved spatial prediction of ETo in Tashkent province. In this paper presented techniques to accurately estimate and spatially predict of ETo using limited and cheaper data set. This analyses can be vital to scientists, engineers and decision makers to assess and set up counter measures against aridity increase in Tashkent province.

3.7 References

Allen R.G., Pereira L.S., Reas D., and Smith M: Crop Evapotranspiration. FAO Irrigation and Drainage Paper 56, Rome, 300 (1998).

Dukhovny V.A., Sorokin A.G., Tuchin A.I., Rysbekov U.H., Stulina G.V., Nerosin S.A., Rusiev I.B., Sorokin D.A., Katz A., Shahov V., Solodky G. 2007 D 34 - Final report on alternative scenarios of sustainable development of water management for the Chirchik Basin, European Commission within the Sixth Framework programme (2002-2006).

Gavilan P., Lorite I.J., Tornero S., Berengena J: Regional calibration of Hargreaves equation for estimating reference ET in a semiarid environment. Agric. Water Management, 81(3): 257-281, (2006).

Goovaerts P: Geostatistics for Natural Resources Evaluation. Oxford University Press, New York, 483pp (1997).

Hargreaves G.H. and Samani Z.A: Reference crop evapotranspiration from ambient air temperature, Paper No. 85-2517 (1985).

Sluiter R: Interpolation methods for climate data Literature review KNMI, De Bilt. Press, (2009).

Lixin, L. and Peter, R: Interpolation Methods for Spatio-Temporal Geographic Data, Computer Science and Engineering Department, University of Nebraska-Lincoln, Lincoln, NE 68588, USA, (2002).

Chapter 4: Development of Hydrological Model Parameters of Chirchik River Basin, Northern Uzbekistan

4.1 Introduction

In chapter 4, presented the generation of hydrological parameters of the Chirchik River Basin for integrated hydrological modeling. The integrated hydrological model was applied to Chirchik River Basin, which consist of coupling of 1 dimensional (1D) stream flow model to the integrated hydrological model. After coupling, model integrated al land phase hydrological process, including irrigation.

The parameters of 1D stream flow model were calibrated using observed daily discharge data from Chinoz gauging station for 2009-2011 and validated for 2012-2013. Simultaneously, integrated hydrological model was also calibrated using observed groundwater data for 2009-2011 and validated for 2012-2013. After calibration, the model produced quantitative results of hydrological parameters of the Chirchik River Basin. The calibration and validation of hydrological parameters and discussion of estimated water balance results were described at the end of this chapter.

4.2 Simulation specification

The hydrological model of Chirchik River Basin includes all water movement parameters such as: overland, river, unsaturated, saturated zone flows and evapotranspiration process. The simulation also includes snow melting and freezing and irrigation process. The integrated hydrological model requires a spatially distributed data set, which includes topography, soil, geological, land use, climate and initial potentiometric head data. These geospatial data were prepared with the ArcGIS 10.2 platform and grid size was carefully selected by considering the studies of Vásquez et al. (2002) and Singh (2010). Vásquez et al. (2002) and Singh (2010) found acceptable changes when MIKE SHE was applied over a range of grid cell sizes (300–1200 m) in a large watersheds. McMichael (2006) concluded that model grid size should be oriented to accurate representation of catchment attributes without placing excessive demands on simulation run time. A grid size of 500 m × 500 m was selected for Chirchik River Basin, because this grid size represents a compromise between detailed representation of basin attributes and simulation time. All these geospatial data were projected to Chirchik River Basin's coordinate system (WGS84 UTM 42N). All data output time steps were set to 24

hours.

The model uses Kristen and Jensen method to calculate actual evapotranspiration (AET). This method requires leaf area index (LAI), root depth (RD) for each vegetation type. Richard's 1D equation is used to calculate unsaturated flow process. The saturated flow component is calculated using Darcy's 3D method. Also, snow melting and freezing processes are simulated using a degree-day empirical approach, which requires a degree-day coefficient of the study area. The MIKE 11 model uses a 1D Saint-Venant equation to compute stream flow computations. The model simulates water releases from stream flow with these releases, then converted to irrigation depth to over-irrigation area. Simulation of the irrigation processes requires irrigation command areas, water sources (rivers, wells or lakes), irrigation time and demand. A detailed explanation of the above mentioned methods can be found in chapter 2 or Graham and Butt (2005) and DHI's user's guide (2012).

4.3 Generation of spatial distributed hydrological parameters

The digital elevation model (DEM) of the Chirchik River Basin was obtained from the NASA Shuttle Terrain Mapping (SRTM) of the United States Geological Survey web database. The original resolution of the DEM data was 30 m. The extraction of the basin boundary consist of two steps: In the first step watershed analyses were conducted using DEM of study area in ArcGIS platform. **Figure 4.1** shows generation procedures of sub watersheds of Tashkent Province. In the result many sub watersheds were generated within DEM. In the second step, the district map of Tashkent Province was overlaid pre generated sub-watersheds as shown in **Figure 4.2.** By using the both geospatial data the boundary of the basin in the upper stream is delineated according to watershed concepts, whereas the downstream is delineated according to the administrative boundaries of the districts of the Tashkent province. The reason is southwestern area (downstream) of the basin is almost topographically plain. Total area of the basin was estimated 5626 km^2.

The topography is used as the top elevation of both unsaturated zone (UZ) and the Saturated Zone (SZ) models. The topography also defines the drainage surface of overland flow. The evapotranspiration surface depth also measured from the topography. In MIKE SHE, the topography defined using either a dfs2 grid file, a point shape file (GIS) or and ASCII XYZ file. In this study DEM (GRID format) data was converted to a dfs2 file using the MIKE zero Toolbox. **Figure 4.3** shows dfs2 format topographical data of the Chirchik River Basin.

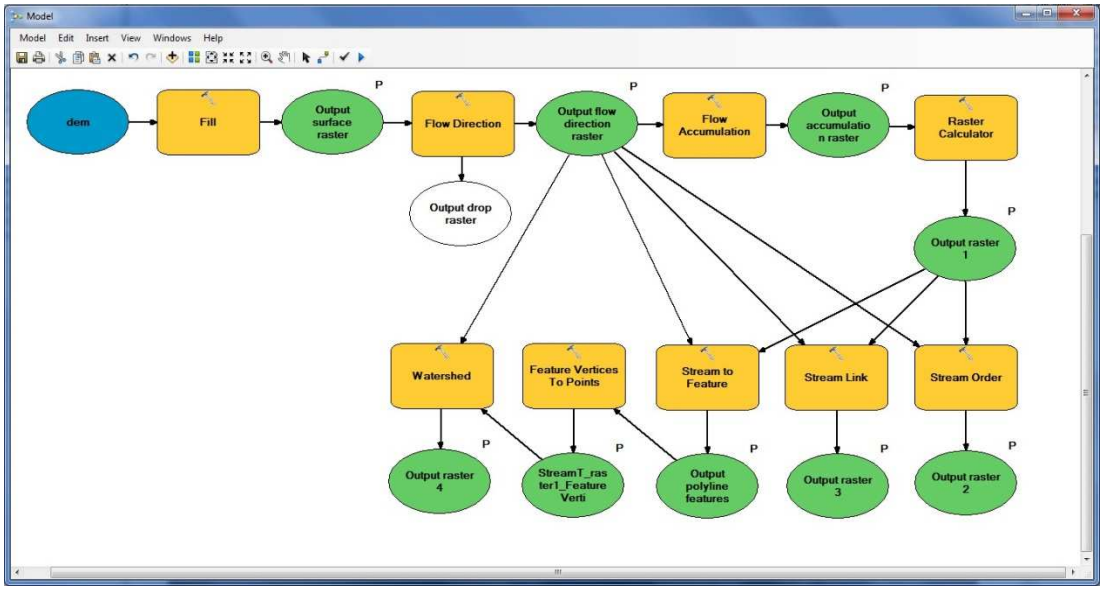

Figure 4.1 Generation process of sub watersheds of Tashkent Province

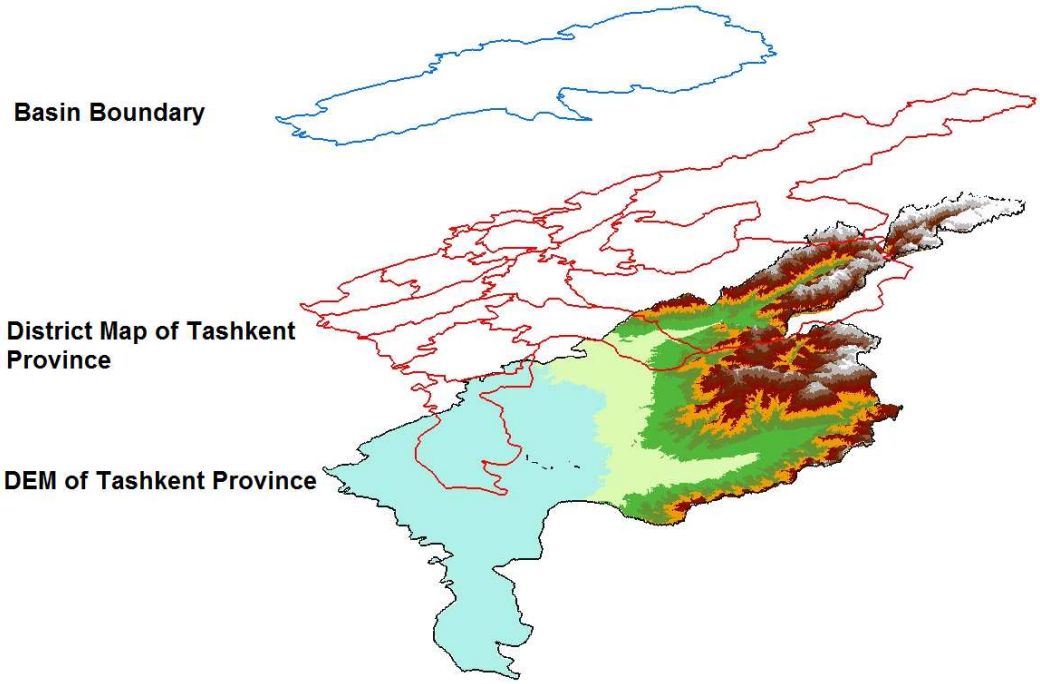

Figure 4.2 Extraction of the Chirchik River Basin boundary from geospatial data

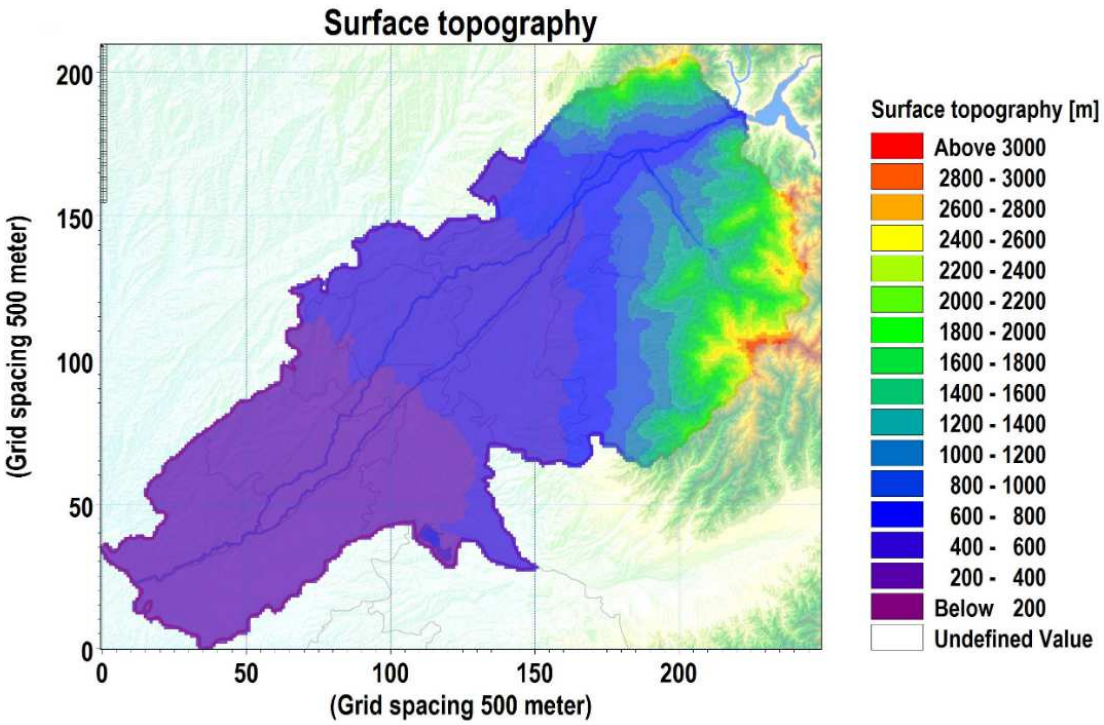

Figure 4.3 Topography of Chirchik River Basin input in MIKE SHE

A land use map of the Chirchik River Basin was obtained from AVNIR-2 (Advanced Visible Near Infrared Radiometer) satellite image (**Figure 4.4**) through a supervised classification method using the Image Analysis toolset in ArcGIS 10.2. Technical Characteristics of AVNIR-2 satellite image is given in **Table 4.1**.

The primary land use data were calibrated with minor modifications were performed using cadastral land use maps of districts in the Tashkent province. The land use of the basin has been classified as agriculture, arable lands, forest, grassland, urban and water body. The main part of the forest is located in the mountainous part of the study area. In **table 4.2** shows explication of each land use class**. Figure 4.5** shows land use map of the Chirchik River Basin.

As stated above, integrated model uses Kristensen-Jensen method to calculate AET. The model estimate AET for each pixel of the model domain using several factors. The model uses meteorological and vegetative data. The meteorological data are reference evapotranspiration (ET_o) and net rainfall. The total evaporation is a sum of the following process: evaporation from the canopy surface (interception of rainfall from the canopy surface), evaporation from the soil surface, and transpiration (based on soil moisture in the unsaturated root zone). The evaporation process in MIKE SHE can be described by following orders:

1. The evaporation from vegetation canopy which rainfall is intercepted.
2. The evaporation from soil surface while water runoff or ponded water.
3. The evaporation of infiltrating water from top soil or transpired by the vegetation.
4. The evaporation from shallow groundwater.
5. The evaporation from melted water from snowpack.

The AET parameters were divided into two groups: one for land use independent parameters and the other for land use dependent parameters. **Table 4.3** shows independent parameters. Crop coefficient (Kc), which is used to adjust the reference evapotranspiration relative to the actual evapotranspiration of the specific crop. In the early crop stages, where LAI of the farm crop is lower than the LAI of the reference grass crop, the evapotranspiration of the farm crop is less from the calculated reference evapotranspiration. This is accounted for in the Kristensen & Jensen ET calculation, since a crop LAI is used as input. Therefore, for most field crops it is therefore not necessary to specify Kc values below 1 in the early crop stages.

The C1 and C2 are empirical parameters that influence the ratio of soil evaporation and transpiration (Kristensen and Jensen, 1975). The estimated value of C1 for agricultural crops and grass is approximately 0.3 and 0.2. C2 has an approximate value between 0 and 0.5. For dynamic simulation using the unsaturated zone description in

MIKE SHE, a value of 0.3 was, however, found to give better results for C2 (Miljøstyrelsen,1981; Jensen, 1983). As parameter for C3, simulations with the unsaturated zone description in MIKE SHE, a value of 20 mm was found more appropriate (Miljøstyrelsen, 1981; Jensen, 1983).

The Aroot influences mainly the uniformity of the water extraction along the root zone. An Aroot value that tends toward zero produces a more uniform water extraction in the root zone, whereas higher values produce more water extraction from the topsoil than other locations in the root zone. As a result, the topsoil dries out faster and restricts further evaporation from soil (DHI, 2003). Evapotranspiration is less for a higher Aroot value. In this study the default model parameters (C1 = 0.3, C2=0.2, C3=20, and Aroot= 0.25) used in the estimation of actual evapotranspiration.

The dependent parameters of AET are considered LAI and RD. The values of seasonal changes for other land use types of LAI and RD data were obtained from the Institute of Water Problems (IWP) in Uzbekistan and literature (Jain et al., 1992; FSI, 2003; WISA, 2005).

IWP recommended a minimum constant value of LAI and RD for urban and water land use classes and this assumption is confirmed by Singh (2010). The minimum value of LAI and RD better simulate evaporation from urban and water bodies (Singh, 2010). Therefore, a minimum constant value were specified for urban and water types throughout the year.

The values of seasonal changes for other land use types of LAI and RD data were carefully selected by considering recommendation of the IWP in Uzbekistan and literature (Jain et al., 1992; FSI, 2003; WISA, 2005).

In Tashkent Province the growing season starts from March to end of October. Therefore, the LAI for forest, agriculture, grass and arable land varies throughout the year are shown in **Figure 4.6.** The RD controls the amount of transpiration through root uptake in the soil profile. The RD values of the forest and arable land have specified a constant value throughout the year. For other land use types (agriculture and grass) RD value is changing depending on LAI changes. Only RD value for forest is uniform throughout the year because changes of root of trees in forest are negligible (Suva, 2007; Sing, 2010). The values of seasonal changes of RD for all land use types of the study area are shown in **Figure 4.7**.

As shown in **Figure 4.8,** the Tashkent Province has a 16 weather stations. However, only 7 (Boshkizilsoy, Chimgan, Kounchi, Sukok, Tashkent and Tuyabuguz) weather stations were selected in simulation process due to its geographic location to study area.

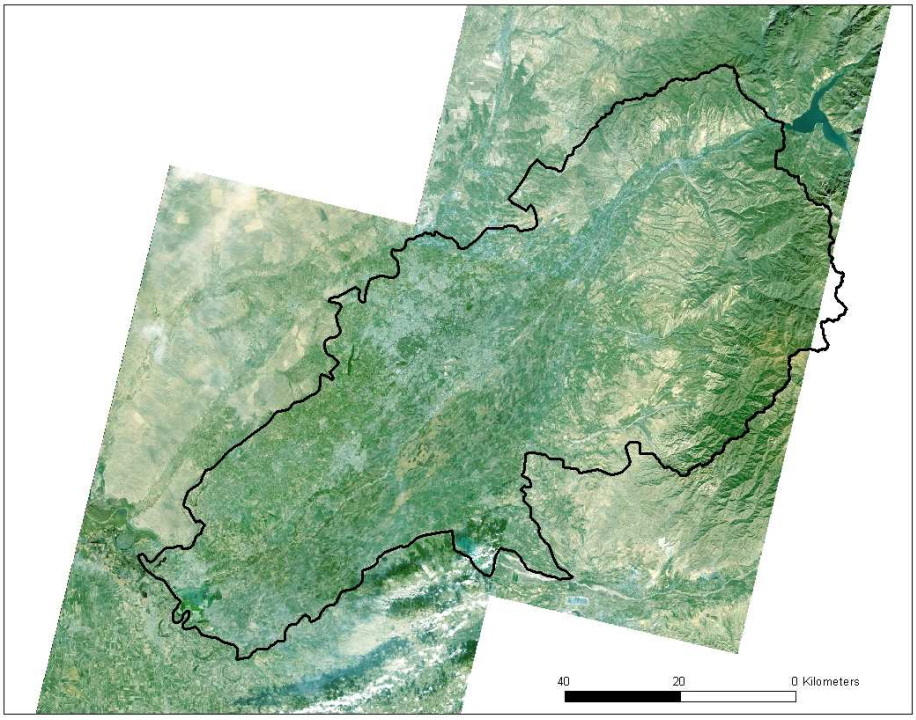

Figure 4.4 ALOS AVNIR-2 satellite image

Table 4.1 Technical Characteristics of AVNIR-2 satellite image

Number of bands	4
Wavelength	Band 1: 0.42 to 0.50 micrometers Band 2: 0.52 to 0.60 micrometers Band 3: 0.61 to 0.69 micrometers Band 4: 0.76 to 0.89 micrometers
Spatial Resolution	10 m (at Nadir)
Swath Width	70 km (at Nadir)
S/N	>200
MTF	Band 1 through 3: >0.25Band 4: >0.20
Number of Detectors	7000/band
Pointing Angle	-44 to + 44 degrees
Bit Length	8 bits
Resolution	10 meters

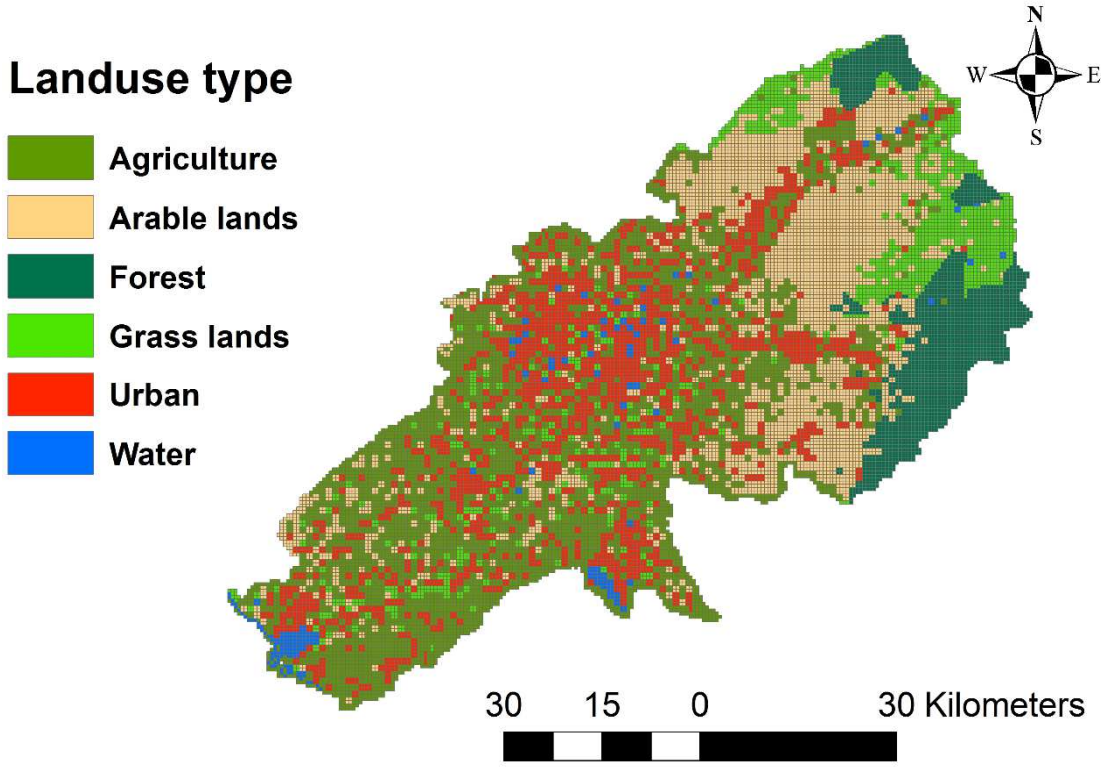

Figure 4.5 Land use map of the Chirchik River Basin

Table 4.2. Explication of each land use classes

N:	**Land use Classes**	**Description**
1	Agriculture	Agricultural area and growing crop field
2	Arable lands	Desert, dry land and no vegetation.
3	Forest	Forest (National parks)
4	Grassland	Grasses, herbs and pasture
5	Urban	Residential, village and inhabited areas
6	Water	River and lake

Table 4.3 Independent ET parameters

Parameters	Value
Canopy interception storage capacity	0.05 mm
Growth cycle	one year
Crop coefficient (K_c)	1
Empirical parameter C1	0.3
Empirical parameter C2	0.2
Empirical parameter C3	20 mm/day
Root mass distribution parameter (Aroot)	0.25 m^{-1}

The climate (precipitation, ET_o, the degree-day melting coefficient and short wave solar radiation data) data from these weather stations were provided by the hydro meteorological Authority of Uzbekistan. **Figure 4.9** shows average annual precipitation data of selected weather stations for 2009-2013. Potential evapotranspiration (ET_o) was calculated using the modified Hargreaves model. **Figure 4.10** shows average annual ET_o data of selected weather stations for 2009-2013. The Thiessen polygon method (Fetter. 2001) was used to spatially distribute these climate parameters over the study area. Proper lapse rates were set to precipitation and temperature data for correction of the Thiessen polygon method in mountainous areas. Rainfall increases 60 mm/year for every 100 meter increase in elevation due to orographic effects.

The overland water flow from snow and glacier melting and its distribution to river formation is an important consideration in basin territory. The two conventional methods are available to simulate snowmelt for daily and shorter time steps. The first comprehensive method is energy balance. This method simulates the energy fluxes to the snowpack. This method is not often used due to intensity of required data. The second alternative method is a degree day empirical approach.

In this approach all energy fluxes assume a unique air temperature. In this study, the snow melting and freezing processes are simulated using a degree-day empirical approach. This method requires a degree-day coefficient and mean daily temperatures of the study area. The degree day factor is the amount of snow that melts per day for every degree the air temperature. The degree day factor is a time varying coefficient because the rate of melting varies as the snow pack changes over the winter. The melting coefficient is often used as a calibration parameter to calibrate the volume of snow melt to the observed runoff. The degree day coefficient of the study area is given in **Table 4.4.** If the air temperature is below the threshold melting temperature (the threshold temperature is usually zero), the rain accumulates as snow.

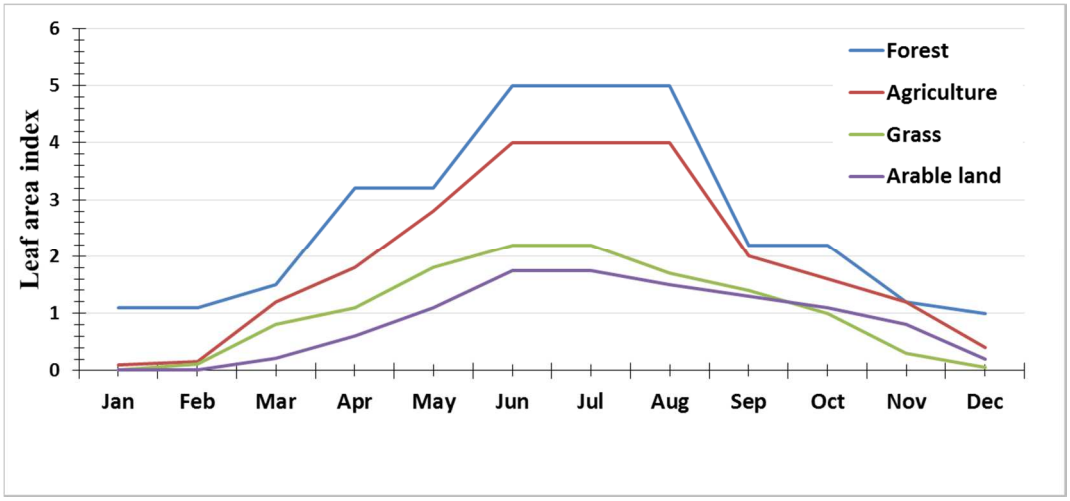

Figure 4.6 Values of seasonal changes of LAI

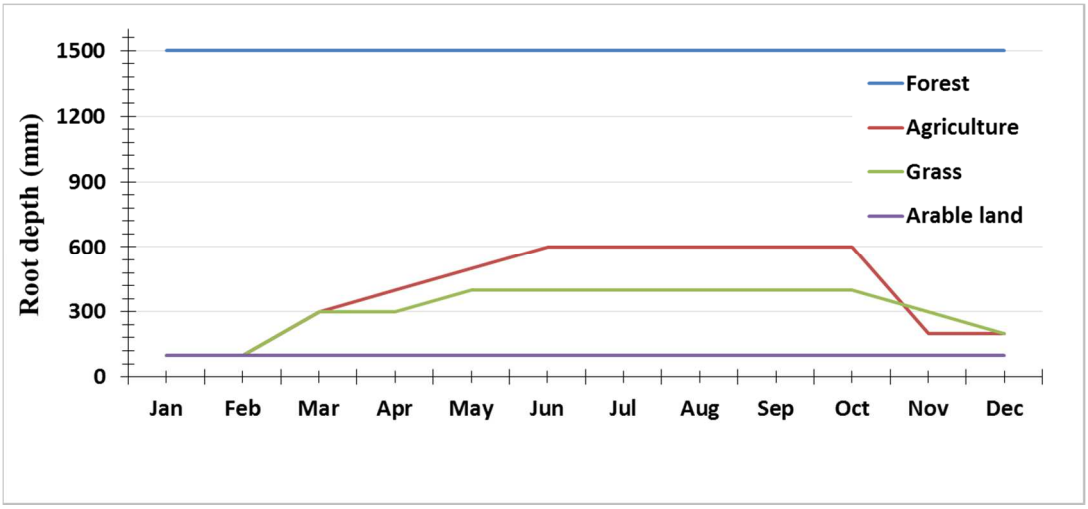

Figure 4.7 Values of seasonal changes of RD

The opposite condition, snow melts at the rate of specified by the Degree-day Melting or Freezing Coefficient. Dry snow acts like a sponge and does not immediately release melting snow. Thus, melting snow is added to wet snow storage. When the amount of wet snow exceeds the maximum wet snow fraction in snow storage, the excess is added to ponded water, which is then free to infiltrate or runoff. The model parameters of a maximum wet snow fraction in snow storage and initial wet snow fraction were set to 0.3 and 0.2 respectively. The model also requires the spatial distributed total initial snow storage. According to literature the maximum snow storage depth can reach 1200 mm/year in high mountainous areas (Chanisheva, S. and Smirnova, E. (2011)). Therefore, spatial distribution snow storage depth was constructed according to this concepts. **Figure 4.11** shows distributed total initial snow storage.

The soil data is one of the essential parameters to simulate the unsaturated zone components. Unsaturated flow computation in the model requires a spatially distributed soil map, and its hydraulic parameters. The distributed soil map was obtained by digitizing 1:800,000 scale soil map of the Tashkent province. Soil types vary depending on geomorphological zoning in the basin. As total 12 soil types were identified in the basin region. Then soil map was discretized to 500 x 500 meter pixel as shown in **Figure 4.12**. This is a generalized soil map as it groups closely similar soil types as one. **Table 4.5** shows the hydrogeological parameters of the soil, which were provided by Institute of water problems of Uzbekistan.

In this study Richards's equation was selected for calculating vertical flow in the unsaturated zone, which are the functions of soil moisture retention curve and effective conductivity. The number of methods are available to for describing these relationships mathematically to solve it by numerical methods. In this study Van Genuchten function (Van Genuchten. 1980; Xu, Y. and Xueyi, Y. 2013) for both curves as they are most widely used soil moisture-pressure hydraulic conductivity relationships.

Saturated zone flow simulated using Darcy's method and solved the finite difference method numerically. This method requires the spatially distributed thickness of the computational geological layers. Only the surficial soil layer was considered in this research due to insufficient information of geological layers within the basin.

Soil layer thickness was constructed using lithological information from a geological borehole dataset (**Figure 4.13**).

The depth of the soil layer continuously increases from the mountains to the downstream areas of the basin, ranging between 5-35 meters. The assumption of soil-layer thickness is consistent within the geological literature (Makhmudov et al., 2014).

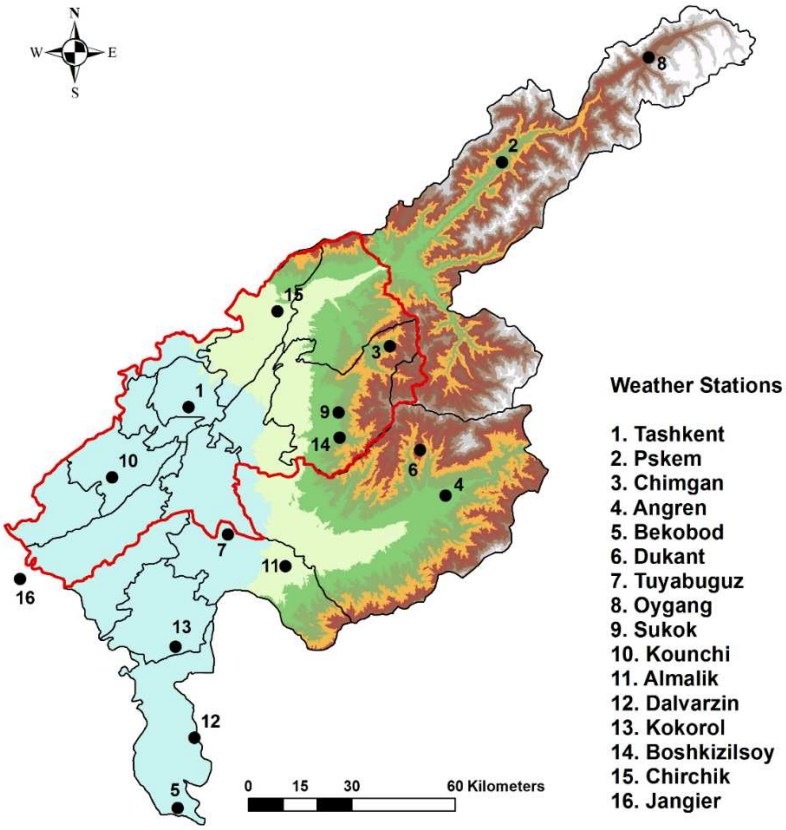

Figure 4.8 Weather stations of Tashkent Province

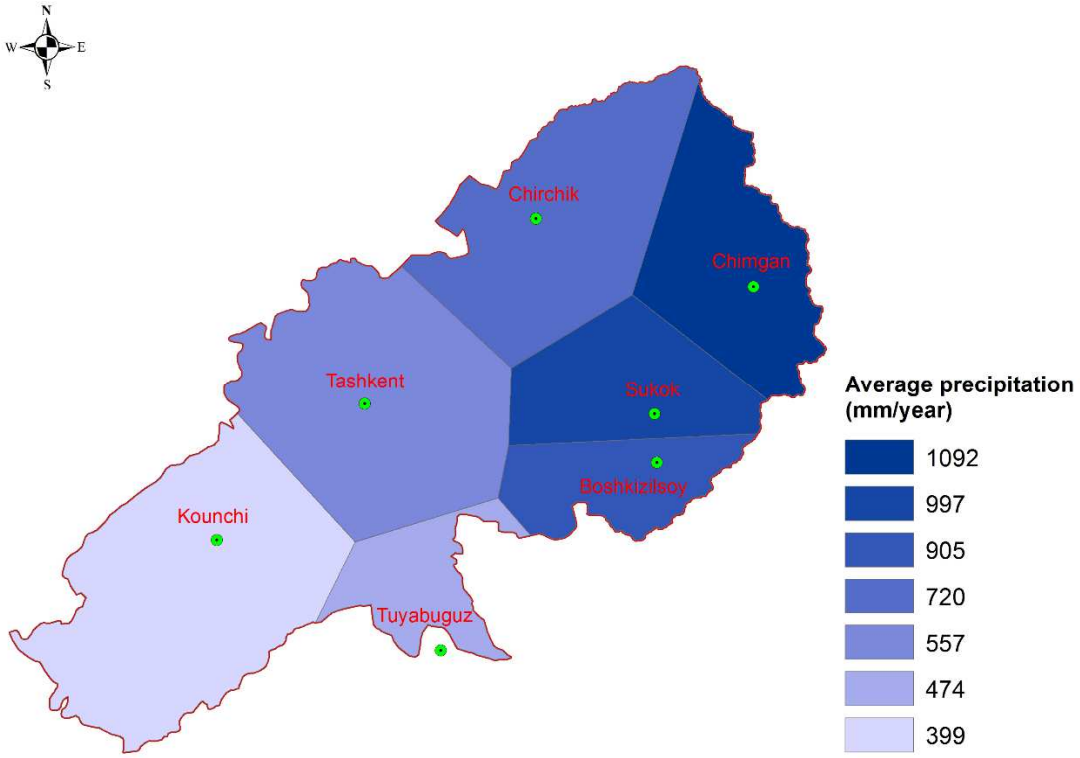

Figure 4.9 Average annual precipitation data of selected weather stations

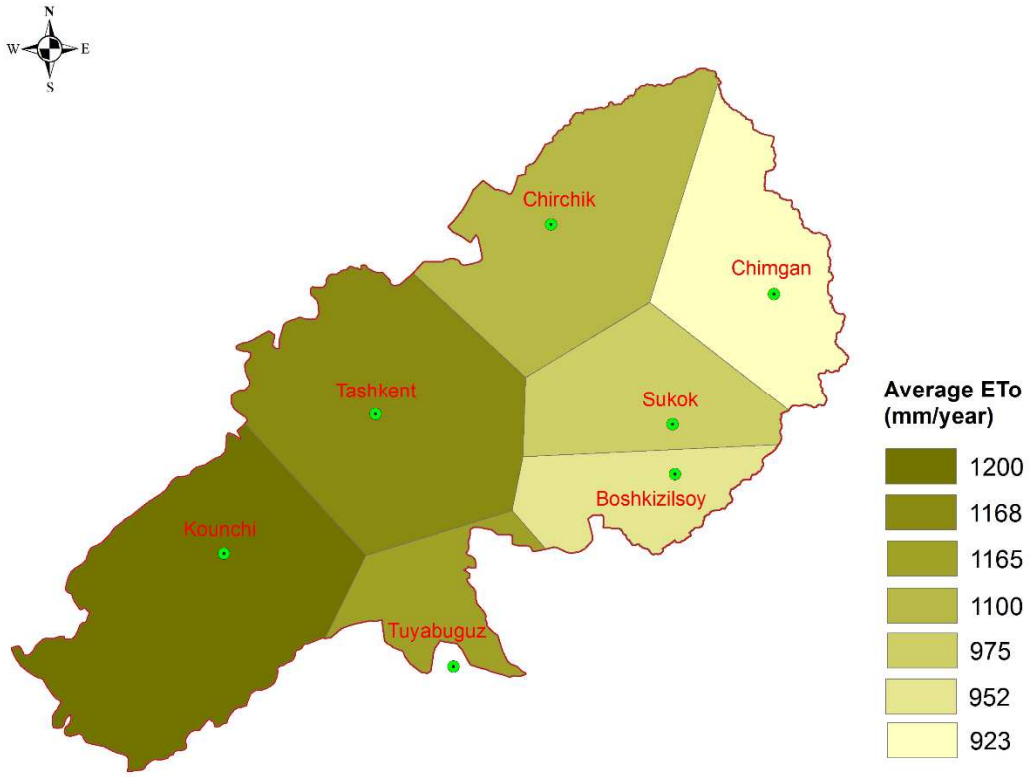

Figure 4.10. Average annual ET_o data of selected weather stations

Table 4.4 Degree day coefficients

Jan	Feb	Mar	Apr	May	Jun	Jul	Aug	Sep	Oct	Nov	Dec
1.4	1.6	1.2	1	0.8	0.6	0.4	0.5	0.6	0.7	0.8	1.3

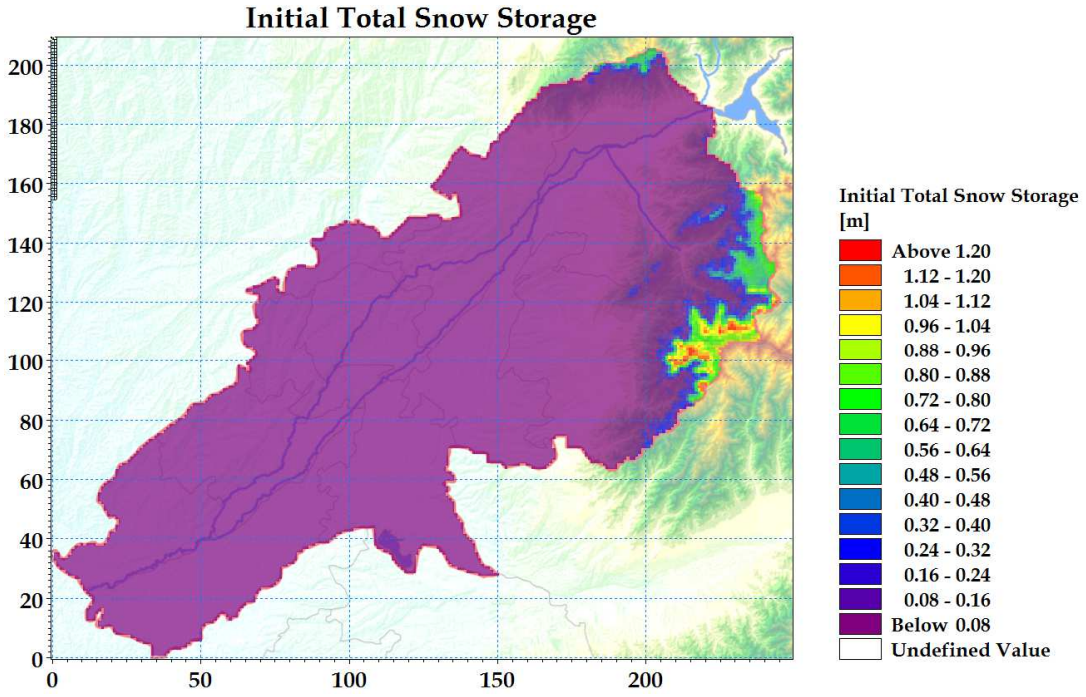

Figure 4.11 Initial snow storage depth of study area

Initial groundwater table data were generated through a geostatistical interpolation method using data from 140 groundwater wells. Then interpolated raster data was converted to vector format as a contour line (**Figure 4.14**). The specified groundwater table is used as the lower boundary condition for the unsaturated model.

In the model unsaturated and saturated zone profiles were vertically discretized as a cell. In this study, fine cells were set for the top of the profile and introduced a smooth transition to coarser cells at the base (**Table 4.6**). The amount of available water in the saturated zone is calculated in the following order:

1. If the groundwater head is below the ground surface, water infiltrates through vertically the unsaturated zone.
2. If the groundwater head is above the ground surface, inudiated water recharge ponded water and then contribute runoff process.
3. Transpiration from the unsaturated and saturated zone, reduces of the recharge.

After input all prepared hydrogeological information (soil data, spatial distributed soil depth and groundwater level data), MIKE SHE combined and preprocessed and generate spatial distributed hydraulic and vertical conductivity in the saturated zone, and specific storage and specific yield of study area. These preprocessed spatial distributed hydrogeological information are shown in **Figure 4.15**.

The overland water movement is one of the central hydrological process, particularly in mountainous areas in the Chirchik River Basin. The MIKE SHE uses two dimensional wave approximation of the Saint Venant method to model the two dimensional movement of water over the land surface.

In nature, overland flow occurs when rainfall cannot infiltrate fast enough or snow and glacier melting. In simulation process, overland flow dynamically coupled to the unsaturated zone model. Because the overland flow becomes subject to infiltration to the unsaturated zone and to evapotranspiration. When the groundwater level would rise above ground level due to head pressure the saturated zone will then directly discharge to overland flow. The overland flow direction is identified by the slope gradients and land surface resistance. In this simulation, Mannings coefficient was assigned based on land use class.

Table 4.5 Hydrogeological parameter of soil in study area

Soil Code	Name	Contents	Vertical conductivity	Horizontal conductivity	Specific yield	Specific storage
1LB	**Light brown**	Light-brown. Heavy loam or clay, rock skeleton and coarse Skelton	**1.8E-09**	**3.47E-08**	**0.16**	0.009
3GB	**Grayish-brown**	Rain fed grey soil, heavy loam or clay.	**1.3E-08**	**1.28E-07**	**0.18**	0.0087
5BS	**Brown Soil**	Typical brown soil with middle-heavy loam.	**1.2E-08**	**1.42E-07**	**0.22**	0.0083
11DG	**Dark gray**	Loess-like heavy loam under ephemeral, couch grass and motley grass cover.	**7.3E-06**	**7.43E-05**	**0.2**	0.0078
13TG	**Typical gray**	Old irrigated, middle loamy and strong and non-strong washed. Often weakly salted	**6.8E-05**	**0.000636**	**0.32**	0.00011
17GG	**Grassland gray**	Rainfed middle and heavy loamy. Weakly skeleton. Weakly and strong washed soil	**5.8E-05**	**0.000527**	**0.25**	0.00073
26NIG	**Newly irrigated grey**	Typical seriozem. Middle and heavy loamy. Weakly washed and sometimes weakly salted.	**5.3E-05**	**0.000519**	**0.27**	0.0054
29OIG	**Old irrigated grey**	Old irrigated, Medow grey, middle loamy, weakly salted and washed soil	**1.5E-06**	**1.48E-05**	**0.28**	0.0066
32OIAG	**Old irrigated alluvial grey**	Old irrigated, meadow alluvial soil with middle loamy.	**1.8E-05**	**0.000154**	**0.3**	0.00023
34NIAG	**Newly irrigated alluvial grey**	New irrigated medow alluvial soil with middle and heavy loamy.	**2.1E-05**	**0.000247**	**0.26**	0.00033
35MSAS	**Meadow and swamp alluvial soil**	Meadow-Swamp alluvial soil with heavy loamy	**3E-07**	**3.17E-06**	**0.1**	0.0098
42SG	**Sand-gravel**	Bench gravel, coarse gravel, pebble-bed	**4E-05**	**0.000413**	**0.24**	0.000084

Table 4.6 Soil vertical discretization

From depth (m)	To depth (m)	Cell height (m)	Number of cells
0	2	0.1	20
2	8	0.2	30
8	23	0.3	50

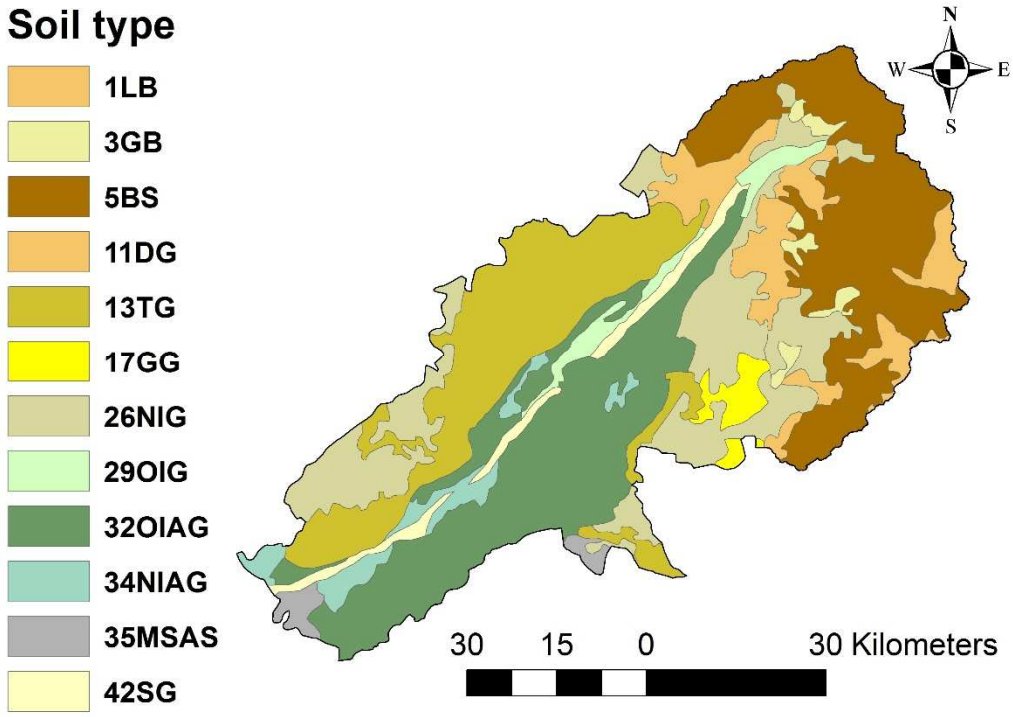

Figure 4.12 Soil map of Chirchik River Basin

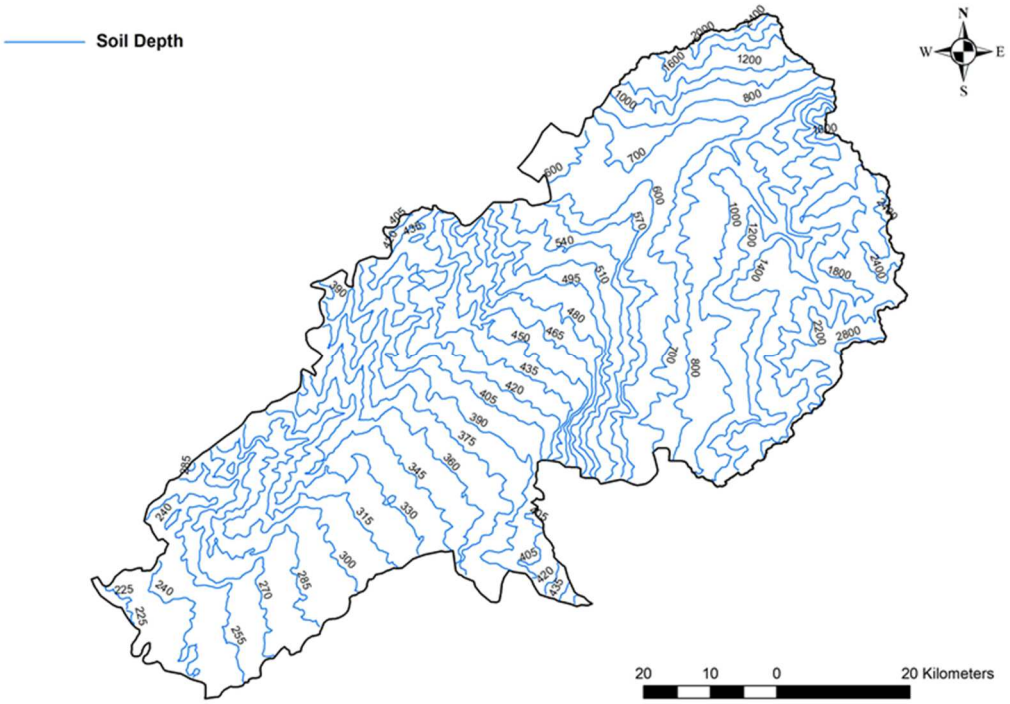

Figure 4.13 Depth of the soil map of Chirchik River Basin

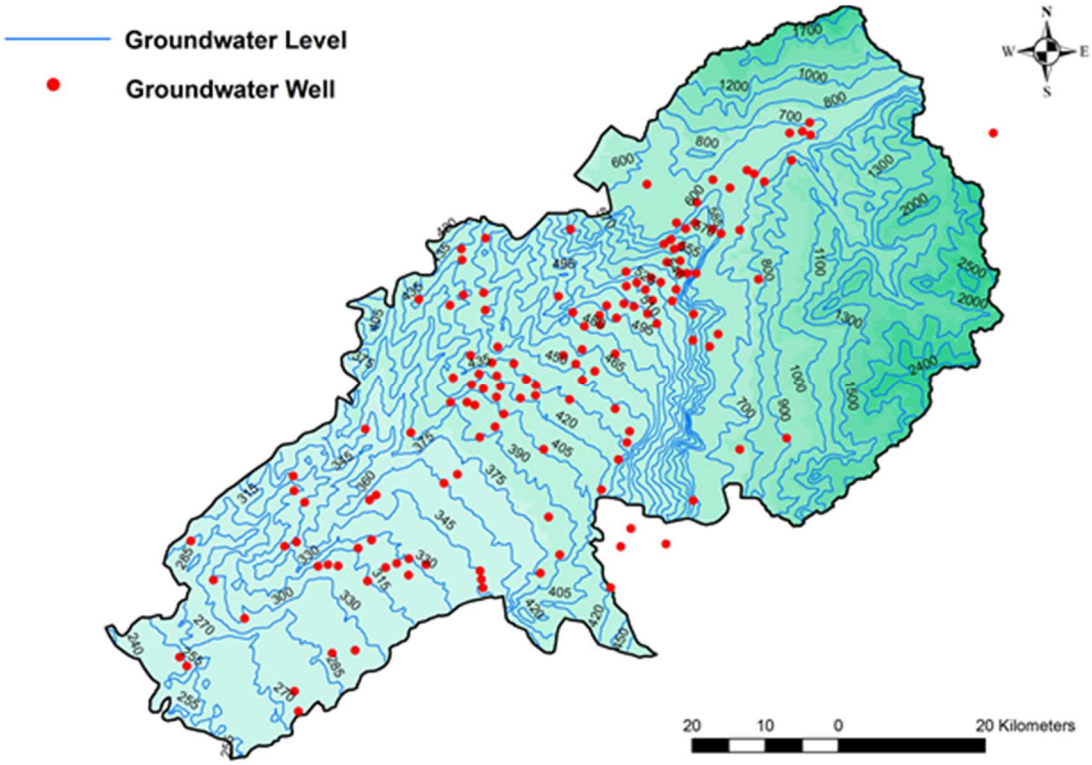

Figure 4.14 Initial groundwater table and wells of Chirchik River Basin

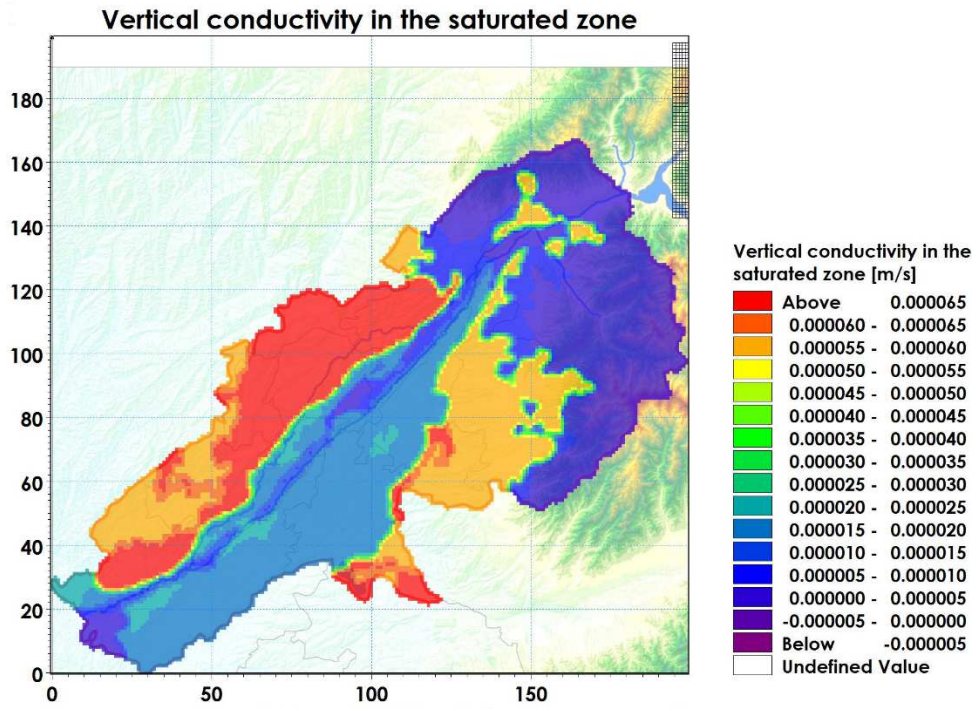

a) Vertical conductivity in the saturated zone

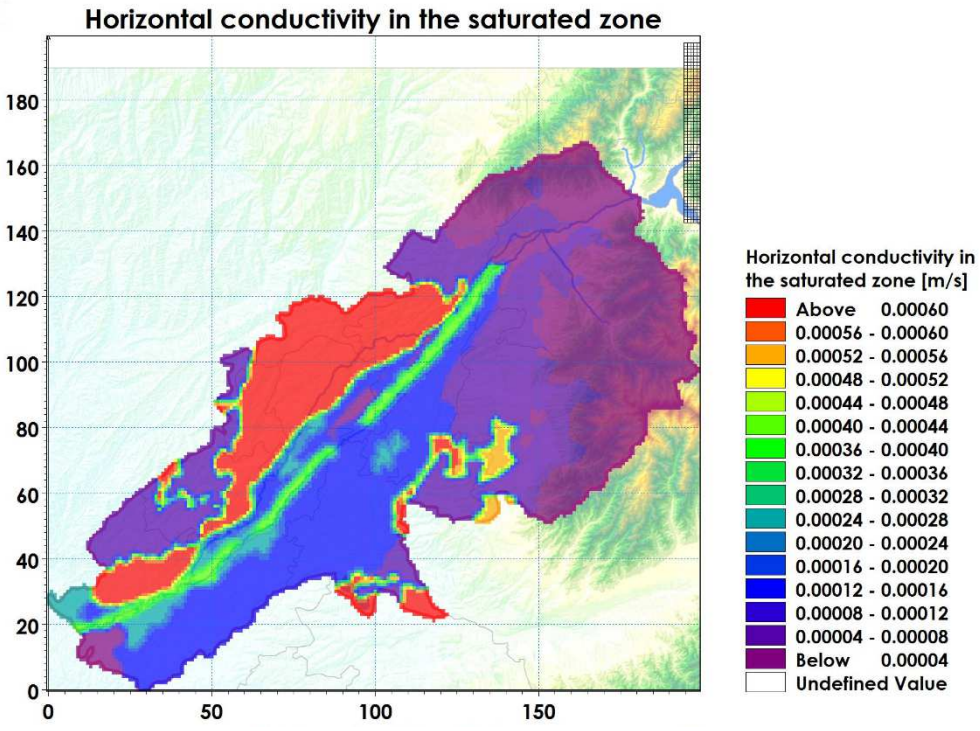

a) Horizontal conductivity in the saturated zone

Figure 4.15 Preprocessed hydrogeological parameters (*cont*.)

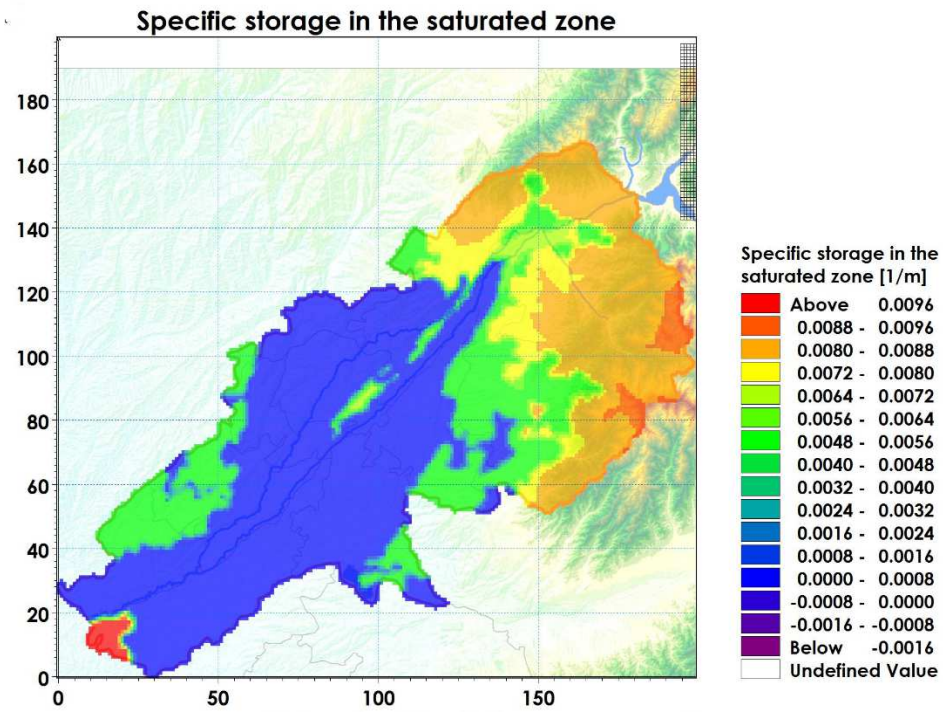

c) Specific storage in the saturated zone

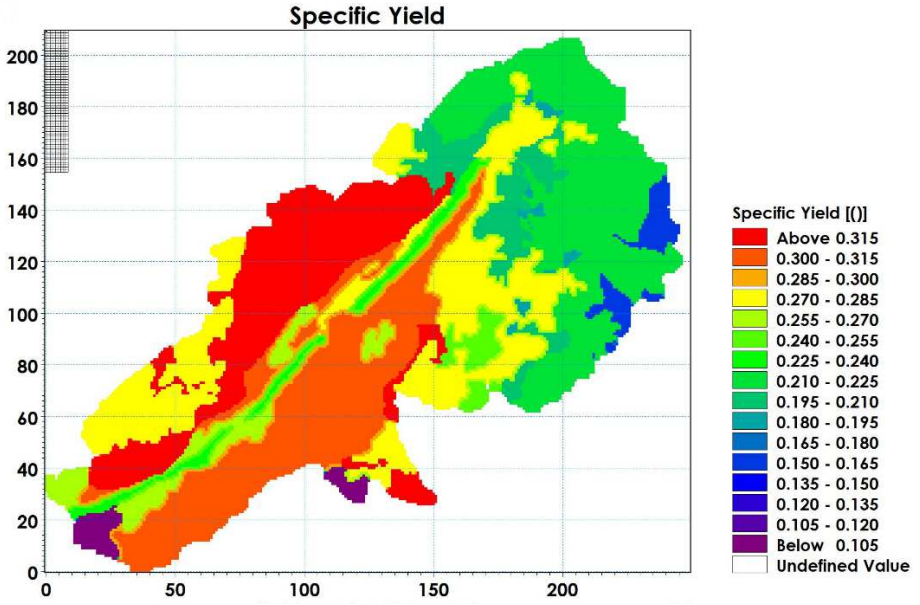

d) Specific yield in the saturated zone

Figure 4.15 Preprocessed hydrogeological parameters

4.4 Stream flow simulation

In this study, the main rivers of the Chirchik River Basin were explicitly modeled using Saint-Venant method. This model is a one dimensional dynamic model to compute the flows and levels of rivers through a series of interconnected channels. The model requires river network, cross section and discharge data of simulated streams. Moreover, the model requires upstream and downstream chainages of modeled rivers. The chainage value is used to measure distance along the length of a river and value increases toward to downstream direction.

River and channel network data were extracted via digitization of the topographical map of the Tashkent province. The network consists of five main rivers: Chirchik, Ugam Rivers and Bozsuv, Parkent, Qorasuv Channels. **Figure 4.16** shows a river network of simulated branches.

Cross-section data were collected by field surveys in each of the simulated branches. **Figure 4.17** shows river cross section measuring process of Chirchik River branches. River cross-sections are profiles of a river bed at a particular chainage, and are used in MIKE 11 to determine the virtual profile of the river. **Table 4.7** shows information of chainages for all branches. Missing cross-sections for Parkent and Qorasuv branches were assumed to be of a regular shape. The created Chirchik stream network consists of 28 cross-section data. An example of the cross-sections set for the Chirchik River are shown in **Figure 4.18**.

Every river branch needs to set an upstream and downstream boundary. If the upstream boundary is not connected to another branch, then it is usually defined as an open inflow boundary. If the downstream boundary is not connected to another branch, then it is usually set to a water level. Daily average discharge data for 2009-2013 of the Ugam River (**Figure 4.19**) and Charvak water reservoir (**Figure 4.20**) were assigned to upstream boundaries of the network.

The storing frequency of the simulation time step was set to 6 sec 6 min. The constant Manning's roughness coefficient was applied for each branch in the stream network. Water withdrawal rate time series data from simulated rivers was set after coupling the stream flow simulation to the integrated model. After coupling, irrigation area and demand were also set to simulate irrigation processes. The model was set to obtain 100% of irrigation water from the simulated streams.

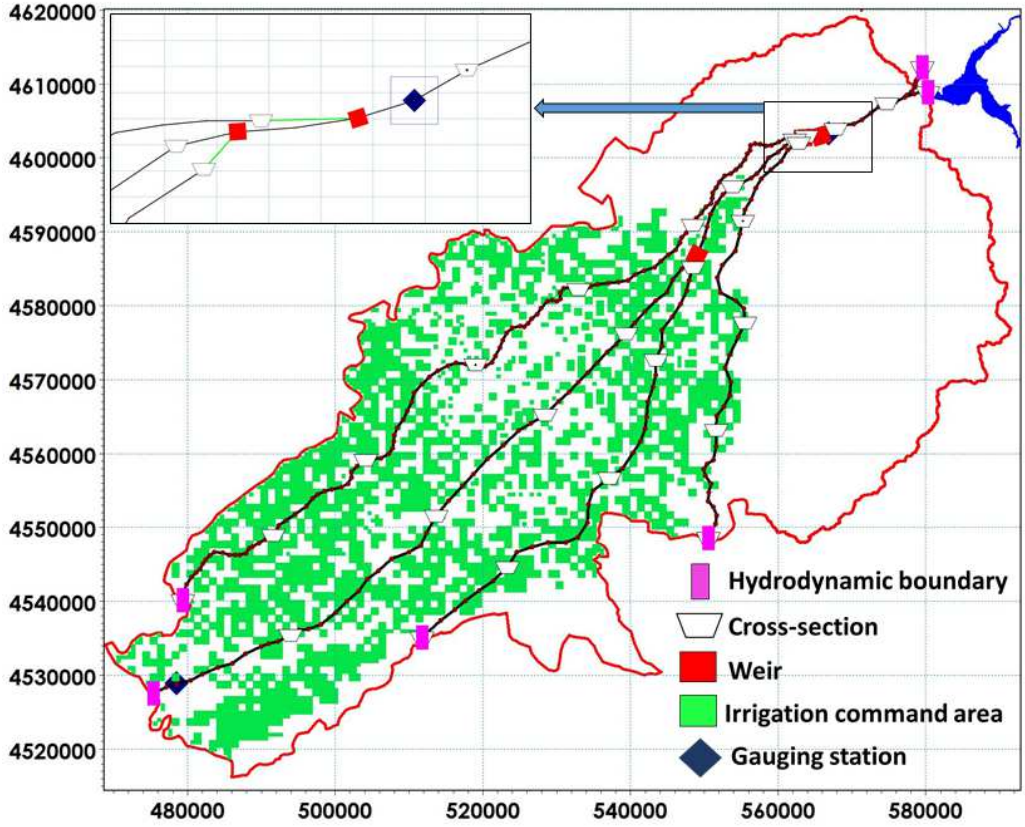

Figure 4.16 River network of simulated branches and irrigated area

Table 4.7 Description of Branch network in MIKE 11 model

N	Name of branch	ID	Upstream Chainage (m)	Down stream Chainage (m)	Branch type
1	Chirchik River	CHR	0	137950.51	Regular
2	Qorasuv Canal	QC	0	67425.939	Regular
3	Bozsuv Canal	BC	0	116499.56	Regular
4	Parkent Canal	PC	0	61817.053	Regular
5	Ugam River	UR	0	4489.3263	Regular

Figure 4.17 Measuring process of river cross section of Chirchik River

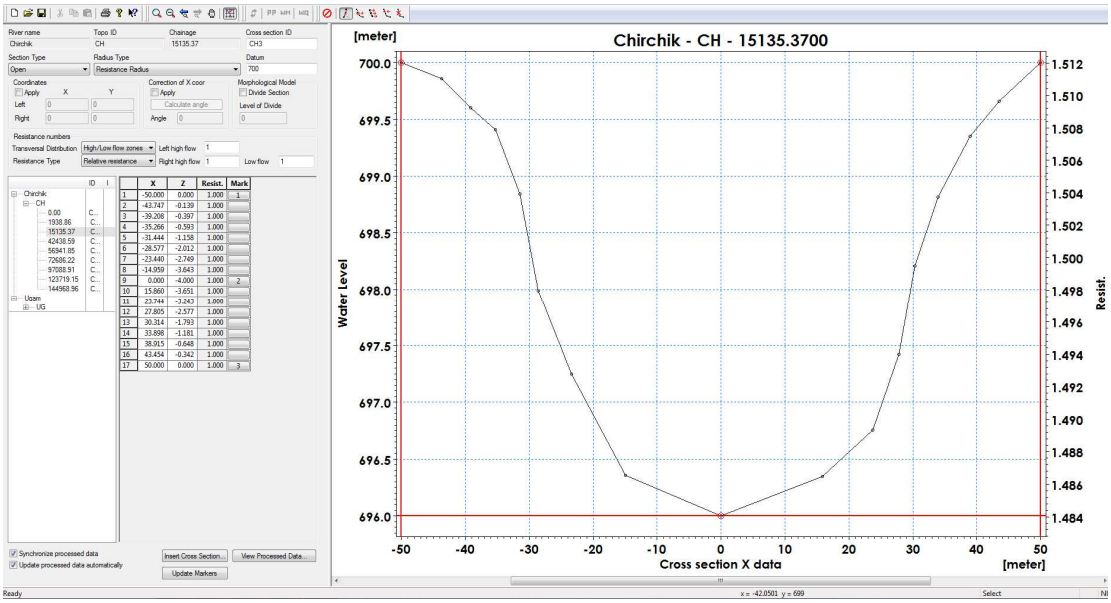

Figure 4.18 An example of the cross-section of the Chirchik River

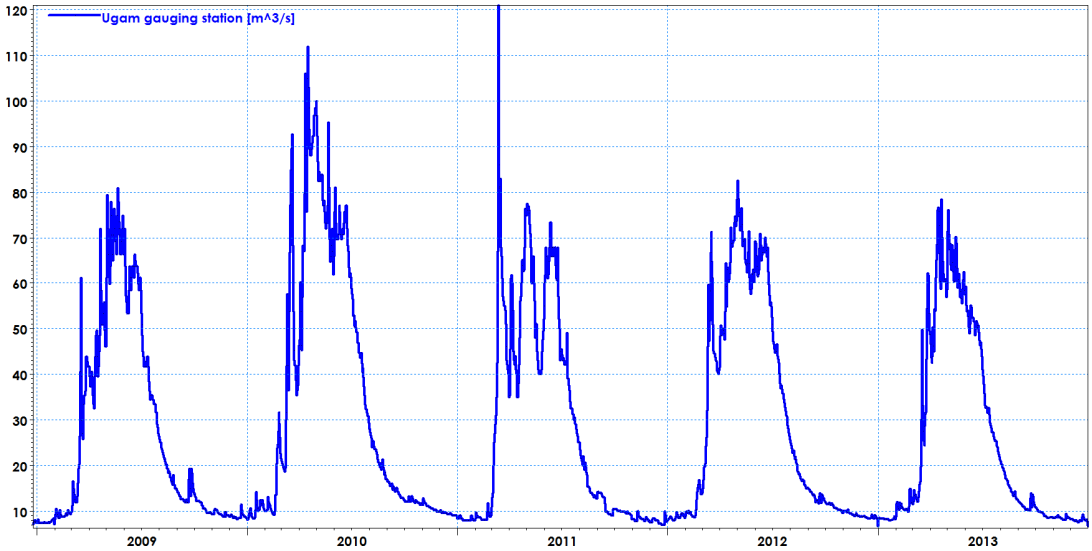

Figure 4.19 Daily discharge data of Ugam gauging station

Figure 4.20 Daily discharge data of Charvak gauging station

4.5 Irrigation process

As stated above, the simulation of the irrigation process in model requires irrigation command areas, irrigation demand and schedule. The conventional and contemporary irrigation techniques are applicable to set separately for each irrigation area. As an irrigation sources surface and groundwater water could be selected to imitate the current irrigation sources. The irrigation standard is Tashkent province is average 5000 m^3/ha and irrigation is conducted normally 5 times in irrigation period. The sequence and quantity of irrigation are based on local standard of Tashkent province. After successful simulation the stream flow was coupled with a hydrological model of the Chirchik River basin to integrate irrigation process to full hydrological model. **Figure 4.16** shows the total simulated irrigation area and streams in the model. The model was set to obtain 100% of irrigation water from the Chirchik River.

4.6 Calibration and validation

Refsgaard and Storm (1995) advised that the initial model parameters should be adjusted to climatic and land phase condition of study area during calibration of a distributed hydrological model. However calibrated parameters should be as small as possible. Initially, climate parameters for modelling snow melting and freezing, including degree-day coefficient and maximum wet snow fraction, were adjusted to climatic conditions of the basin. The next step of calibration process focused on adjusting horizontal and vertical conductivity, and specific storage of saturated zone parameters. The initial calibration model runs were carried out by modifying above mentioned hydrological parameters for 2009-2011.

Simulation results were calibrated and validated for 2009-2011 and 2012-2013 against stream flow discharge at Chinoz gauging stations and groundwater level data. **Figure 4.21** shows location of gauging stations and groundwater well within Chirchik River Basin. Model performance was evaluated using mean error (ME), mean absolute error (MEA), root mean square error (RMSE), correlation coefficient (R^2) and the Nash and Sutcliffe coefficient (EF) (Nash and Sutcliffe 1970).

4.7 Stream flow hydrograph

Figure 4.22 and **Figure 4.23** shows simulated and observed hydrographs for the calibration and validation period in the Chinoz gauging station. The model was generally good, simulating daily stream flow discharge with an average of 0.91 (2009-2013) and 0.77 (2009-2013) of R^2 and EF. The hydrographs show over and under estimation of stream flow discharge. **Table 4.8** presents the performance statistics of stream flow simulation.

The Chrichik River discharge mainly depends on water release rate of Charvak water reservoir, the rate of contribution from tributaries and temperature degree that melts of snow storage. Apart from this the discharge also depends on water withdrawal quantity from the Chirchik River for irrigation. These phenomena make different tendency of Chirchik River flow. Simulated river flow shows numerical imbalance when river water starts to be withdrawn for irrigation. This is clearly shown in March 2013 (validation period). Relatively high overestimation was detected from July to November immediately after peak discharge rate. The main reason for this discrepancy is the absence of the operation information of small irrigation canals, reservoirs and hydro-engineering structures.

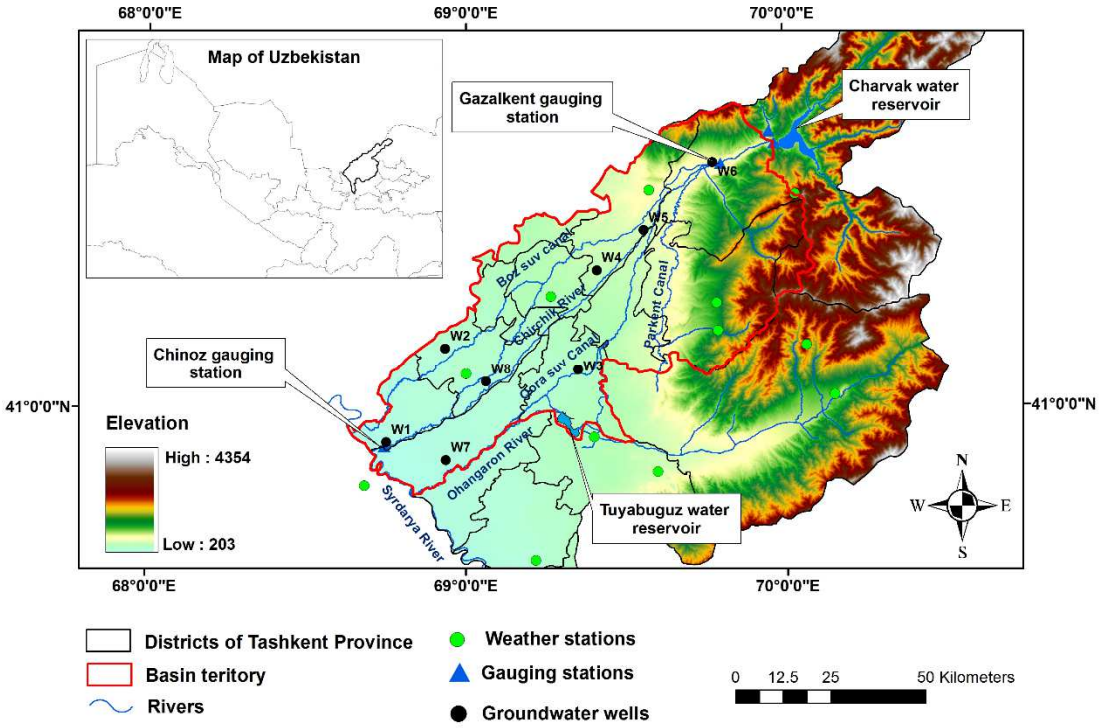

Figure 4.21 Location of gauging stations in Chirchik River Basin

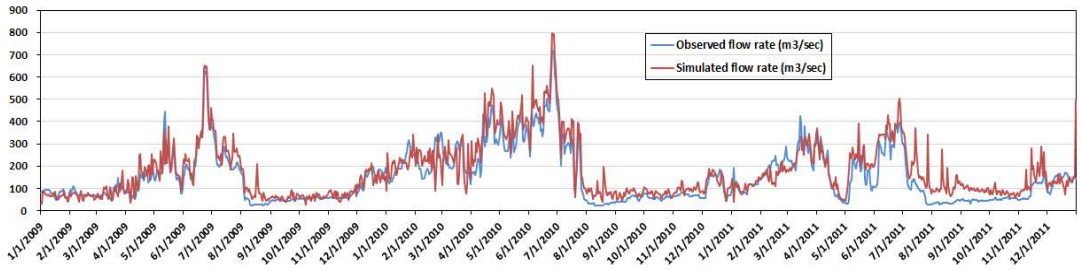

Figure 4.22 Calibration of simulated stream flow in Chinoz gauging station

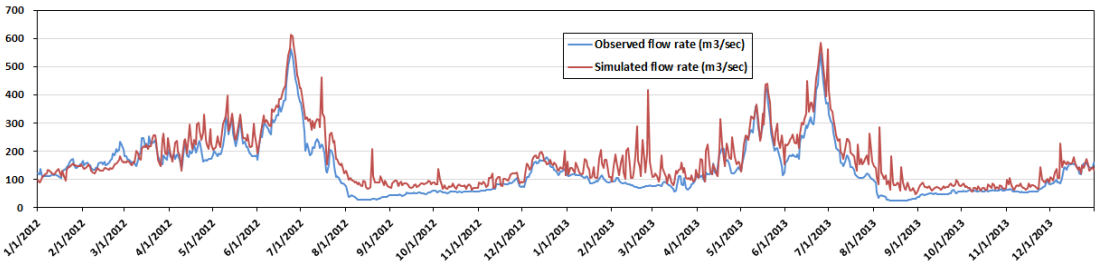

Figure 4.23 Validation of simulated stream flow in Chinoz gauging station

Table 4.8 The performance of streamflow simulation at Chinoz gauging station

Statistical indicators	Calibration Period (2009-2011)	Validation Period (2012-2013)
ME	-42.87	-28.36
MAE	53.83	32.92
RMSE	104.38	45.90
R^2	0.78	0.93
EF	0.22	0.76

Not accounting for the exchange between river water and saturated zone due to insufficient geologic data may also explain this.

4.8 Groundwater dynamics

Simulations of groundwater level dynamics were calibrated and validated against average monthly observed well data for 2009-2011 and 2012-2013 respectively. In this study, data from a total of eight ground water wells was used. These groundwater wells are located at up (W5, W6), middle (W4, W3) and downstream (W1, W2, W7 and W8) sites in the basin. The location of groundwater wells assists appraisal of model performance in different zones. The performance of groundwater simulations are provided in **Tables 4.9** and **Table 4.10**. **Figure 4.24** and **Figure 4.25** shows comparison of observed and simulated groundwater depth. Simulated groundwater dynamics show a satisfactory match with observed data at each location. Hydrographs show the groundwater table reaching its maximum level from April to May, and dropping to minimum levels at the end of September and October. **Figure 4.26** shows estimated groundwater level during May, 2009.

In general, the model underestimated the groundwater level during peak recharge period. All hydrographs show consistent dependence on precipitation in terms of timing and quantity. Simulated groundwater elevations across the middle and downstream sites varied up to an average of 0.66 m during the study period in response to precipitation events. This value was equal to an average of 1.7 m in upstream sites. This shows that the fluctuation amplitude of the groundwater table in upstream sites is relatively higher. Potentiometric surface maps show the general direction of groundwater flows from Northeast to Southwest towards the Syrdarya River. This clearly underlines how groundwater flows contribute hugely to the Syrdarya River through base flows. This is an estimated average of 55 mm/year.

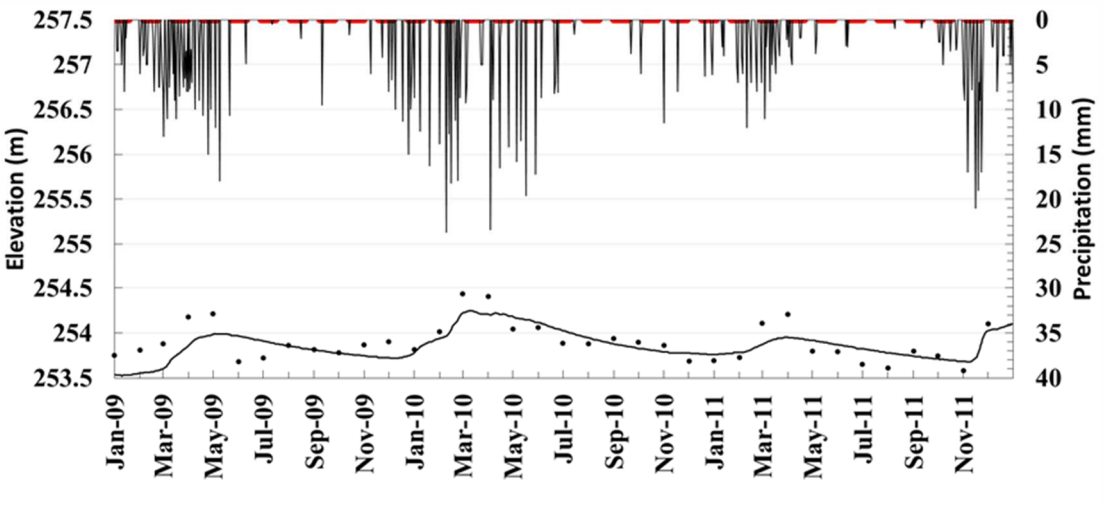

a) Well ID: W1

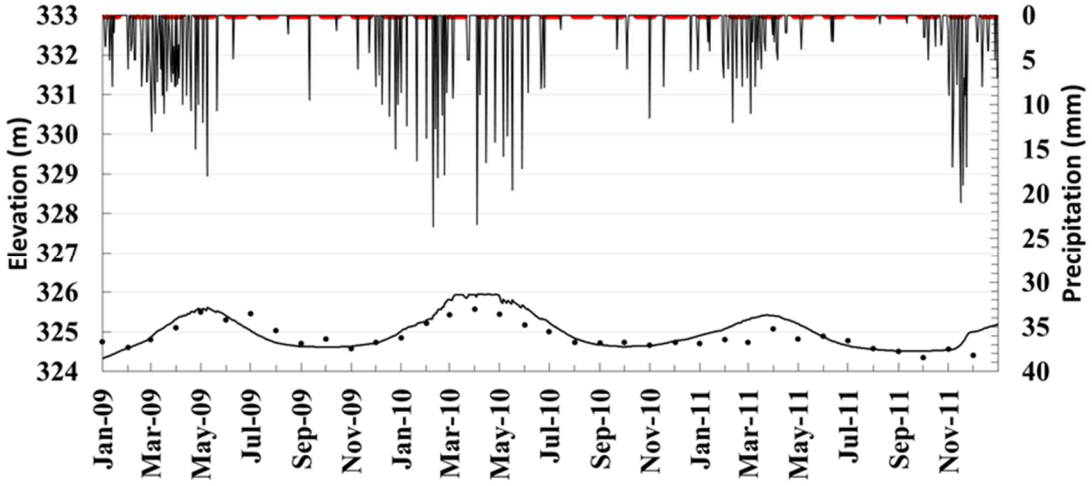

b) Well ID: W2

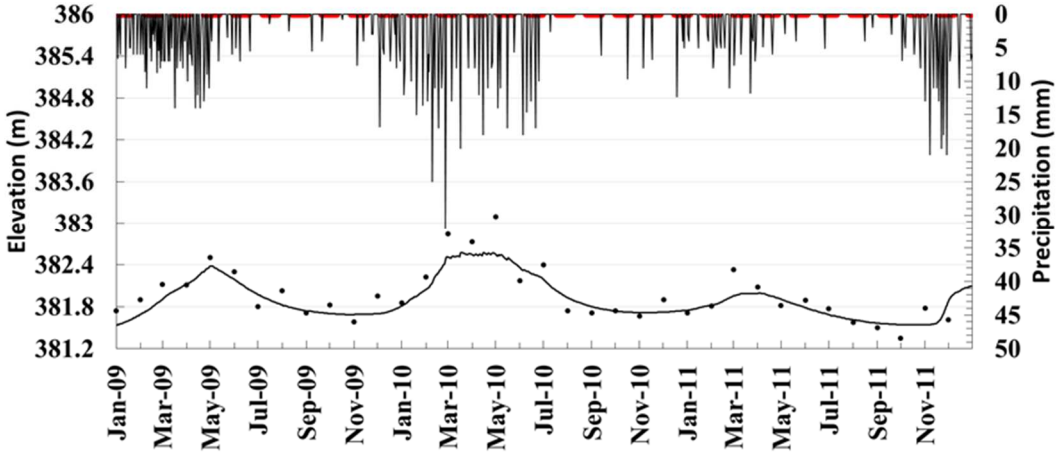

c) Well ID: W3

Figure 4.24 Simulated and observed groundwater level for 2009-2011 (*cont.*)

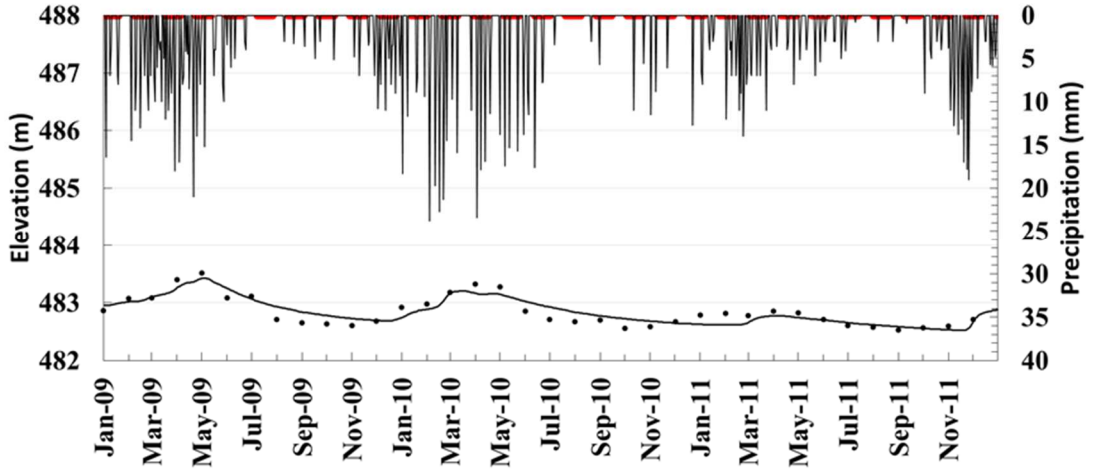

d) Well ID: W4

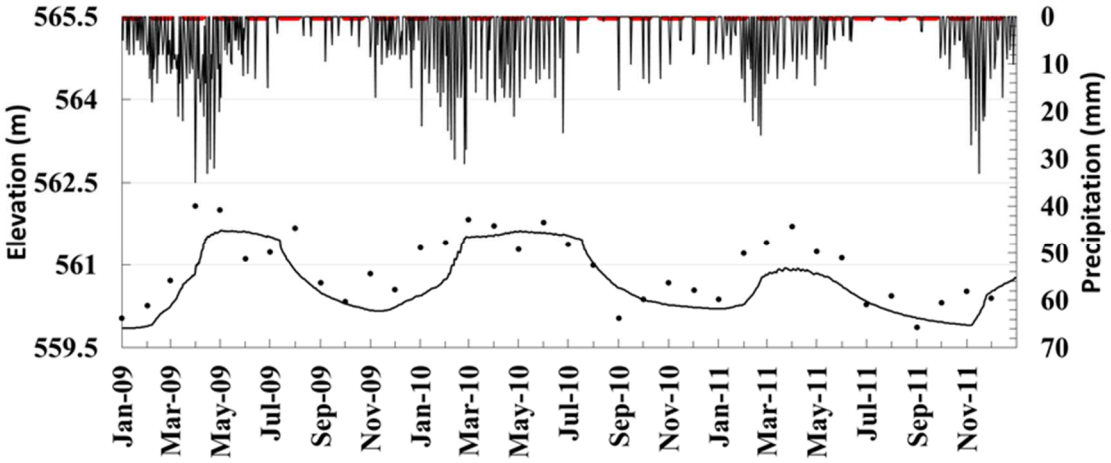

e) Well ID: W5

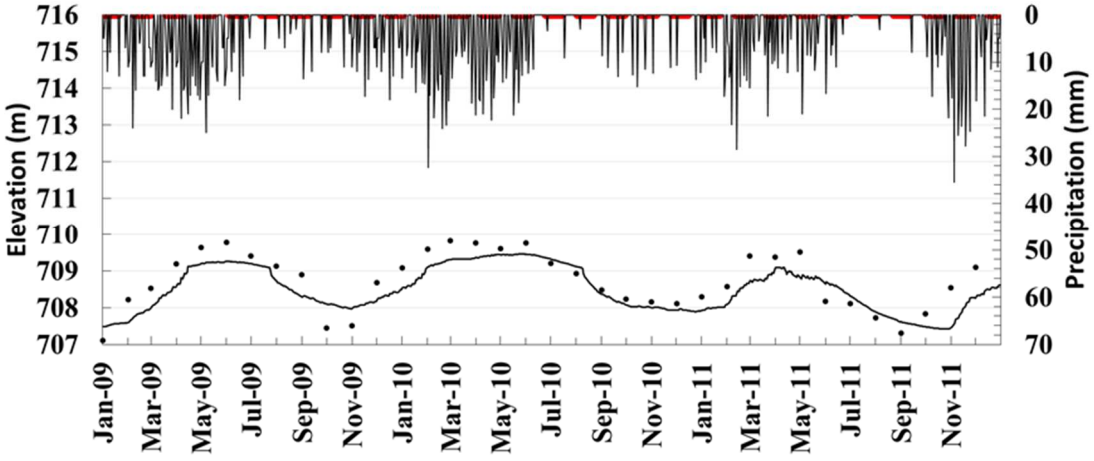

f) Well ID: W6

Figure 4.24 Simulated and observed groundwater level for 2009-2011 (*cont.*)

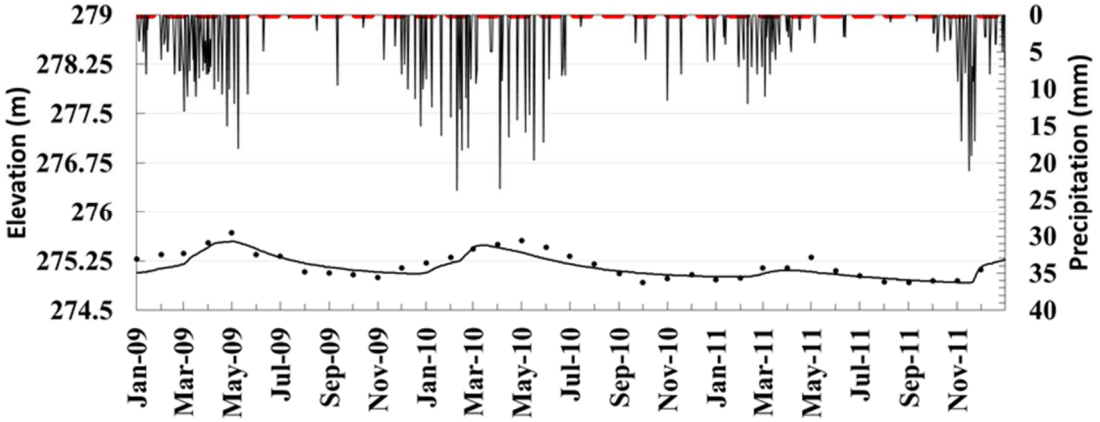

g) Well ID: W7

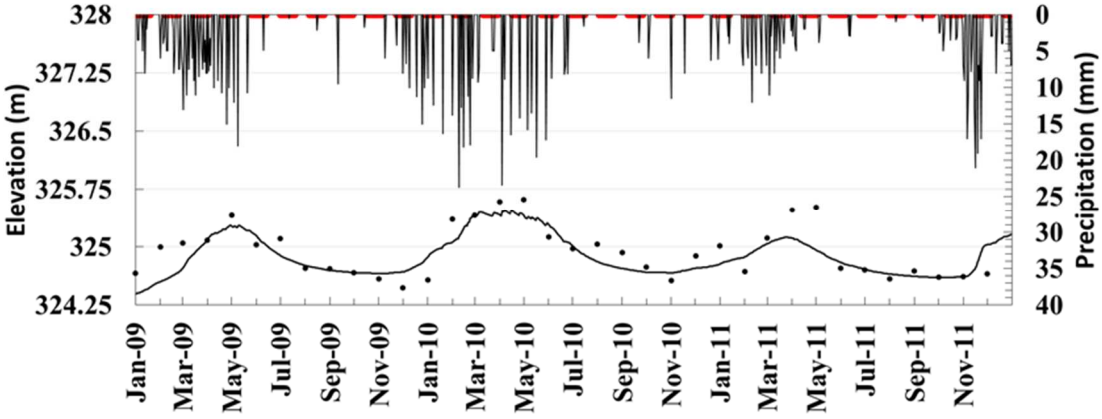

h) Well ID: W8

Figure 4.24 Simulated and observed groundwater level for 2009-2011.

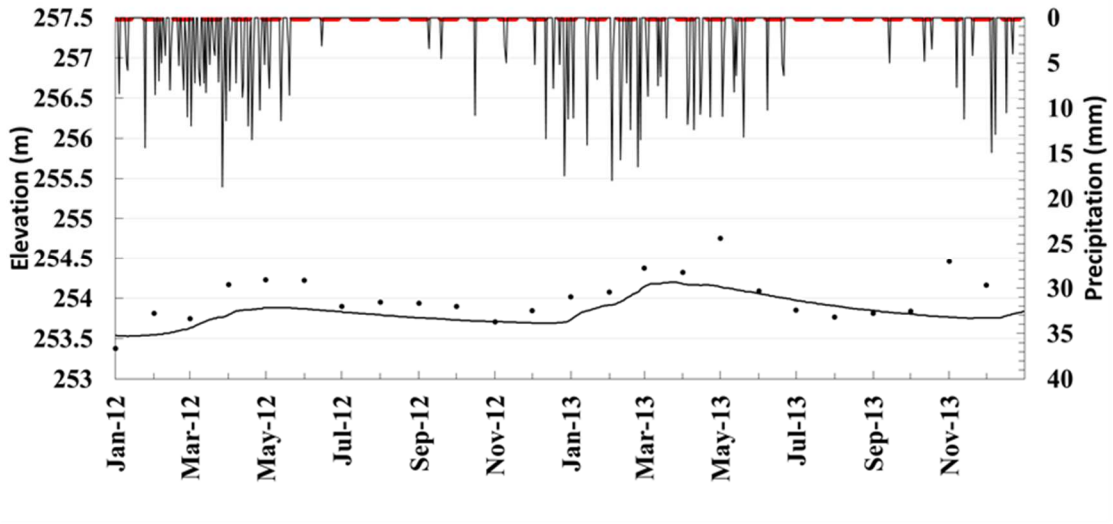

a) Well ID: W1

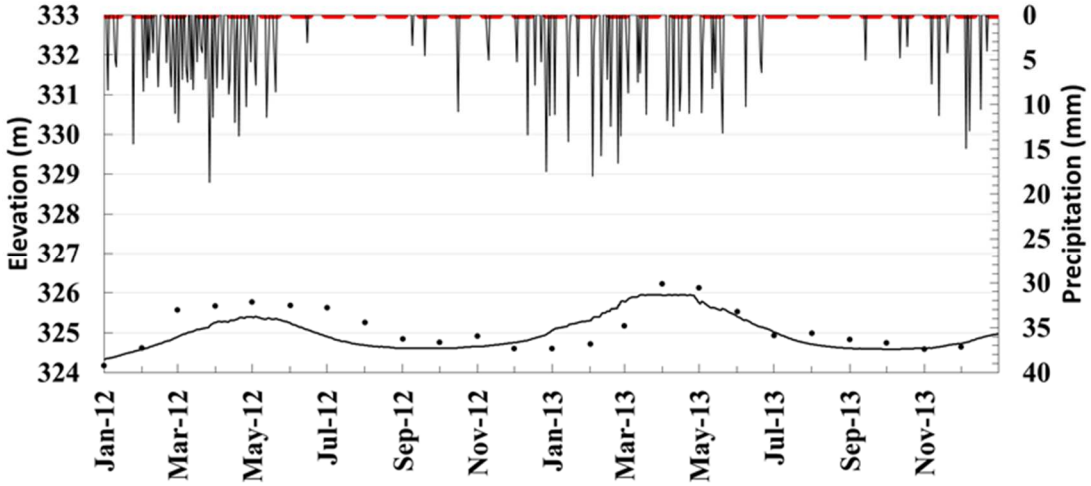

b) Well ID: W2

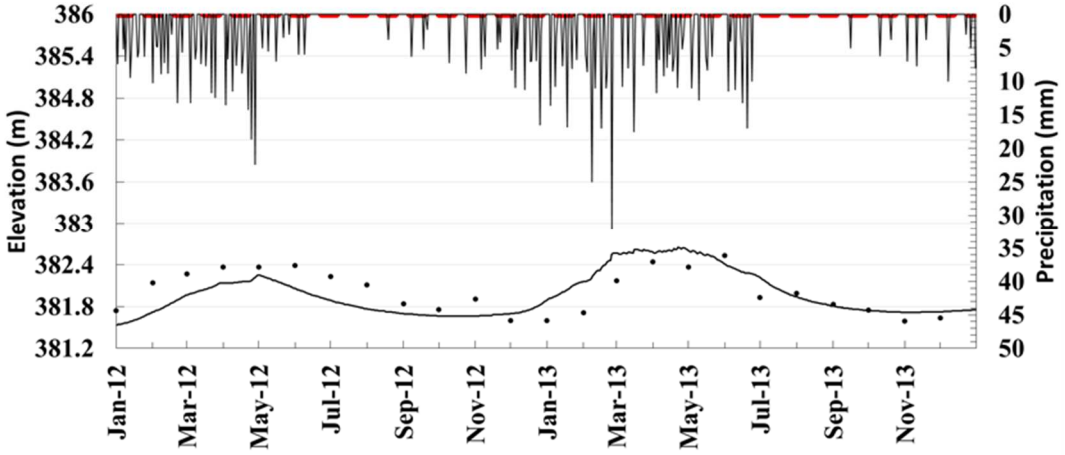

c) Well ID: W3

Figure 4.25 Simulated and observed groundwater level for 2012-2013 (*cont.*)

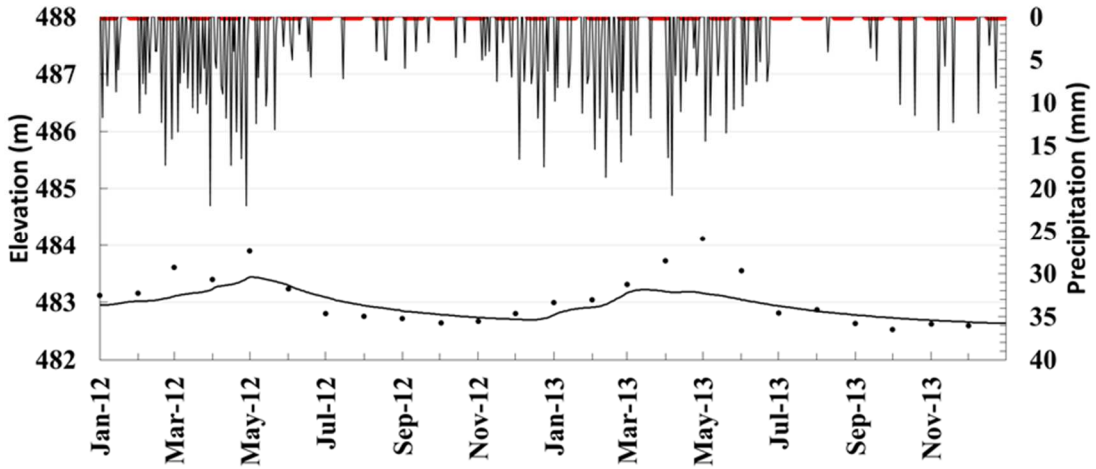

d) Well ID: W4

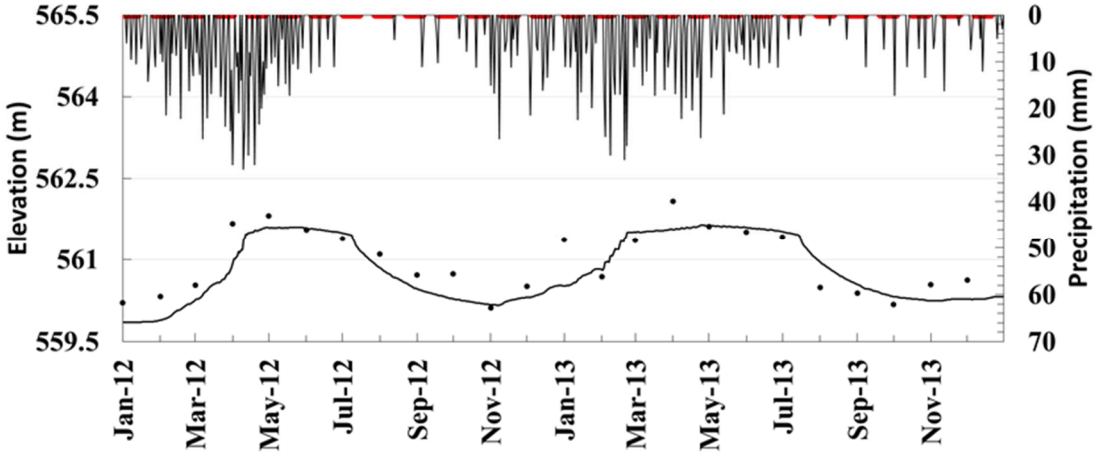

e) Well ID: W5

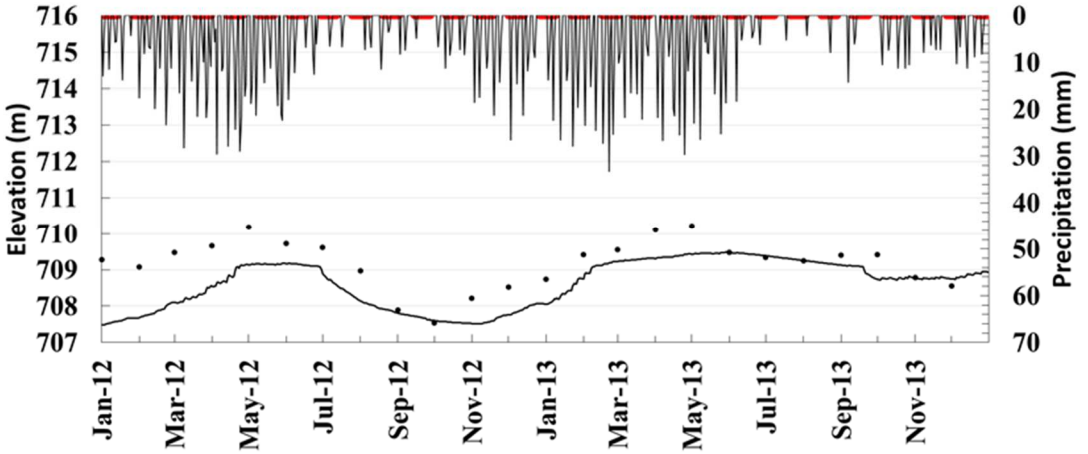

f) Well ID: W6

Figure 4.25 Simulated and observed groundwater level for 2012-2013 (*cont*.)

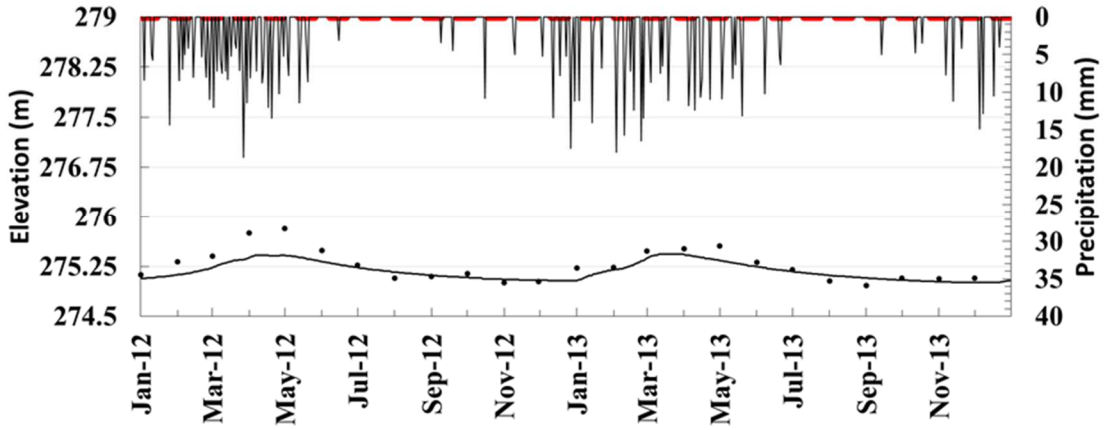

g) Well ID: W7

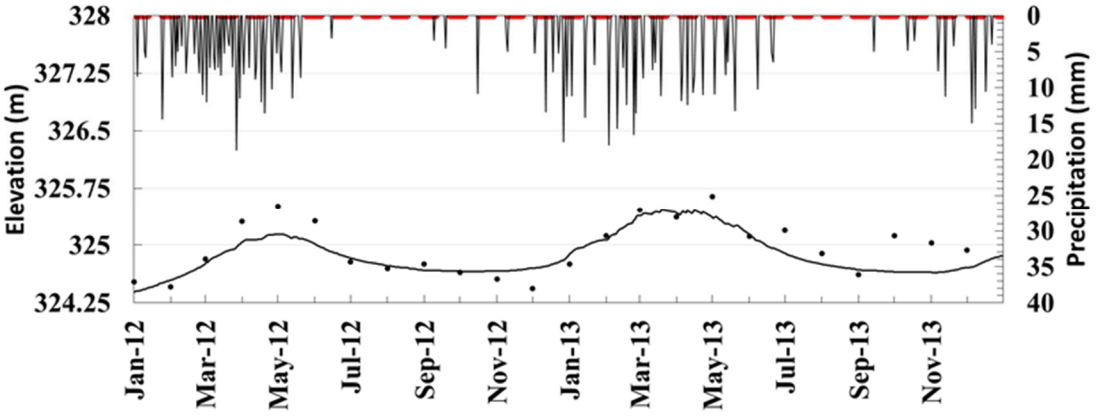

h) Well ID: W8

Figure 4.25 Simulated and observed groundwater level for 2012-2013.

Table 4.9 Calibration results of groundwater simulation

Groundwater well ID	ME	MAE	RMSE	R	EF
W1	0.03	0.13	0.16	0.68	0.42
W2	-0.09	0.20	0.26	0.82	0.30
W3	0.06	0.15	0.19	0.89	0.75
W4	-0.008	0.10	0.12	0.88	0.77
W5	0.78	0.40	0.48	0.77	0.36
W6	0.26	0.42	0.47	0.85	0.61
W7	0.03	0.08	0.10	0.88	0.74
W8	0.01	0.16	0.2	0.78	0.60

Table 4.10 Validation results of groundwater simulation

Groundwater well ID	ME	MAE	RMSE	R	EF
W1	0.18	0.22	0.28	0.67	0.04
W2	0.13	0.31	0.37	0.75	0.50
W3	0.03	0.21	0.25	0.68	0.33
W4	0.05	0.19	0.27	0.81	0.55
W5	0.11	0.26	0.32	0.86	0.65
W6	0.57	0.62	0.78	0.70	-0.28
W7	0.08	0.11	0.15	0.90	0.58
W8	0.04	0.16	0.20	0.84	0.68

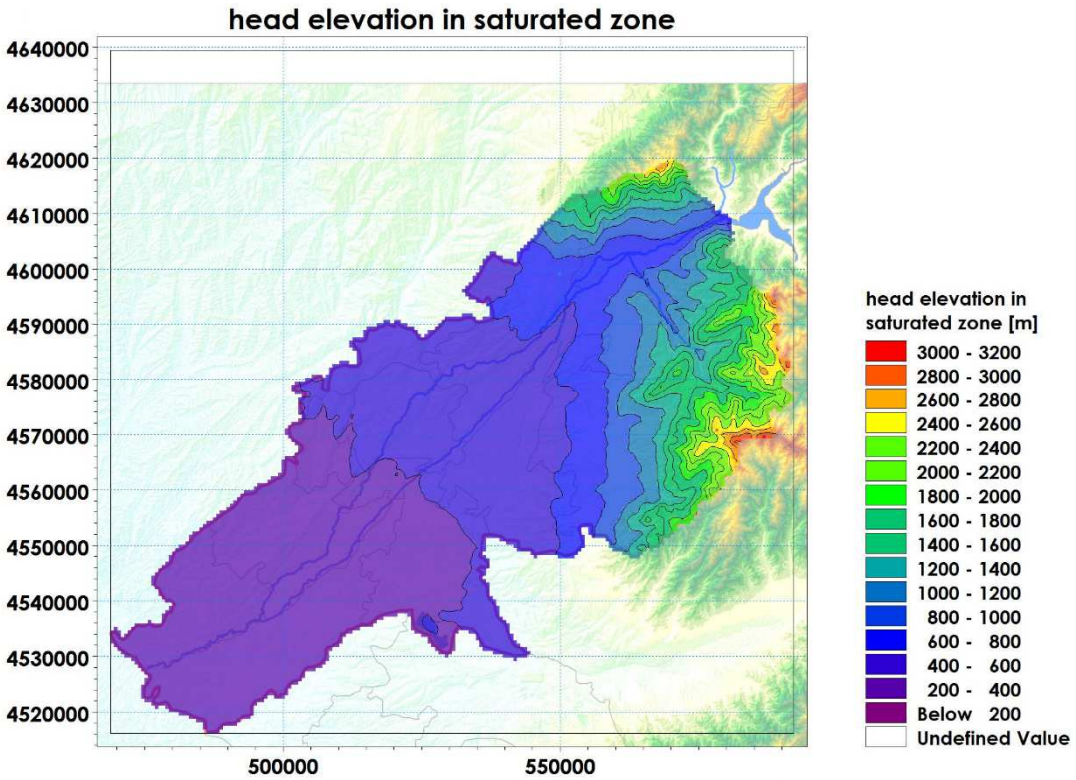

Figure 4.26 Estimated groundwater level during May, 2009

4.9 Water balance results of Chirchik River Basin

The hydrological balance of the Chirchik River Basin is strongly dependent on agricultural activity and the climatic conditions of the basin. The model simulated the main hydrological processes, including evapotranspiration, overland unsaturated and saturated zone storage changes for calibration (2009-2011), and validation (2012-2013) periods.

Table 4.11 shows the contribution of each water balance component in the basin (mm/year). In simulation, precipitation and irrigation water are the main hydrological inputs to the water cycle. The overland water from snow and glacier melting are estimated at around 4% of total income. The results indicate the main proportion of this water was lost through AET during the vegetation period (March-September) due to applied irrigation water.

Total AET was estimated at an average of 821 mm/year. This is corresponds to 77% of the total water budget. The estimated average AET is exceeds around 8% from average annual total precipitation. AET from snow surface was an estimated average of 89 mm/year or 10% of the total average AET. AET is highly variable across the watershed, and it predominantly increases in downstream sites in the basin. This is occurs because PET increases with decreasing elevation (Usmanov et al., 2015). The spatial range of AET is a varied average of 1211-692 mm/year. **Figure 4.27** and **Figure 4.28** show daily spatial distributed AET in irrigation and non-irrigation period respectively. High AET (1211 mm/year) was estimated in downstream irrigation areas. This is almost two times greater than precipitation, and it occurs during non-rainy periods. The high evaporative power of the atmosphere to be compensated by irrigation water.

It should be stated that decreased irrigation water causes of increased aridity in the basin. Simulation shows that the main recharge of groundwater is mainly provided by precipitation and irrigation water. During the study period the total recharges varied between 180-221 mm/year (last row in **Table 4.11**). This ranges between 17 - 20 % of the total income. Groundwater recharge largely occurs from March to May (average 90-60 mm/month) when the amount of rainfall and snow melting increases in middle and downstream sites. In contrast, mountainous area recharge lasts until the end of June, and then starts to decrease, depending on variations in the amount of rainfall. A maximum recharge of 221 mm/year was estimated in 2010, when high amounts of precipitation occurred. The results indicate that in mountainous areas around 51% of total precipitation falls as a snow during the cold season. This proportion equaled an average of 29% in downstream sites.

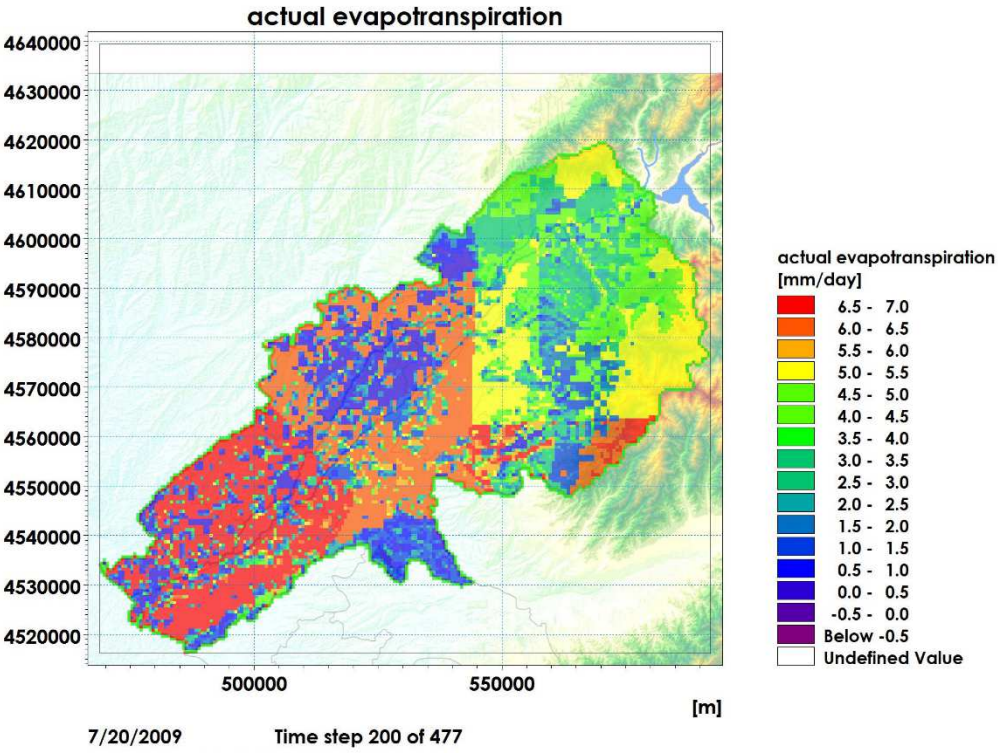

Figure 4.27 Daily spatial distributed AET in irrigation period

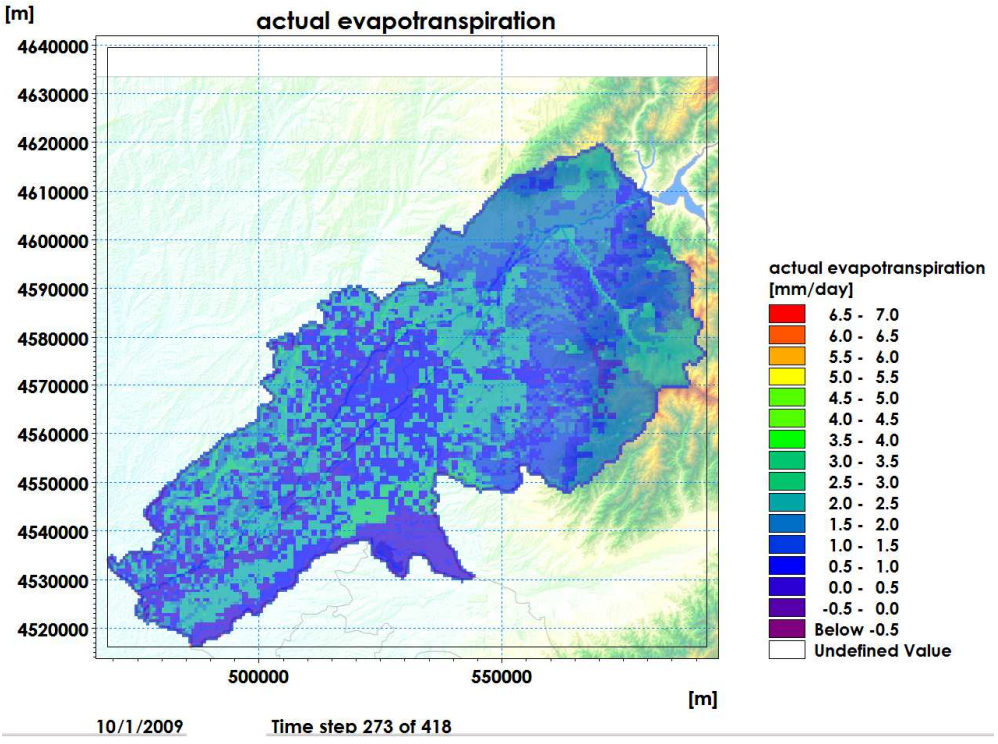

Figure 4.28 Daily spatial distributed AET in non-irrigation period

Snow storage mainly occurs from December to the end of February. Additionally, the results indicate overland flow peaks in mountainous areas of the basin in spring and fall with seasonal heavy rains and the beginning of snow melt on low infiltration ground surfaces. Snow pack melt-water contributed an average of 34% of total overland flows. In this way, overland flow substantially feeds the source of the Chirchik River. This amount is an estimated average of 77 mm/year, which is 3% of the average total of precipitation. A small amount of water outflows from the basin boundary, particularly from downstream sites. This is an estimated average of 89 mm/year, or 4% of total precipitation. The overall water balance error was averaged at 2% and 3% during the calibration and validation period. This shows incoming and outgoing water balance parameters were well satisfied. **Figure 4.29** and **Figure 4.30** show spatial distributed water balance error in calibration and validation periods respectively.

Table 4.11 Contribution of hydrological parameters to water balance

Hydrological Parameter	Calibration		Validation			Average	Water
	2009	2010	2011	2012	2013		
	mm	mm	mm	mm	mm	mm	%
Precipitation	-803	-720	-662	-848	-750	-757	-71
Irrigation	-279	-282	-310	-346	-364	-316	-29
Snow storage change	-5	-20	-12	-23	-10	-14	-1
UZ-storage change	-7	-26	-0	-17	-8	-14	-1
ET	770	854	777	845	860	821	77
OL-storage change	61	0	15	61	30	33	3
OL-boundary outflow	56	111	62	54	151	87	8
OL-flow to river	66	91	50	59	118	77	7
SZ-storage change	143	-38	112	204	-34	77	7
Total error	2	-30	22	-11	-7	-5	0
Recharge	143	105	218	204	171	168	16

UZ, unsaturated zone; ET, evapotranspiration; OL, overland flow; SZ, saturated zone

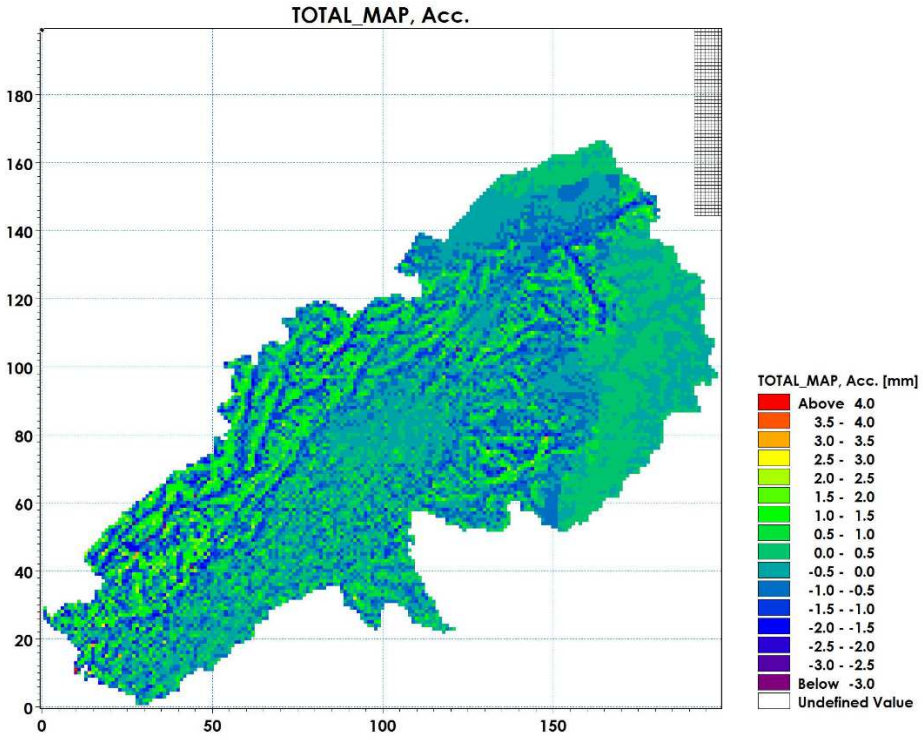

Figure 4.29 Average water balance error in calibration period (2009-2011)

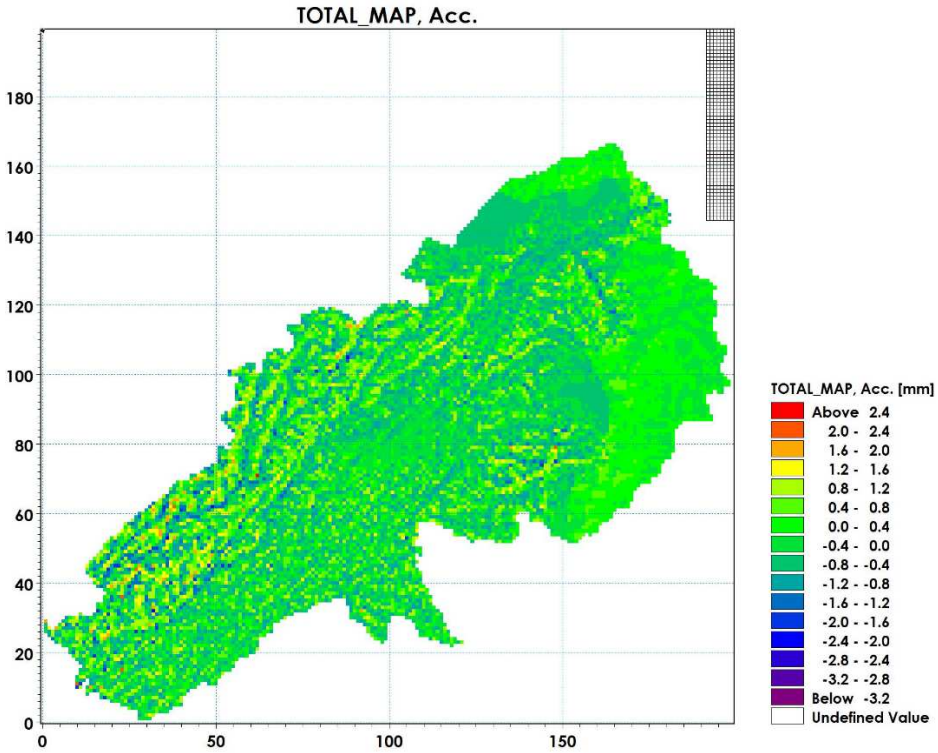

Figure 4.30 Average water balance error in validation period (2011-2012)

4.10 Conclusions

The MIKE SHE integrated hydrological model was used to study the hydrological balance of the CRB. The model was constructed with several assumptions when preparing the geospatial data set of unsaturated and saturated zones, and climate and land use parameters. This hydrological study of the CRB allows for the following main conclusions:

I. MIKE SHE as a physical-based mathematical model uses a large number of hydrological parameters. All need to be adjusted to the climatic conditions of the study area to reach satisfactory results that correspond to reality.
II. Evapotranspiration was found to be the main water loss factor among water balance components, with an average of 821mm/year (77% of total water budget). As an arid land, AET is strongly dependent on irrigation water quantity irrespective of rainfall in downstream sites.
III. AET is highly variable across the basin, with increases toward to downstream sites. The estimated AET in irrigation areas at downstream sites was almost two times higher than upstream sites. Therefore decreased irrigation water causes increased aridity, particularly in downstream site.
IV. Estimated groundwater recharge varied between 180-221 mm/year, making up 17-20% of the total water budget. The highest groundwater recharge occurs from March to May with an average of 90-60 mm/month.
V. The general direction of groundwater flow is toward the Syrdarya River. Base flow from basin boundary into the Syrdarya River was estimated at an average of 55 mm/year.
VI. The Chirchik River is gaining upper stream sites by overland flow on average 77 mm/year.
VII. The main water balance error was obtained from simulated overland flow. Adjusting the climate parameters of the model to the basin environment optimises this. The overall water balance error estimated a 2.5% average, which demonstrates that interacting hydrological components and parameters are well matched.
VIII. Accurate irrigation schedule and operational information of hydro-engineering structures are critical model inputs in order to improve daily streamflow simulation and minimize numerical errors.
IX. This study confirmed that in arid and semi-arid regions with intensive agricultural, integrated modelling is valuable for understanding water cycles in large basins.

4.11 References

Chanisheva, S. and Smirnova, E: Climate Characteristics of Tashkent Province. Uzhydrometeorological Bureau Press., Tashkent, Uzbekistan (2011).

DHI, MIKE SHE User's Manual, Volume 1 and 2: An Integrated Hydrological Modelling Framework (2012).

Fetter, C., Applied Hydrogeology, Fourth edition by Prentice-Hall, Inc, p33-37 (2001).

FSI. 2003. The State of Forest Report. Forest Survey of India, Ministry of Environment and Forests, Dehradun, India.

Graham, D. and Butt, M. Watershed Models: Flexible integrated watershed modelling with MIKE SHE. Taylor and Francis Group Press., Boca Raton, Florida (2005).

Jain, S.K., Storm, B., Bathurst, J.C., Refsgaard, J.C. and Singh, R.D. Application of the SHE to Catchments in India 2. Field experiments and simulation studies with the SHE on the Kolar subcatchment of the Narmada River. Journal of Hydrology 140, 25-47 (1992).

Makhmudov, E. Rahimov, Sh., Chen, S. and Tzilili: Water Resources and Its Utilization in Uzbekistan. Pliograf Group Press., Tashkent, Uzbekistan (2013).

McMichael, C E., Hope, A.S. and. Loaiciga, H.A. 2006. Distributed hydrological modelling in California semi-arid shrub lands: MIKE SHE model calibration and uncertainty estimation. Journal of Hydrology 317. 307–324 (2006).

Nash, J. and Sutcliffe, J: River flow forecasting through conceptual models. Journal of Hydrology, 10, 282-290 (1970).

Refsgaard, J.C. and Storm, B: MIKE SHE. In: Singh, V.P. (Ed.), Computer Models of Watershed Hydrology.Water Resource Publications, CO, USA, 806-846 (1995).

Singh Rajagopal: Hydrological and hydraulic modelling for the restoration and management of Loktak Lake, Northeast India. Doctoral thesis, UCL (2010).

Suva Shakya: Use of MIKE SHE for Estimation of Evapotranspiration in the Sprague River Basin. Doctoral thesis, Oregon State University (2007).

Usmanov, S., Yasuhiro, M. and Tetsuya, K: Evaluation of Interpolation Methods for Spatial Modelling of Refer-ence Evapotranspiration Using Modified Hargreaves Equation. Journal of Arid land Studies, 25, 141-144 (2015).

Van Genuchten, M: A closed form equation for predicting the hydraulic conductivity of unsaturated soils. Soil Sci. Soc. Am. J. 44: 892–898 (1980).

Vázquez, R.F., Feyen, L., Feyen, J. and Refsgaard, J.C. Effect of grid size on effective parameters and model performance on the MIKE SHE code, in Hydrological Processes v16, 355-372 (2002).

Xu Yang and Xueyi You: Estimating Parameters of Van Genuchten Model for Soil Water Retention Curve by Intelligent Algorithms. Inf. Sci. 7, No. 5, 1997-1983 (2013).

WISA. 2005. Conservation and management of Loktak Lake and Associated Wetlands Integrating Manipur River Basin: Detailed Project Report. Wetlands International-South Asia, New Delhi, India.

.

Chapter 5: Integrated Approach to Detect the Spatial and Temporal Variation of Groundwater Level in Quyi Chirchik District, Uzbekistan

5.1 Introduction

This chapter focuses the development of a new method to spatial detection of high groundwater table area and subsequent application for water balance studies in an irrigation dominated districts. In this study distributed hydrological model was applied to develop a hydrological model of Quyi Chirchik district. MIKE 11 model was used for simulation of irrigation channel flow and water releases to irrigate fields. The model parameters were successful calibrated using observed groundwater well data for 2009-2011. The model then validated for 2012-2013 using well-tuned model parameters. After successful calibration, the model produced integrated and fully distributed hydrological model of the study area. Using the model results and Arc GIS tools, the shallow and low groundwater level were spatially detected and its contribution to other hydrological parameters were examined. In general, this chapter demonstrates the applicability of the new method and its inputs to the water resources management in arid areas.

The Water Quality Index (WQI) method has been applied to assess ground water quality status in Quyi Chirchik district. The research also studies the relationship between spatial and temporal variation of groundwater level and salinity. A total of twelve shallow ground water samples was collected from the study area and its physico-chemicals properties were analyzed.

5.2 Problems in groundwater management

The Quyi Chirchik is one of the downstream districts of Tashkent Province (**Figure 5.1**). In Quyi Chirchik, district one of the most subjected issues are salinization of irrigated lands, increasing groundwater mineralization and raising the groundwater table (Rakhmatullaev et al., 2013). The salinization and soil degradation lead to reduced crop yields. The loss of productivity is managed by the extensive use of fertilizers. The soil salinity is reduced by leaching process. As a result the groundwater table depth has reached to 2-3 meters in irrigated areas. In extensive leaching irrigated lands groundwater table depth has passed from critical points which is 1-2 meters. The level of Total Dissolved Solids (TDS) is measured more than 1000 mg/l in 32 % of irrigated lands. The value of TDS has observed more than 1300 mg/l in areas where groundwater is most close to the ground surface (JICA. 2010). Accumulation of water in the subsurface from irrigation and a leaching process make clear the reason of the groundwater table rise, but the spatial variation of groundwater quality depending on groundwater table has not been studied sufficiently. Moreover, over polluted groundwater is not considered as a usable resources anymore. On the contrary, it harms ecosystems and brings economical ecological damages. Shallow groundwater quality is most sensitive and strongly depends on land use activities in the region.

Therefore, develop the countermeasures and study the spatial variations of groundwater are one of the important tasks of water resources management in the district (Makhmudov et al., 2013). Over the years, various models have been developed for modeling groundwater flow and its spatial characteristics under various condition. MIKE SHE fully distributed hydrological model have been used widely by many researchers to study the spatial and temporal variation of groundwater dynamics (Foster et al., 2015; Singh et al., 1998). Compared with other conventional methods, the model has the advantage of fully integrating the surface, subsurface, irrigation process and their interactions in hydrological simulation (Fatema et al., 2012; Golmar et al., 2014). Therefore the objectives of this study were to develop an integrated hydrological model for Quyi Chirchik district and to investigate spatiotemporal variations of groundwater depth. Then the model results were used to study the formation of salinity of origin and assess water quality index of groundwater in Quyi Chirchik district (WQI) (Horton. 1965). The research also studies the relationship between spatial and temporal variation of groundwater level and salinity.

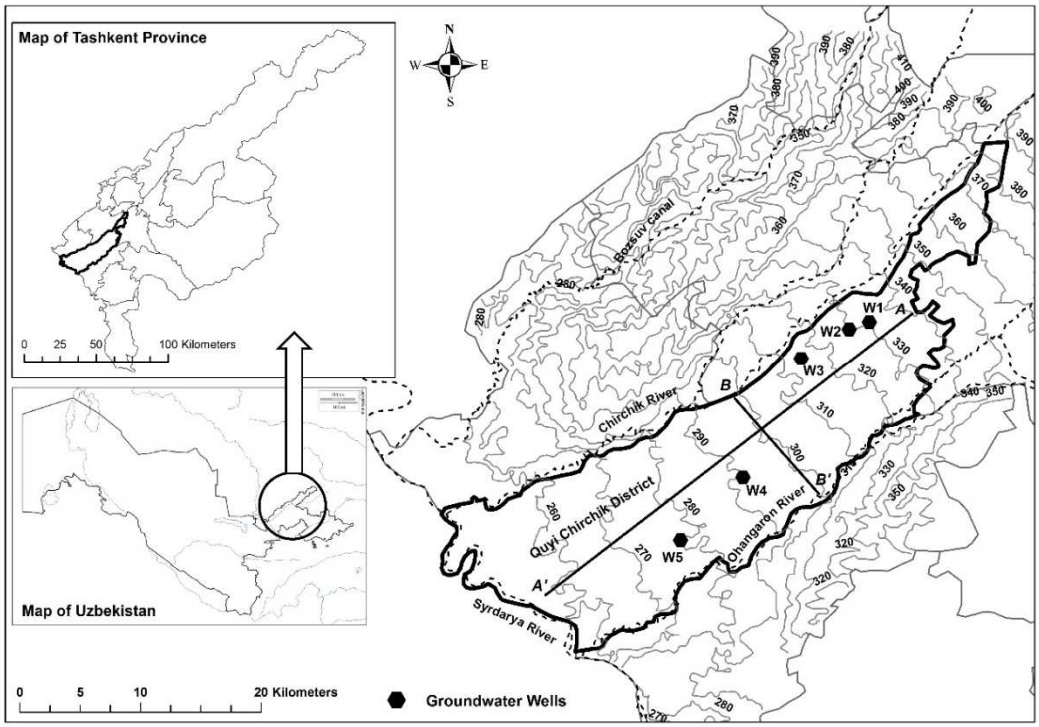

Figure 5.1 Location of Quyi Chirchik district in Tashkent Province, Uzbekistan

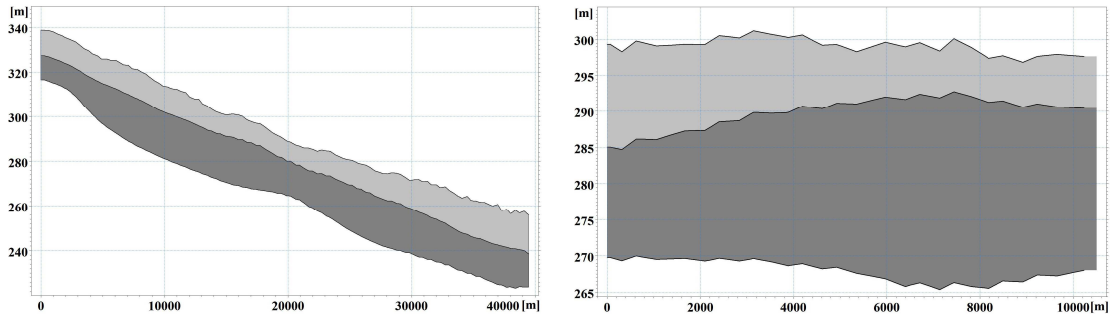

a) A-A^{I} b) B-B^{I}

Figure 5.2 Hydrogeological cross-section of Quyi Chirchik district

5.3 Hydrological model development

The Quyi Chirchik district is 560 km^2 and located between the Chirchik and Ohangaron rivers in downstream site in Tashkent Province (**Figure 5.1**). The district has a population of around 100 thousand people. The climate is continental arid with mean yearly precipitation is 250-300 mm. The average yearly potential evapotranspiration is 800 mm. The summer is long dry with an average 26-27^o C temperature. In winter temperature is around 1.5^o C (Chanisheva et al., 2011). The topography is almost plain and varies from 300 to 200 meters. The average 68% area of the district is irrigated lands. Every year average 283 million m^3 are used for irrigation. The alluvial soil type is dominant in the district. The thickness of the soil layer may vary from 4 m to 13 m. The beneath the soil lies Quaternary unconsolidated sediments consisting mainly of boulder-pebble and gravel-conglomerates. The depth of the second layer ranging between 5-25 meters. The hydraulic connection is good between the first and second layers because they are all unconfined aquifers. The high groundwater table became one of the main problems of the district. A lot of shallow aquifer salinized or involved into salinization process. Salinization results from agricultural practices but is also related to the sodic nature of soil like solonetz and solontchaks.

The MIKE SHE integrated hydrological model uses a spatially distributed hydrological parameters of topography, soil, geology, land use, climate and initial groundwater table data. These parameters were prepared with the ArcGIS 10.2 platform and discretized to 500 x 500 meter mesh format. Digital elevation model of the study area was obtained from the Shuttle Terrain Mapping (SRTM) of the US Geological Survey. All these geospatial data were projected to Quyi Chirchiq's coordinate system (WGS84 UTM 42N). The development of geospatial model parameters is described in detail in chapter 2 and 3.

In this research two geological layers were considered in the simulation process. The first is a surficial soil layer. The second geological layer is the Quaternary unconsolidated sediments. The geological cross-sections of these layers are presented in **Figure 5.2** (location of sectional lines is given in **Figure 5.1**). The total 4 soil types were identified in the district (**Figure 5.3)**. This figure shows most dominated soil type is old irrigated alluvial grey. This soil type is covered most of the agricultural lands. The spatial distributed depth of the first and second layer were generated by Kriging interpolation methods using data from the 8 boreholes (**Figure 5.4** and **Figure 5.5**). Hydrogeological parameters of analytical layers are given in **Table 5.1**. Development of spatially distributed initial potential head (**Figure 5.6**) and other parameters were described in

chapter 3. The calculation method and scheme of hydrological balance and parameters were conducted same as Chirchik River Basin. The detail information of integrated hydrological methods and equations is provided in Chapter 2 and chapter 3.

A land use map was obtained from multi band satellite image (Advanced Visible Near Infrared Radiometer) of the study area using a supervised classification method in ArcGIS 10.2. The cadastral map was used to correct the primary land use map. The land use of the basin has been classified as agriculture, arable lands, grassland urban and water body (**Figure 5.7**). The values of seasonal changes of leaf area index (LAI) and root depth (RD) data were obtained from the Institute of Water Problems of Uzbekistan, and assigned to each land use class. The values of LAI and RD parameters were given in chapter 3. The single weather station data were used in this study and potential evapotranspiration (PET) was calculated using the modified Hargreaves model. The PET (**Figure 5.8**) and daily-accumulated precipitation data (**Figure 5.9**) were uniformly distributed over the study area.

The agricultural sector of the Quyi Chirchik district is strongly depends irrigation waters which are 95 % derived from Chirchik and Ohangaron Rivers. The district has an around 35000 ha. The irrigation standard is average 5000 m^3/ha and irrigation is conducted 5 times in irrigation period. The sequence and quantity of irrigation are based on local standard of Quyi Chirchik district. The irrigation quantity for 2009-2013 is given in **Table 5.2**. The four main irrigation channels serve in agricultural areas. The stream flow of irrigation channels is simulated using MIKE 11 model package and coupled with an integrated hydrological model of Quyi Chirchik. The irrigated area and channels of the MIKE 11 model are shown in **Figure 5.10**.

Table 5.1 Hydrogeological parameters of Quyi Chirchik district

Hydrogeological Parameters	**Layer 1**	**Layer 2**
Thickness (m)	4-22	5-25
Material	Soil	Boulder-pebble and gravel-conglomerates
Type	Shallow aquifer	Quaternary unconsolidated sediments
Horizontal hydraulic conductivity (m/s)	$0.317*10^{-5}$ - $0.413*10^{-3}$	$1.1*10^{-5}$
Vertical hydraulic conductivity (m/s)	$0.\ 34*10^{-6}$ - $0.21*10^{-3}$	$1.3*10^{-6}$
Storage coefficient	0.0098-0.00023	0.001

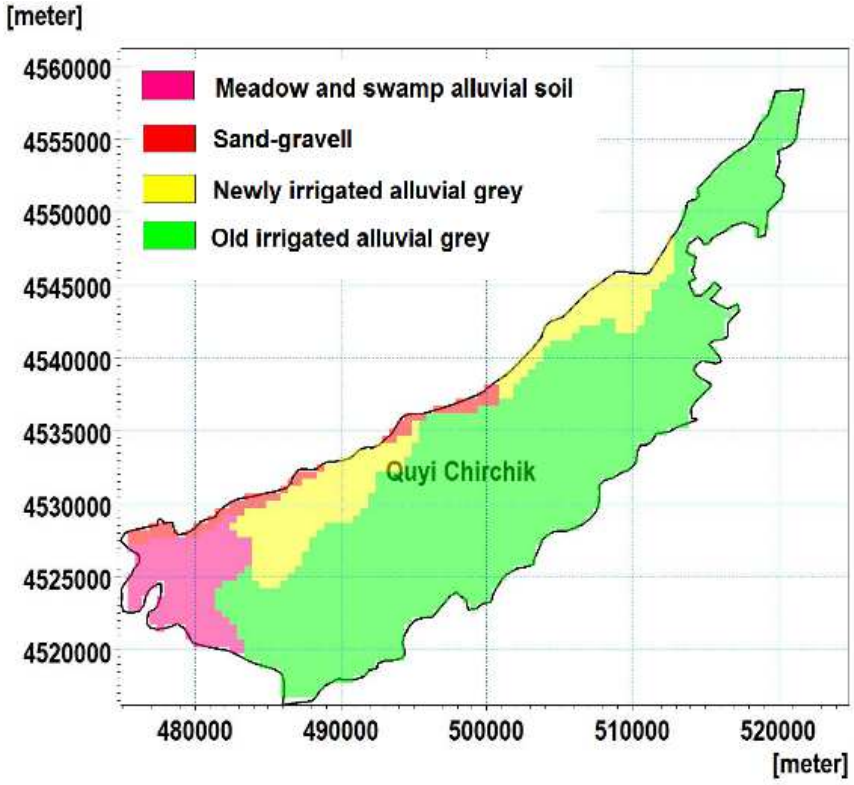

Figure 5.3 Soil types of Quyi Chirchik district

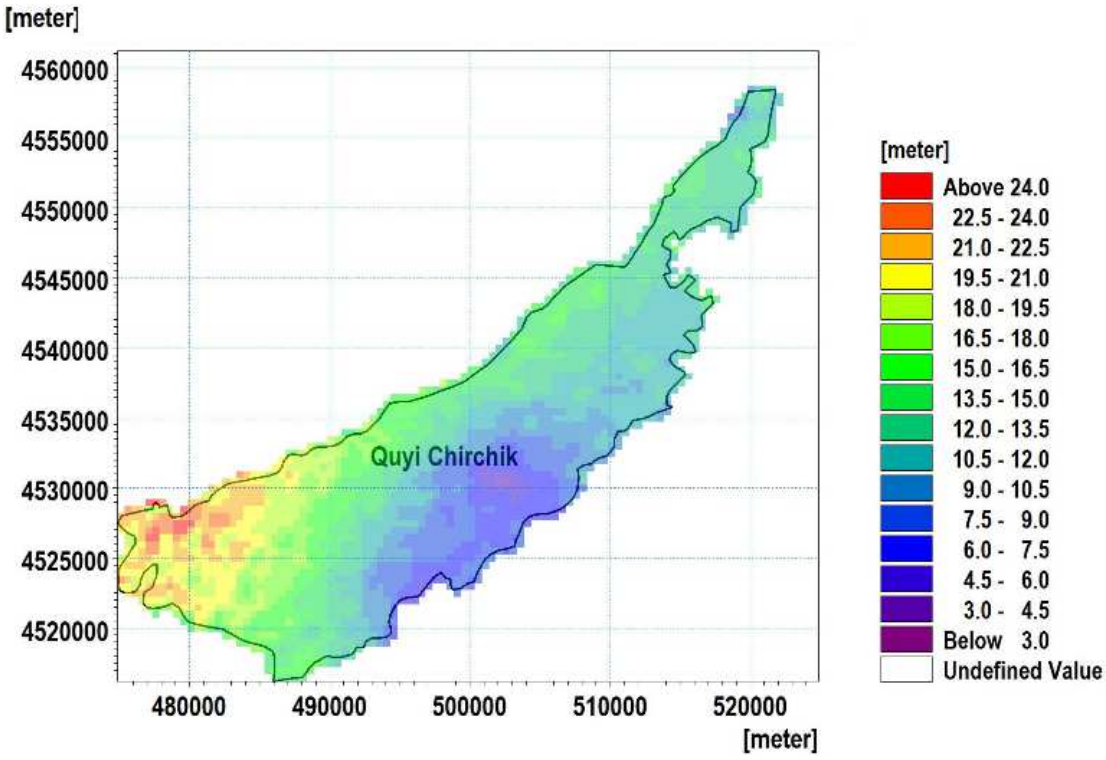

Figure 5.4 Soil depth of Quyi Chirchik district

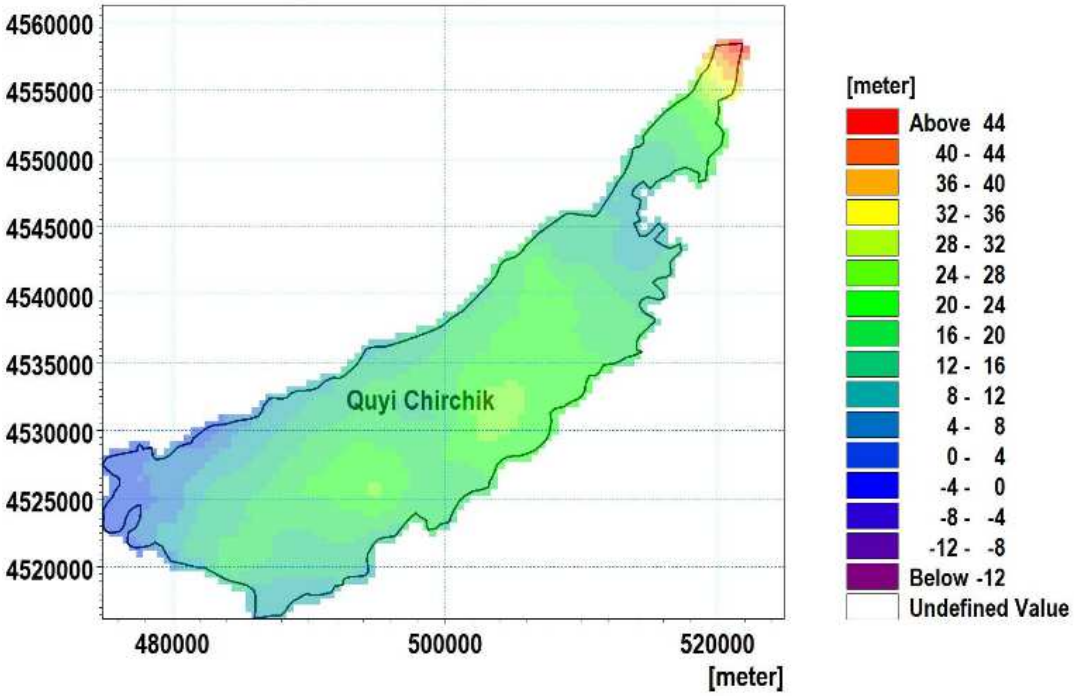

Figure 5.5. Unconsolidated layer depth of Quyi Chirchik district

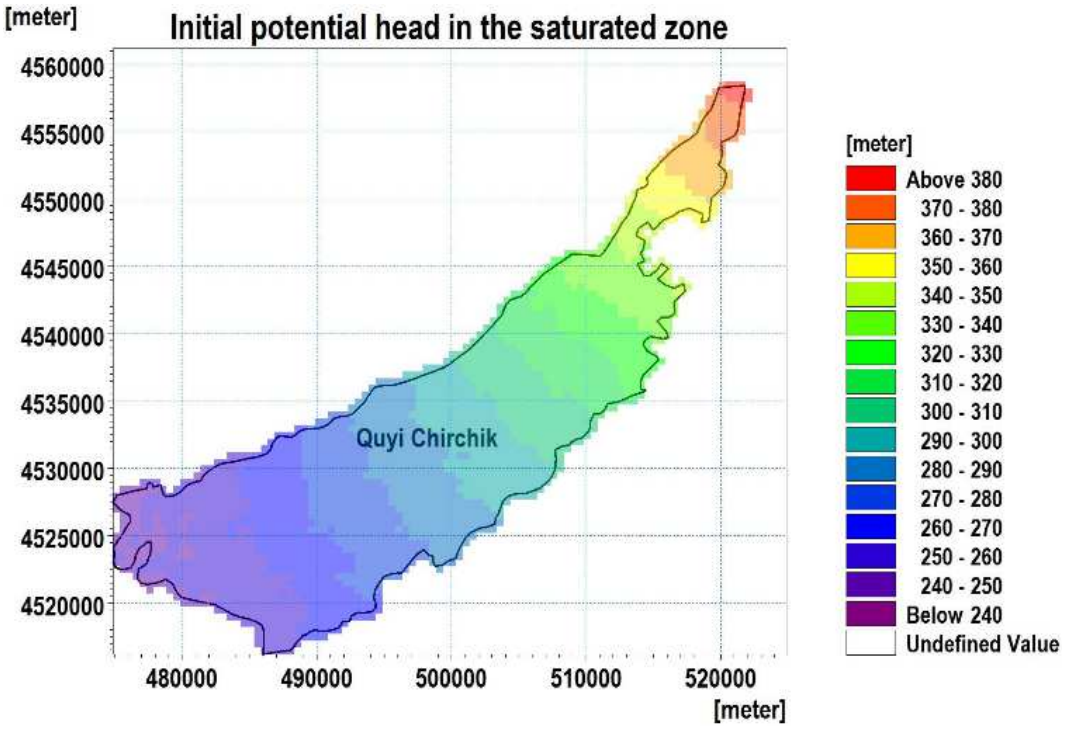

Figure 5.6. Initial groundwater depth of Quyi Chirchik district

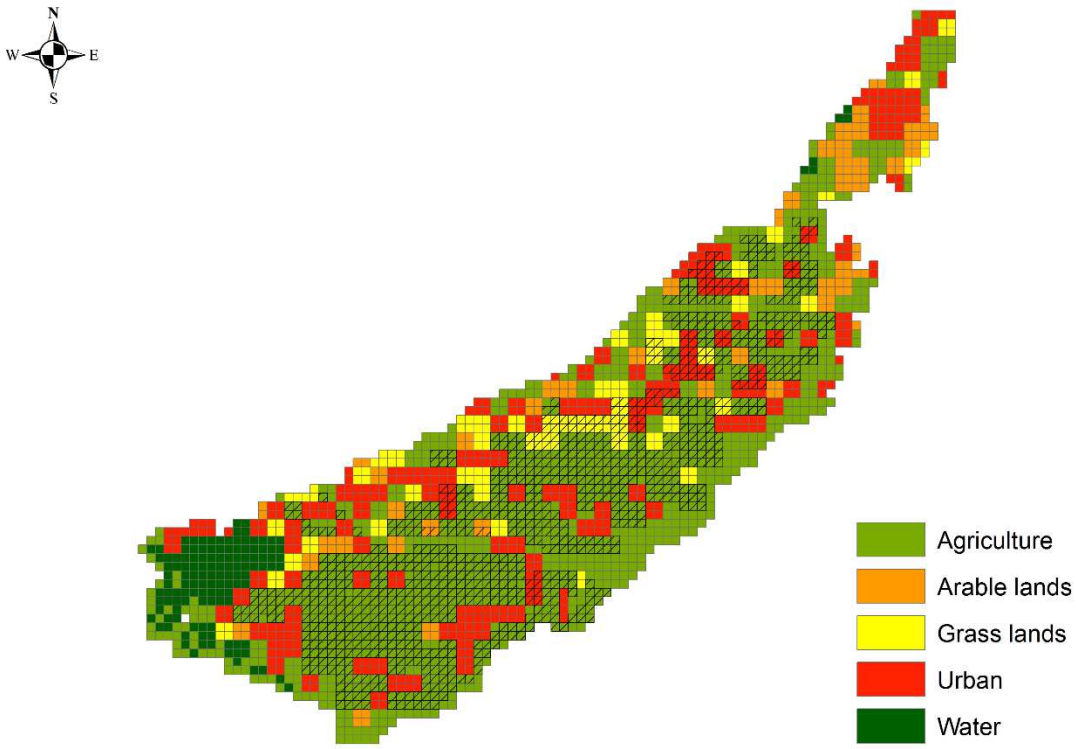

Figure 5.7 Land use map of Quyi Chirchik district

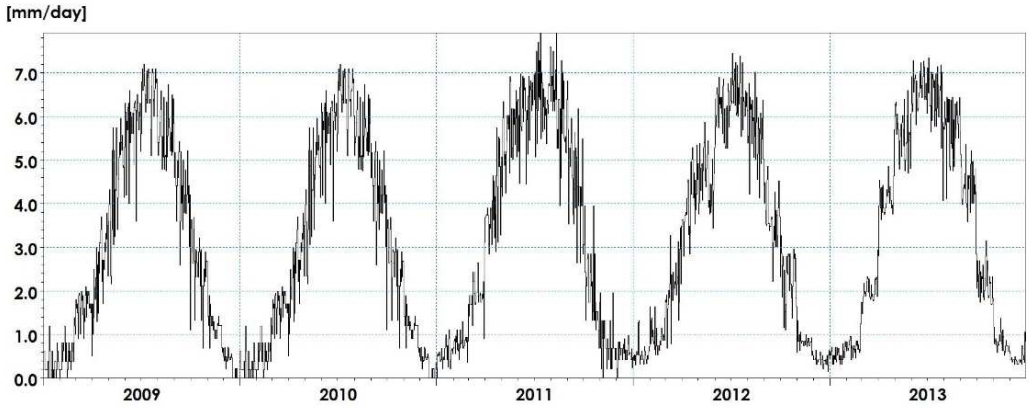

Figure 5.8 Potential evapotranspiration of Quyi Chirchik district

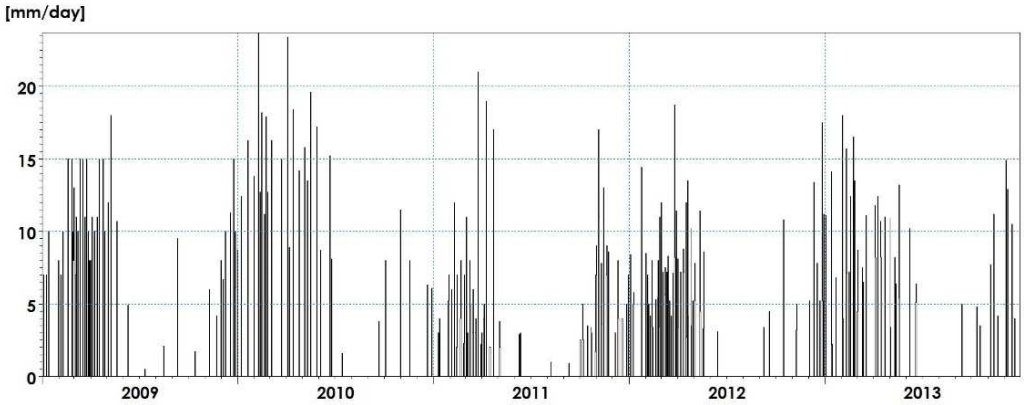

Figure 5.9 Daily precipitation of Quyi Chirchik district

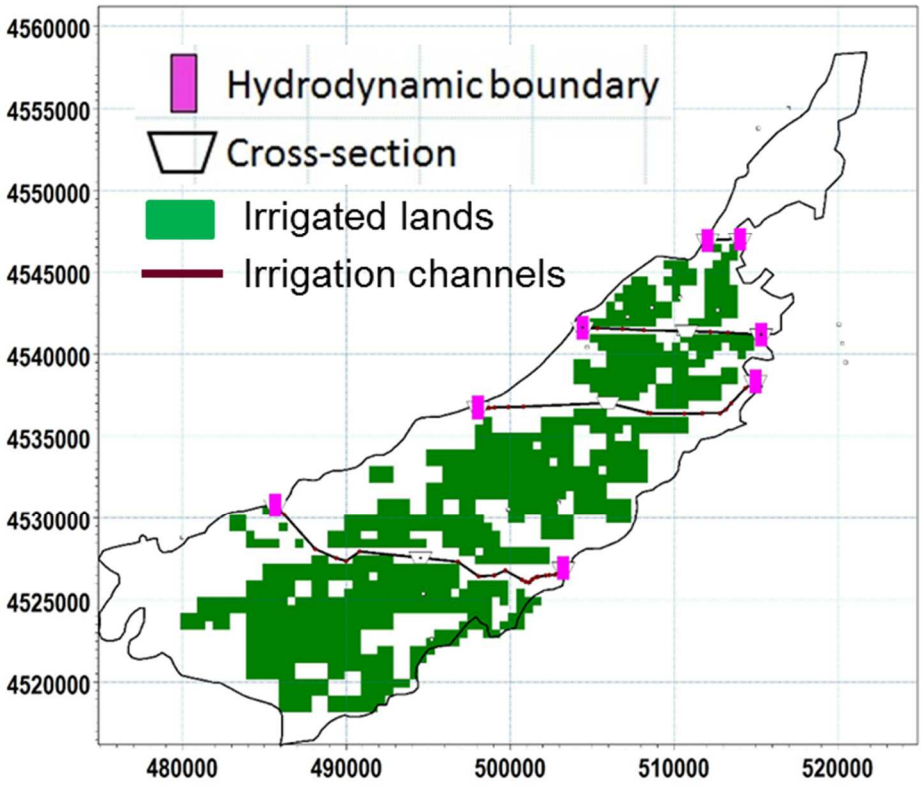

Figure 5.10 Irrigation channels and irrigation area of Quyi Chirchik district

5.4 Results and discussion

After successful calibration of hydrogeological parameters, the model produced quantitative results of water balance of Quyi Chirchik district. **Table 5.2** shows the contribution of each water balance component in the basin (mm/year). **Figure 5.11** shows incremental results of water balance parameters for 2009 - 2013.

In this model, main hydrological inputs are precipitation and irrigation water. **Figure 5.11** tells main part of precipitation occurs in the fall and spring, the non-irrigation period. Therefore, water demand of agricultural crops is compensated by irrigation water. The results shows, around 29 % of total precipitation falls as a snow. During the non-irrigation period actual evapotranspiration is becoming dependent only to irrigation volume and intensity.

The total AET was estimated at an average of 770 mm/year. This is almost two times greater than average precipitation. The estimated AET constitutes around 89 % of total hydrological income. This value includes the evaporation from snow and soil surfaces, apparently main part is from transpiration from vegetation. **Figure 5.12** and **Figure 5.13** show daily spatial distributed AET in irrigation and non-irrigation period. The spatial range of AET is varied average 520-820 mm/year.

This is characterized that shallow groundwater areas are also contribute to ATE process, particularly in irrigation area. According to pervious researches (Makhmudov et al., 2013), AET from subsurface starts 3 meters depth from the ground surface. The satisfactory water balance error was obtained from simulation and this show hydrological parameters are well sustained each other. **Figure 5.14** and **Figure 5.15** show spatial distributed water balance error in calibration and validation periods respectively.

In irrigated areas, the unsaturated zone is very shallow during the irrigation period, therefore infiltration and AET are considered the main hydrological recharge that manage rate of recharge in simulation. The total groundwater recharge was estimated from 180-317 mm/year in simulation period. This is about 25 % of the total input (precipitation and irrigation water). **Figure 5.16** and **Figure 5.17** show total average groundwater recharge map for calibration and validation period in study area.

The simulation of groundwater results were calibrated and validated using monthly observed well data for 2009-2011 and 2012-2013 respectively. **Figure 5.1** shows the location of groundwater wells in the study area. Model performance was evaluated using the mean error (ME), mean absolute error (MEA), root mean square error (RMSE), correlation coefficient (R^2) and the Nash and Sutcliffe coefficient (EF). **Figure 5.18** shows a comparison of observed and simulated groundwater level data. Simulated

groundwater dynamics show a satisfactory match with observed data at each location. Simulation statistics in **Table 5.3** shows the model simulated groundwater flow with satisfactory level.

Table 5.2 Estimated water balance parameters of hydrological model

Year	2009	2010	2011	2012	2013
Precipitation	-435.70	-381.50	-358.40	-431.10	-377.10
Irrigation	-421.09	-423.49	-572.41	-450.38	-456.13
Canopy storage change	0.01	0.01	0.00	0.00	0.00
AET	686.14	743.65	779.35	822.47	820.29
Overland storage change	1.90	3.36	5.78	1.91	-2.41
Boundary outflow	3.16	22.53	28.12	35.22	26.33
Overland to river	0.94	12.16	16.77	27.86	21.06
Sub surface storage change	164.40	23.44	100.58	-5.90	-31.81
Error	-0.24	0.17	-0.20	0.08	0.24

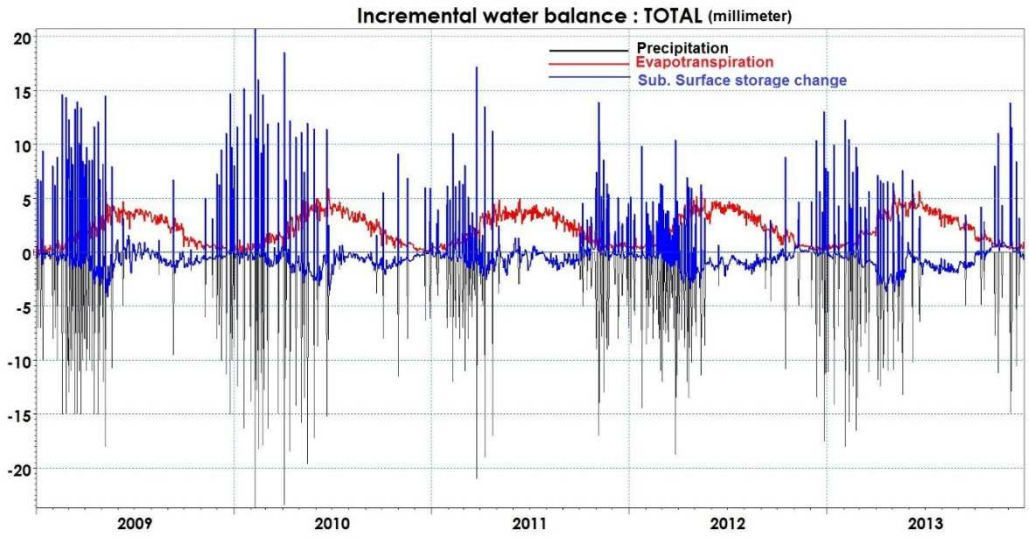

Figure 5.11 Incremental water balance results of Quyi Chirchik district

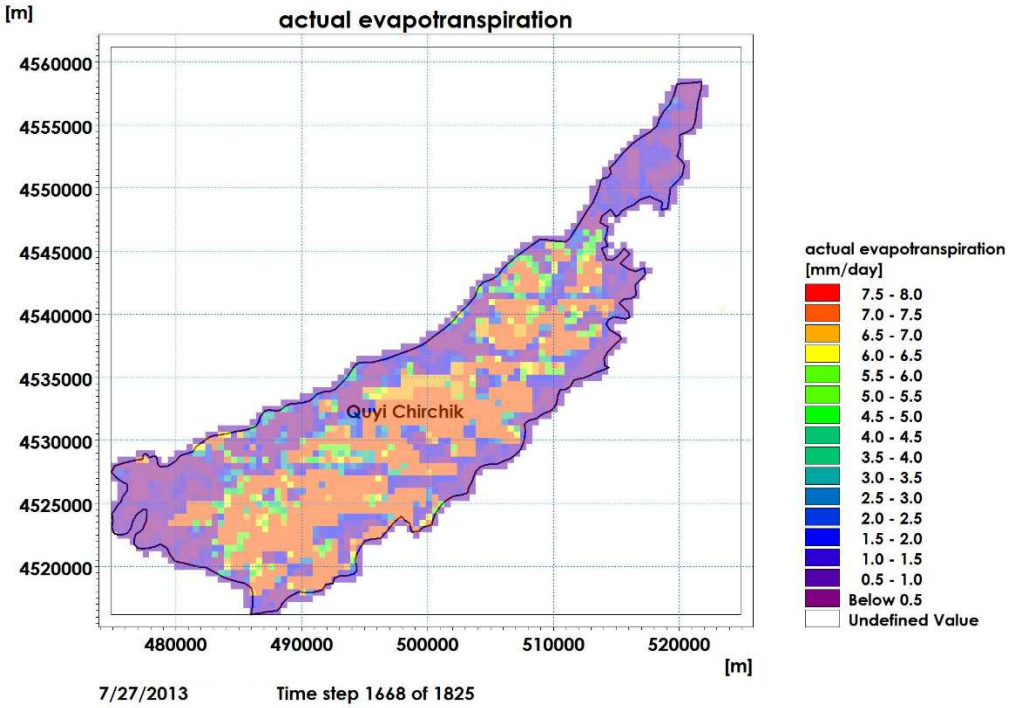

Figure 5.12 Daily spatial distributed AET in irrigation period

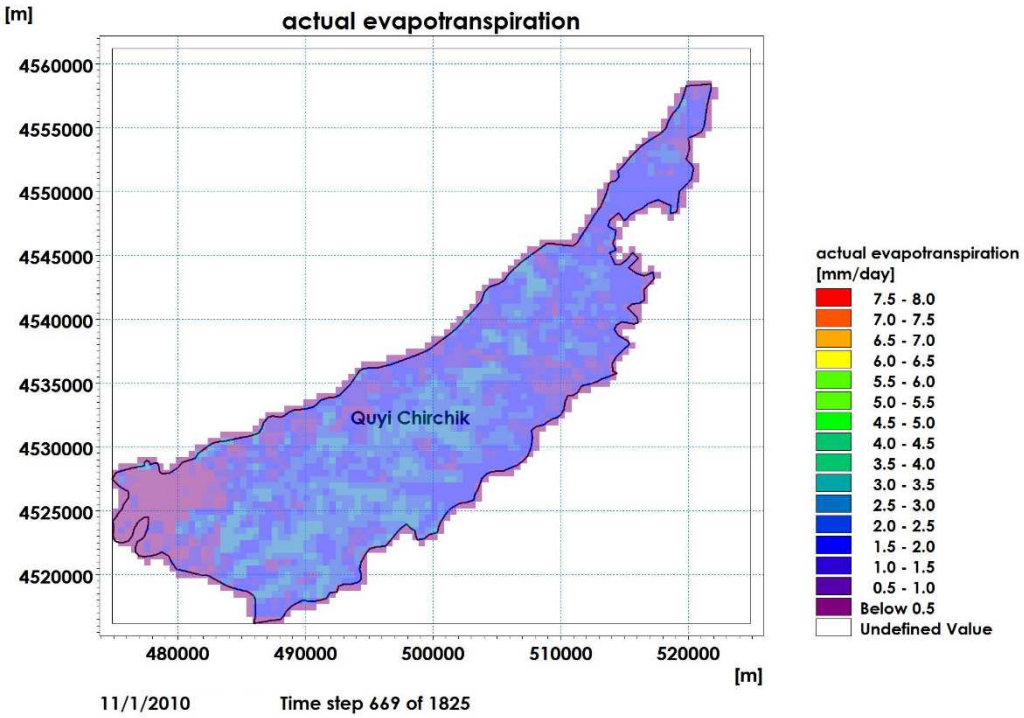

Figure 5.13 Daily spatial distributed AET in non-irrigation period

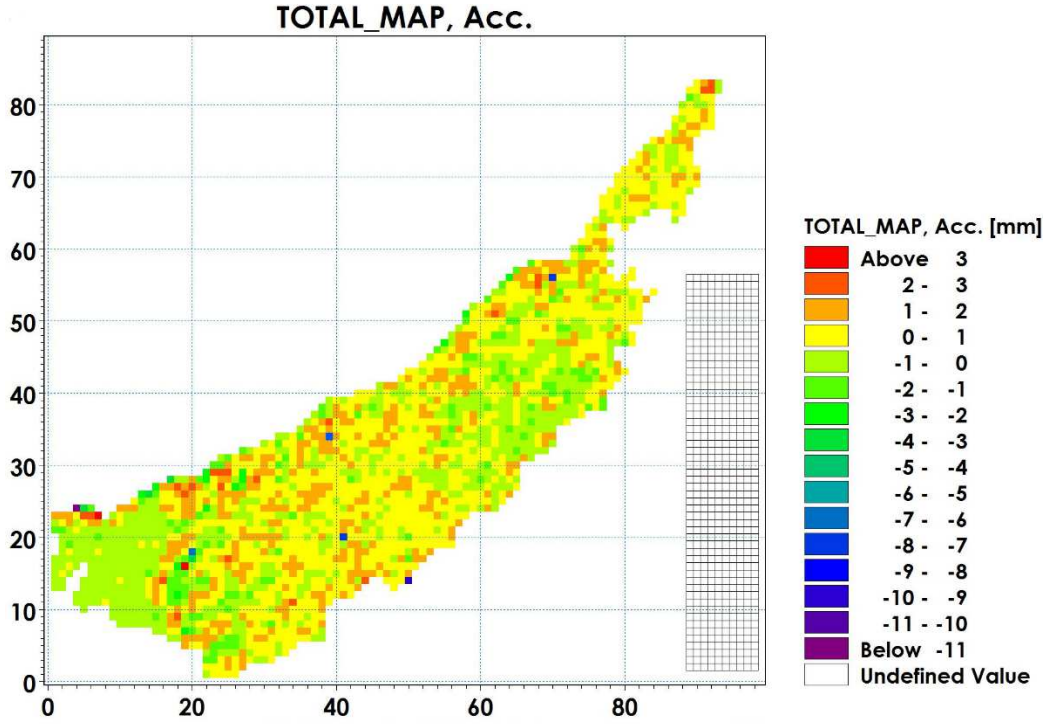

Figure 5.14 Average water balance error in calibration period (2009-2011)

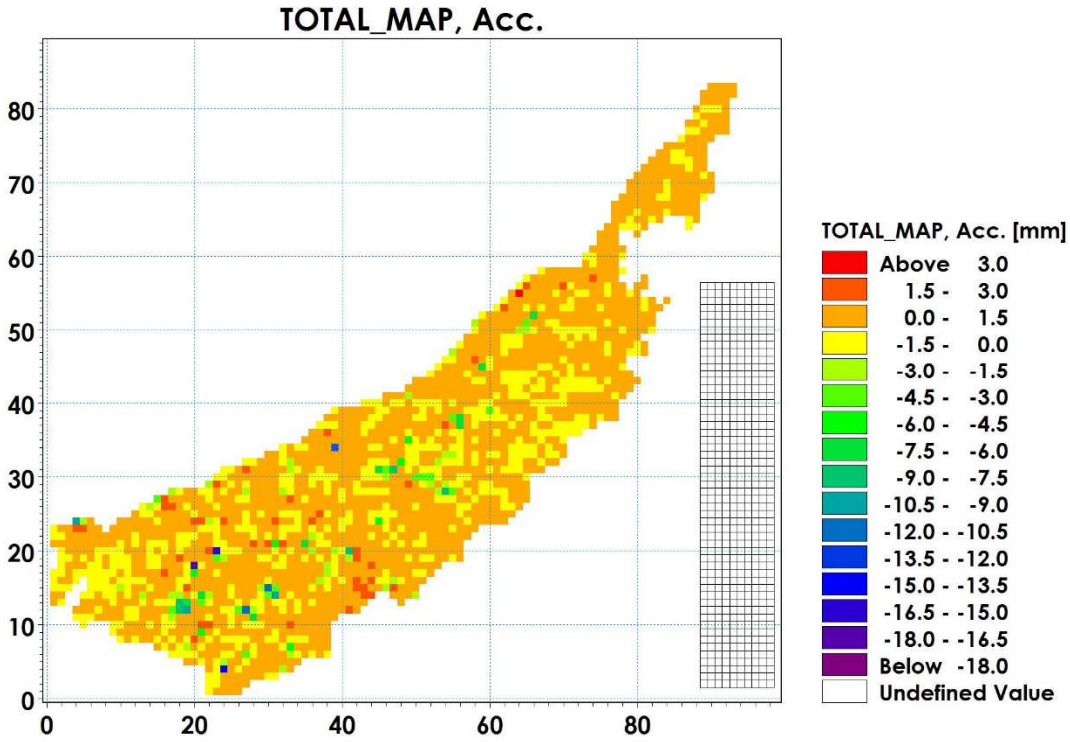

Figure 5.15 Average water balance error in validation period (2012-2013)

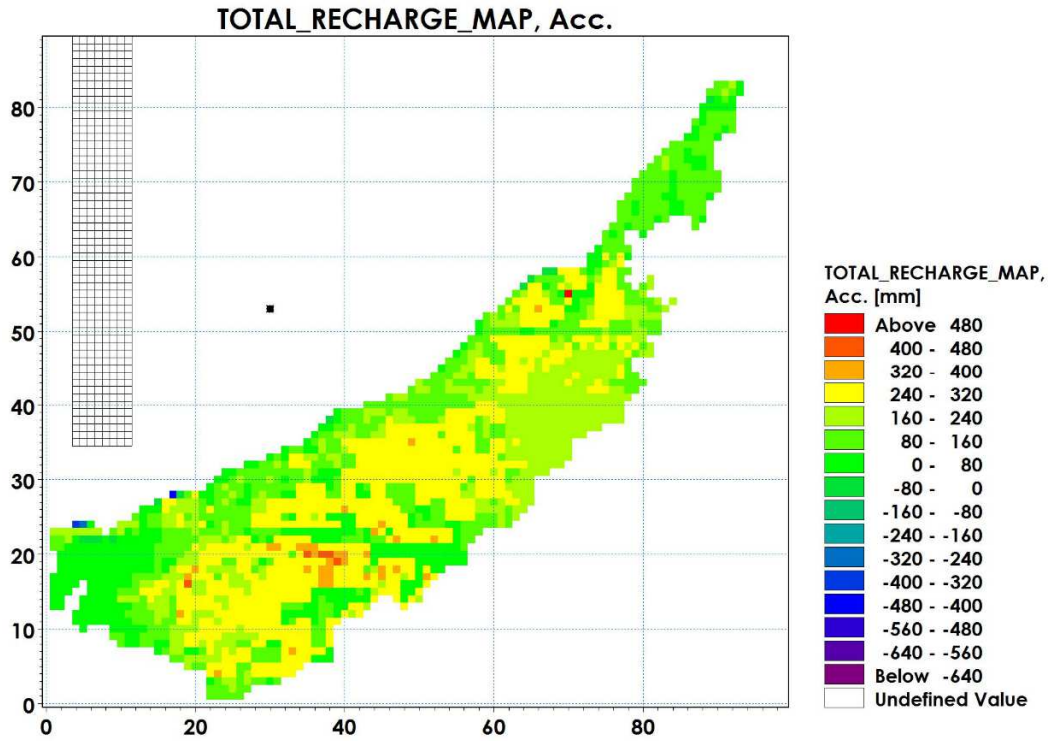

Figure 5.16 Accumulated average groundwater recharge map in calibration period (2009-2011)

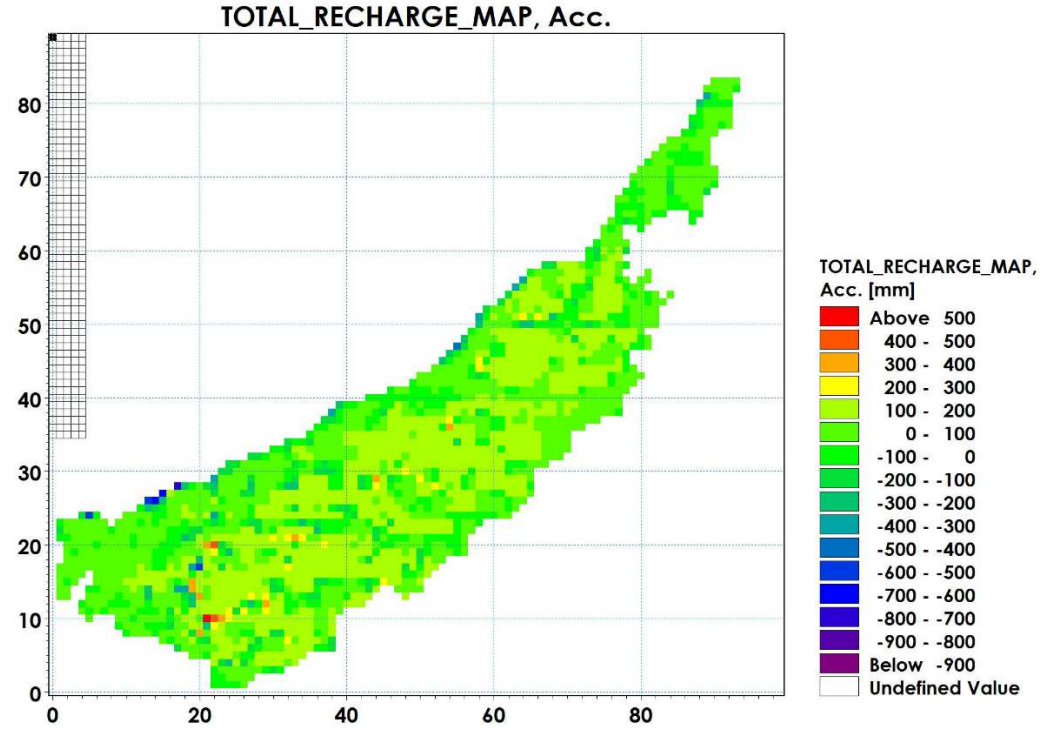

Figure 5.17 Accumulated average groundwater recharge map in validation period (2012-2013)

Table 5.3 Statistics of groundwater simulation

Well ID	ME	MAE	RMSE	R	R2
W1	0.117	0.176	0.2	0.765	-0.166
W2	-0.105	0.256	0.318	0.604	0.277
W3	0.345	0.392	0.441	0.585	-4.658
W4	-0.369	0.387	0.426	0.658	-1.316
W5	0.06	0.195	0.231	0.825	0.644

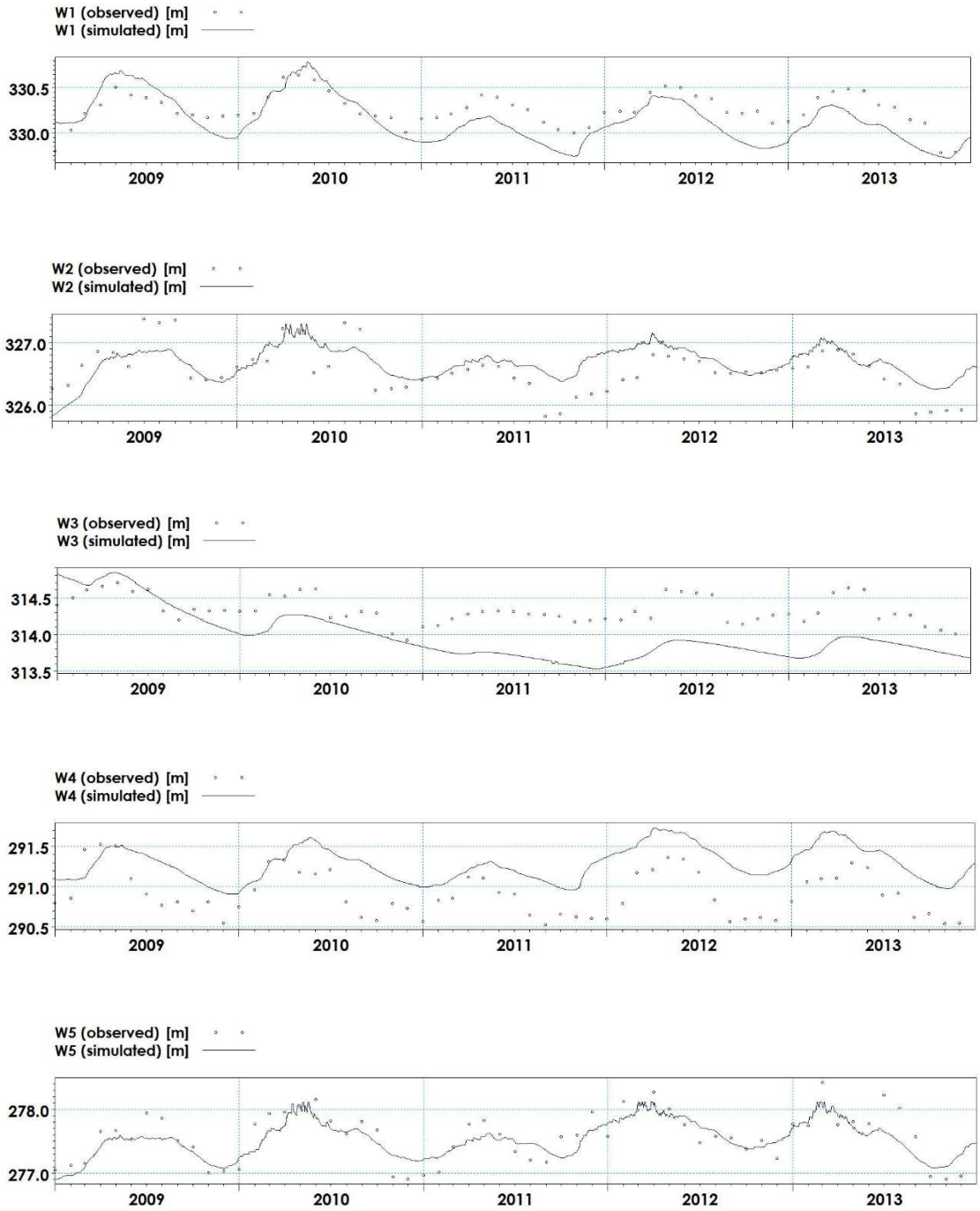

Figure 5.18 Observed and simulated groundwater level in study period

5.5 Spatial analyses of groundwater table

After obtaining fully distributed hydrological model of Quyi Chirchik district, groundwater table map was constructed through a number of procedures. Initially spatially distributed (depth integrated) saturated storage data were generated using a water balance package of MIKE SHE for 2009-2013. This data shows groundwater fluctuation in dfs2 (2D) format. As stated above, maximum groundwater rise observed end of May in the study area. Therefore from dfs2 file was extracted only groundwater depth end of May using MIKE ZERO toolbox. Then these data were transformed to shape file for mapping of groundwater level. The generated groundwater table map of Quyi Chirchik district is given in **Figure 5.19**. **Figure 5.20** shows a geometrical model of groundwater height or saturated zone height while end of May, when it is maximum closer to ground surface. The spatial analyses of the water table map show, around 925 ha area impacted by high groundwater level, which is passed from 2.5 meters depth. The 2.5 meter depth considered threshold level for all districts of Tashkent provinces. The groundwater depth between 3-4 meter occupied areas was estimated about 1625 ha. It should be noted that, about 86 % of these lands corresponds to irrigated agricultural lands. The main part of this area were located in southwestern part of Quyi Chirchik district. This map also shows some portion of urban area also threaten by water table rise.

This groundwater depth map was compared to government elaborated water table map (**Figure 5.21**) to assess the accuracy. Visual comparison of these maps shows groundwater raised areas in both map areas spatially overlapped by 70 %. This assessment confirms that this is an accurate approach to spatial and temporal analyses of groundwater dynamics under irrigation dominated area. The government elaborated map also shows high groundwater impacted areas in another district in Tashkent province. This shows the tool is very important not only in Quyi Chirchik district, but also to neighboring districts. This method can be utilized to identify shallow groundwater impacted areas and assist accurately and effectively perform countermeasures against aridity increase and soil salinization issues. Moreover, this model can be used in water resources planning and development department to appraise water quality and quantity condition, and assist to estimate water budgets of the district.

The limitations and uncertainty of the model related to data availability and degree of calibration. Limitation of data can be seen mainly describing the geometry of subsurface environment, particularly depth of analytical layers. Limited borehole data were available to construct geometry of geological layers and initial groundwater depth, thus additional data would be to an increased level of confidence of the model results.

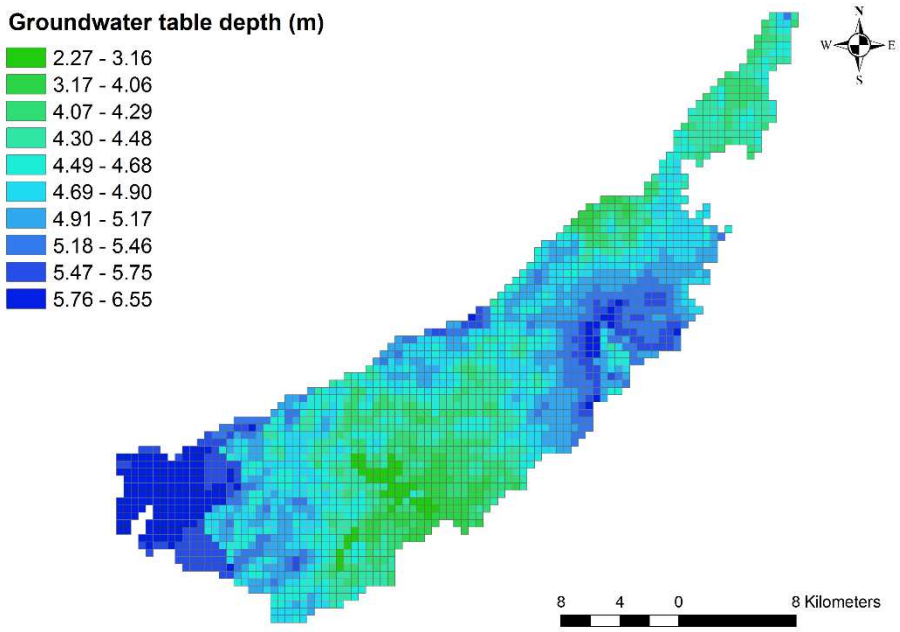

Figure 5.19 Groundwater depth of Quyi Chirchik district

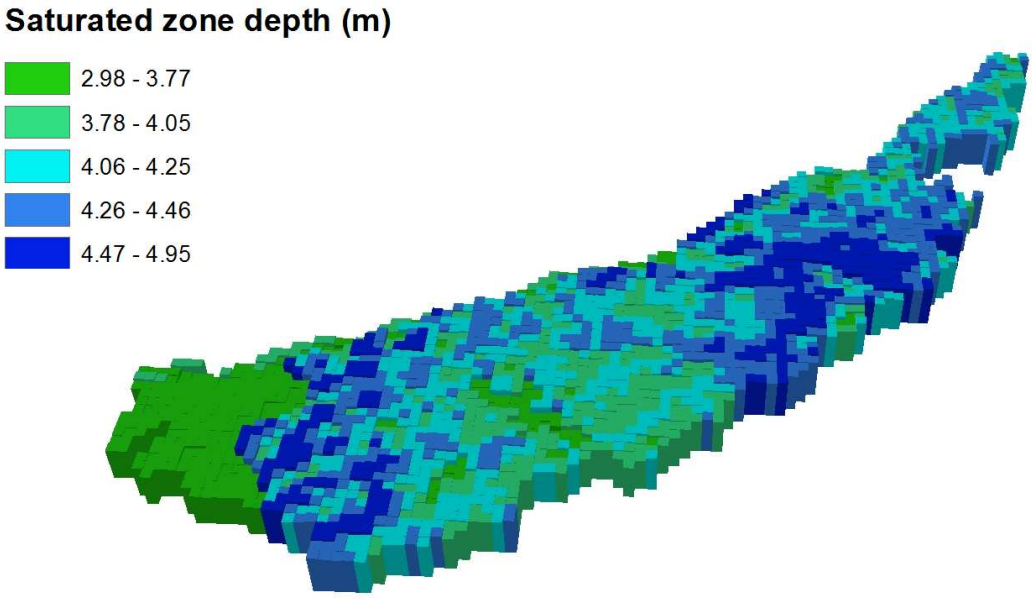

Figure 5.20 Geometrical model of groundwater height

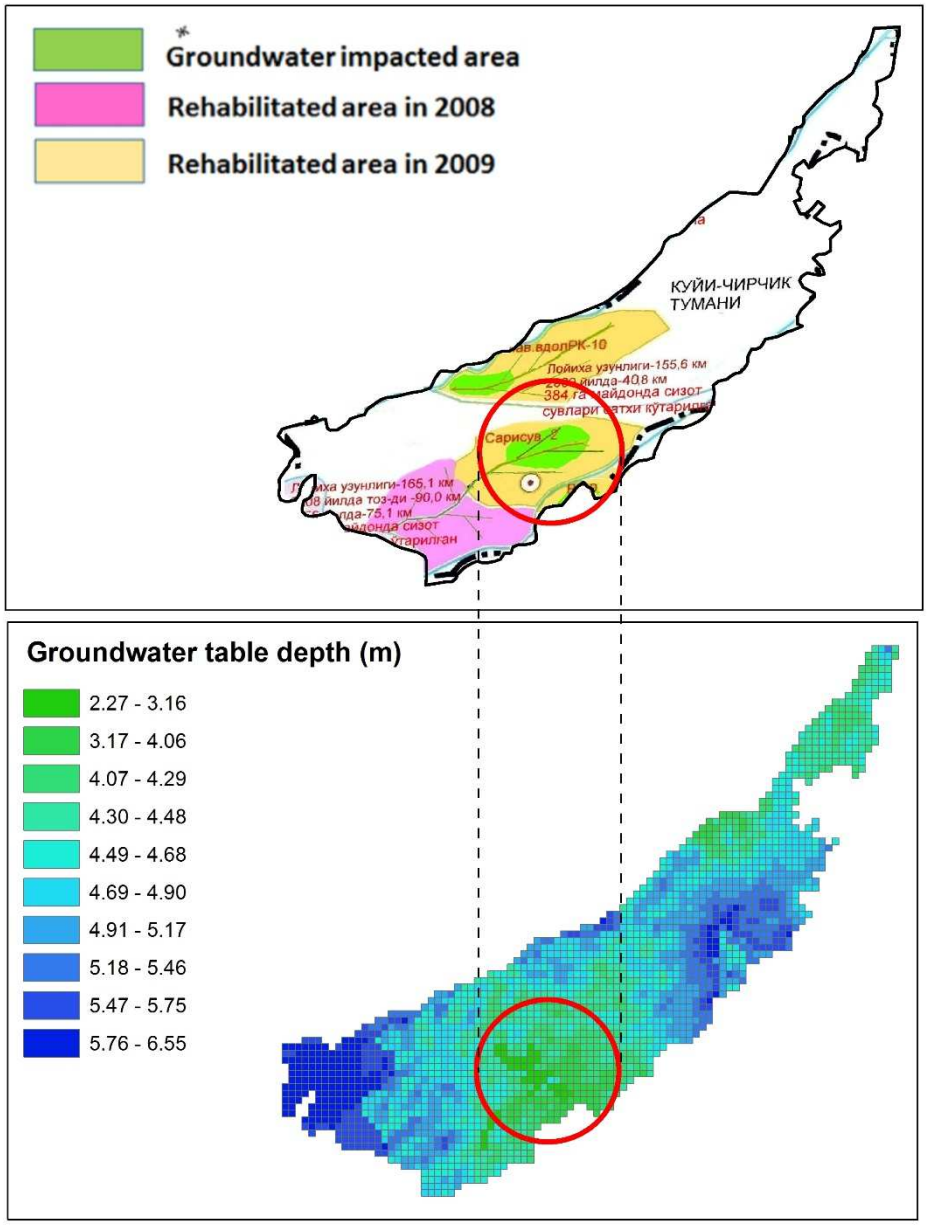

Figure 5.21 Comparison of groundwater table depth with government elaborated water table map in districts of Tashkent Province

5.6 Groundwater Quality Assessment by Using Water Quality Index in Quyi Chirchik District

Groundwater samples were collected from 12 places end of May when groundwater reaches its high level during the year (2013). **Figure 5.22** shows location of these samples in Quyi Chirchik district.

Each sample was analyzed for 11 chemical parameters. The following chemical elements are analyzed in this study: Total hardness (TH), TDS, pH, bicarbonate (HCO_3^-), chloride (Cl^-), sulfate (SO_4^{-2}), nitrate (NO_3^{2-}), calcium (Ca^{2+}), magnesium (Mg^{2+}), potassium (K^+) and sodium (Na^+). Initially WQI was estimated to check the overall quality of groundwater at sampling location. The calculation method of WQI is described in detail by many researchers (Backman et al., 1998; Soltan, 1999; Ramakrishnalah et al., 2009; Rizwan and Gurdeep, 2010). There are three stages for computing WQI. On the first stages the specific weights (wi) have been assigned to all chemical parameters according to the perceived effects in the water quality. The most influence able parameters have a weight of 5 and the lower important a weight of 1. The maximum weight of 5 has been assigned to nitrate due to its perceived effects on primary health (**Table 5.4**). Then the specific weight is used to calculate the relative weight (Wi) using **Equation (5.1)**:

$$W_i = \frac{w_i}{\sum_{i=1}^{n} w_i} \quad \textbf{(5.1)}$$

In the second stage the quality rating scale (qi) is calculated using **Equation (5.2)**:

$$q_i = \frac{C_i}{S_i} \times 100 \quad \textbf{(5.2)}$$

Where *Ci* is the observed concentration of each chemical parameter in each water sample and *Si* is the World Health Organization (WHO) (WHO, 1993) standard for each chemical parameter. In final stage sub-index of ith parameter (*SI*i) is determined for each chemical parameter using **Equation (5.3)**, and then used to compute the WQI according to **Equation (5.4)**:

$$SI_i = W_i \times q_i \quad \textbf{(5.3)}$$

$$WQI = \sum SI_i \quad \textbf{(5.4)}$$

Estimated WQI values are classified into five categories (**Table 5.5**): Good, fair, poor and very poor. The sample data of groundwater chemicals and estimated WQI are given in **Table 5.6**. The statistical analyses were also carried out to appraise the linear relationship between any of the chemical parameters. The fully distributed integrated model was used to simulate spatial and temporal variation of groundwater level in Quyi Chirchik district. The model integrates the surface, subsurface, irrigation process and their interactions in hydrological simulation. The detail information of the groundwater model is given in the previous chapter. This study attempts to establish detail information of formation and origin of salinity and water quality parameters.

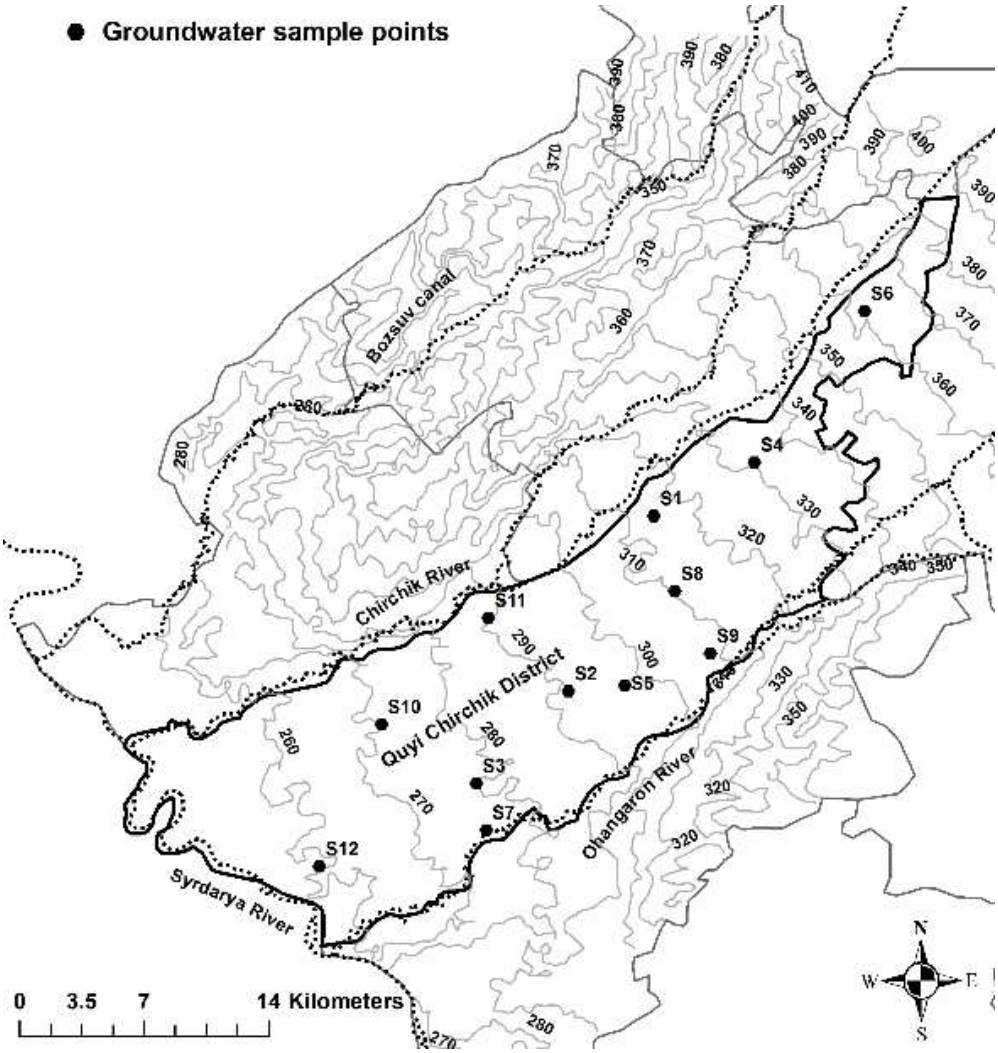

Figure 5.22 Map of Quyi Chirchik district and location of groundwater samples

5.6 Results and discussion

The estimated WQI values for 12 wells in Quyi Chirchik districts range from 76.58 to 132.88 as shown in **Table 5.6**. According to **Table 5.5**, nine samples are placed in "Fair" water classification and other 9 samples fall to "poor" water quality standard. This shows 75 % of the samples are in fair and 25 % of the samples are in poor condition. The higher value of WQI is mainly due to the higher values of TDS. The accumulation of TDS in shallow groundwater is mainly caused by anthropogenic factors. TDS in all study area varies from 775 to 1285.5 mg/l. This shows TDS values in all measured samples are exceeded from water quality standard.

The correlation coefficient matrix of chemicals in **Table 5.7** shows that NO_3^{2-}, Ca^{2+}, SO_4^{2-}, Na^{+} and Cl^{-} are the main contributions of TDS. For instance nitrate concentration showed good correlation with TDS (0.78) and WQI (0.88). The concentration of nitrate varies from 14.11 to 72.35 mg/l in the study area. The sulfate concentration is exceeded from the standard level of almost 100 % of the samples. For instance nitrate concentration showed good correlation with TDS (0.78) and WQI (0.88). The concentration of nitrate varies from 14.11 to 72.35 mg/l in the study area. The sodium and nitrate concentrations are also exceeded in five and four number of samples due to intensive agricultural activities and over application of fertilizers. The high positive correlation also exists between Ca^{2+} and SO_4^{2-} (R=0.68). This presents the unique origin of these two elements, which is the dissolution of gypsum. The correlation coefficient is also high between Mg^{2+} and SO_4^{2-} (R=0.6) and this is possibly formatted from the dissolution of sulfate minerals.

Table 5.4 Relative weight for each chemical parameter

Chemical parameter	S_i	w_i	W_i
TH	300	2	0.061
TDS	500	4	0.121
pH	8.5	4	0.121
HCO_3^-	250	3	0.091
Cl^-	250	3	0.091
SO_4^{2-}	200	4	0.121
NO_3^{2-}	45	5	0.152
Ca^{2+}	75	2	0.061
Mg^{2+}	30	2	0.061
K^+	12	2	0.061
Na^+	200	2	0.061

Table 5.5 Water quality classification based on WQI

WQI value	Class	Water quality	Water samples
<50	I	Good	0
50-100	II	Fair	9
100-200	III	Poor	3
200-300	IV	Very poor	0

Table 5.6 Sample data of groundwater chemicals (mg/l) and estimated WQI

Chemical parameter	S1	S2	S3	S4	S5	S6	S7	S8	S9	S10	S11	S12
TH	6.8	6.5	4.3	4.3	10	7.2	5	7.6	8.3	6.1	5.1	5.7
TDS	775	1188	1285.5	911	866	980	1104.7	822	832	963	912	931
pH	7.33	8.31	6.84	7.52	7.68	7.65	9.12	8.2	7.3	7.12	7.65	7.54
HCO_3^-	327.4	387.52	300.25	327	326	332.3	364.21	322.5	322	345.4	329.3	320.1
Cl^-	35.4	64.34	58.47	40.25	35.47	62.3	53.25	31.97	31.47	68.3	51.3	51.23
SO_4^{2-}	254.3	326.32	388.72	265.32	248.87	268.12	312.21	245.37	244.87	254.12	265.12	245.63
NO_3^{2-}	14.11	72.35	58.52	22.35	19.54	30.01	42.31	16.04	15.54	29.21	27.01	24.2
Ca^{2+}	45.3	89.65	83.64	58.34	54.02	54.21	75.63	50.52	50.02	48.51	51.21	68.25
Mg^{2+}	23.6	68.87	75.63	42.32	37.64	23.32	52.21	34.14	33.64	23.32	20.32	54.21
K^+	2.74	7.12	6.21	5.87	6.32	7	6.87	2.82	2.32	5.21	4	4.21
Na^+	133.09	223.54	245.62	157.34	146.82	208.21	212.32	143.32	142.82	188.21	205.21	139.82
WQI	76.58	132.88	123.56	90.85	86.56	94.45	114.80	81.68	80.01	90.87	88.61	92.80

Table 5.7 Correlation coefficient matrix

Chemical Parameters	TH	TDS	pH	HCO_3^-	Cl^-	SO_4^{2-}	NO_3^{2-}	Ca^{2+}	Mg^{2+}	K^+	Na^+	WQI
TH	1											
TDS	0.26	1										
pH	0.00	0.01	1									
HCO_3^-	0.00	0.09	0.46	1								
Cl^-	0.208	0.51	0.00	0.189	1							
SO_4^{2-}	0.267	**0.86**	0.001	0.015	0.24	1						
NO_3^{2-}	0.162	**0.88**	0.048	0.266	0.49	**0.74**	1					
Ca^{2+}	0.18	**0.8**	0.09	0.153	0.24	**0.68**	**0.82**	1				
Mg^{2+}	0.122	**0.62**	0.02	0.023	0.07	**0.6**	0.58	**0.8**	1			
K^+	0.047	0.5	0.08	0.201	0.42	0.31	0.45	0.3	0.2	1		
Na^+	0.252	**0.79**	0.016	0.104	**0.61**	**0.68**	**0.71**	0.4	0.2	0.4	1	
WQI	0.192	**0.95**	0.058	0.213	0.51	**0.83**	**0.91**	**0.9**	**0.68**	0.5	**0.67**	1

5.7 Correlation of the groundwater table and land use with water quality

The productivity of the irrigated land in study area strongly depends on the groundwater table rise and its mineralization. Therefore groundwater table is a critical factor for maintaining an adequate condition of irrigated lands. High water table strengthens the capillary rise of salts up to the top soil layer. This process increases soil salinization and land degradation.

The study was carried out to find the existing correlation between ground water table depth and water quality. As stated above the groundwater table and chemical parameters were obtained at the end of spring when groundwater table is maximum. **Figure 5.23** shows spatial distributed groundwater table depth of the study area with WQI. The maximum groundwater table depth varies from 2.2 to 6.5 m. The map denotes that relatively high groundwater table area has occupied the southwestern site of the district and water quality is also most salinized according to WQI. The most critical situation is when the groundwater table depth is less than 2.5 meters from the ground surface because salt movement is observed by capillary rise toward to root zone and thus has a direct effect on crop yield and soil salinity. It can be concluded that as the groundwater table increase water quality decreases, particularly in arid agricultural areas. The excessive leaching process will be worsening this issues unless providing proper drainage systems. Unfortunately Quyi Chirchik district is plain region and drainage system is not functioning efficiently.

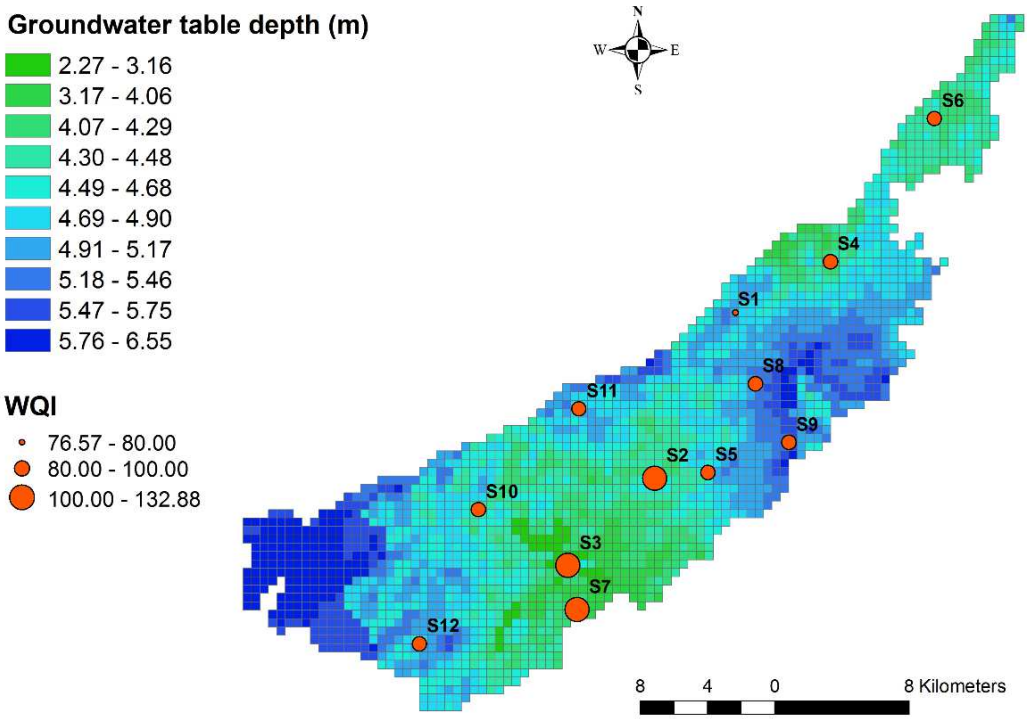

Figure 5.23 Correlation between groundwater table depth and WQI

5.8 Conclusion

The proposing method in this chapter focuses the solution of one of the actual hydrological related problems in Quyi Chirchik district. The high groundwater level is not issue only in Quyi Chirchik district, but also neighboring districts in Tashkent province. The model was constructed with several assumptions in the geospatial data preparation, particularly the spatial distributed depth of geological layers. The model parameters were calibrated using observed groundwater well data for 2009-2013. The model then validated with well-tuned parameters for 2012-2013. After model produced quantitative results of water balance of Quyi Chirchik district. Using model results spatial and temporal variation of ground water dynamics was investigated. The spatial analyses show southwestern part of Quyi Chirchik district is impacted by high groundwater table. In 925 ha area groundwater depth were estimated 2.5 meters in end of May. This groundwater depth considered critical level due to its negative effects. Because from this level groundwater expose to evaporation and create good environment for soil salinization process. It should be noted that, about 86 % of these lands corresponds to irrigated agricultural lands. Visual comparison of the model generated groundwater depth map with government elaborated map is spatially overlapped by 70 %. This shows that this is an accurate approach to detect the high water table impacted areas under irrigation process. This method can be important to water resources managers to perform countermeasures against aridity increase and soil salinization issues.

In this study water quality index has been computed to assess groundwater quality and origin of salt in Quyi Chirchik district, Uzbekistan. Twelve groundwater samples were collected from different sites to estimate WQI, eleven chemical parameters have been considered: Total hardness, TDS, pH, bicarbonate, chloride, sulfate, nitrate, calcium, magnesium, potassium and sodium. The results shows that 75 % of water samples falls in “Fair” classification and 25 % samples falls in “Poor” categories of WQI. This shows that shallow groundwater in the study area is not suitable for drinking purposes.

The study has revealed that good correlation exists the between groundwater table depth and total dissolved solids. The maximum groundwater table depth varies from 2.2 to 6.5 m. The spatial distributed groundwater table map denotes relatively high groundwater table area has occupied in southwestern site of the district and water quality is also most salinized places according to WQI.

The statistical analyses show that the high value of WQI and TDS of this site has been found mainly from the higher values of sulfate, nitrate, calcium, magnesium and

sodium. The excessive concentration of sulfate and nitrate in samples depicts intensive application of inorganic fertilizers. The study also found that a strong correlation exists between the groundwater table depth and TDS. The spatial distributed groundwater table depth and WQI map provide valuable tools for managers to understand the status of water quality specially and assist making adequate decisions. Based on this study, it is advised to increase density of drainage systems, particularly where groundwater table depth is higher and increase the efficiency of both irrigation and the drainage system. And most important is the increase of quality of irrigation waters which mainly comes from Chirchik and Ohangaron rivers. These rivers, especially Chirchik River receives many untreated drainage waters from urban and upper stream irrigation sites until coming to downstream sites.

5.9 References

Backman, B., Bodis, D., Lahermo, P., Rapant, S., and Tarvainen, T. "Application of a groundwater contamination index in Finland and Slovakia" (1998).

Fatema, A., Rasul, M., Khan. M and Amir M. A Comparative View of Groundwater Flow Simulation Using Two Modelling Software - MODFLOW and MIKE SHE. Proceedings of the 18th Australasian Fluid Mechanics Conference, Launceston, Australia, 3-7 December 2012.

Foster S. and Allen D. Groundwater-Surface Water Interaction in a Mountain-to-Coast Watershed: Effects of Climate Change and Human stressors. *Advances in Meteorology,* 22 (2015). http://dx.doi.org/10.1155/2015/861805

Golmar, G., Shiv, P., Ali, M. and Ramesh, R. Evaluating Three Hydrological Distributed Watershed Models: MIKE-SHE, APEX, and SWAT. Hydrology, 1, 20-39 (2014). http://dx.doi.org/10.3390/hydrology1010020

Horton, R. K., An index number system for rating water quality. Journal-Water Pollution Control Federation, 10, pp: 300-305 (1965).

JICA report on "Water Resources Utilization in Tashkent Province, Uzbekistan", (2010).

Makhmudov, E. Rahimov, Sh., Chen, S. and Tzilili, A. Water Resources and Its Utilization in Uzbekistan. Pliograf Group Press., Tashkent, Uzbekistan (2013).

Rakhmatullaev, S., Frederic, H., Kazbekov, J., Helene, C. J., Mikael, M. H., Philippe, Le C. and Jumanov, J. Groundwater Resources of Uzbekistan: An Environmental and Operational Overview (2013).

Ramakrishnalah, C. R., Sadas hivalah C. and Ranganna G. Assessment of water quality index for the groundwater in Tumur Taluk, Karnataka state, India. E journal of chemistry. 6(2), pp. 523-530.

Rizvan, R., and Gurdeep, S. Assessment of Groundwater Quality status by using Water Quality Index Method in Orissa, India. World Applied Sciences. 9(12), pp. 1392-1397.

Singh, R., Subramaniana, K. and Refsgaard, C. Hydrological Modelling of a Small Watershed Using MIKE SHE for Irrigation Planning. Agricultural Water Management, 41, 149-166 (1998).

Soltan, M. E: Evaluation of groundwater quality in Dakhla Oasis (Egyptian Western Desert). Environmental Monitoring and Assessment. 57(2), pp.157-168 (1999).

Usmanov, S. and Yasuhiro M. Integrated Approach to Detect the Spatial and Temporal Variation of Groundwater Level in Quyi Chirchik District, Uzbekistan. The 37th West Japan Symposium on Rock Engineering (2016).

WHO, Guidelines for drinking water quality (2nd Ed., Vol. 1, pp. 188). Recommendation,

Geneva and World Health Organization (1993).

Chapter 6: Conclusions and Future Work

6.1 Conclusion

Hargreaves model was modified under local climatic conditions of the Tashkent province using standard Penman Monteih FAO 56 (FAO-56 PM) model estimates for every month of the years. The HM showed a good performance with locally calibrated empirical coefficients in Tashkent province as an arid and semi-arid region. Over and under estimations of ETo with the original HM were reduced by 65 % as an average using new empirical coefficients for all 16 weather stations. Then the suitable interpolation methods were determined among deterministic, geostatistical and regression methods to spatial modeling of reference evapotranspiration over the Tashkent province using modified Hargreaves model estimates. The ordinary co-kriging method is better predicted estimated ETo in Tashkent province using elevation data as a covariance. The results revealed that the incorporation of elevation data improved spatial prediction of ETo in Tashkent province.

By using estimated reference evapotranspiration, a fully integrated hydrological model was developed to study the hydrological balance of the Chirchik River Basin, Uzbekistan. The model was constructed with several assumptions when preparing the geospatial data set of unsaturated and saturated zones, climate and land use parameters. Parameters in the model were calibrated and simulated results were validated for the periods 2009-2011 and 2012-2013 in term of two observed hydrological parameters; stream flow rate and groundwater table.

After the successful calibration of the parameters, the model produced quantitative results of the hydrological parameters. Using the model results, the groundwater and surface water interaction and spatial variability of hydrological parameters are analyzed.

Precipitation and irrigation water plays a major role in the entire surface and subsurface hydrological cycle. Evapotranspiration was found to be the main water loss factor among water balance components, with an average of a 714 mm / year (77% of the total water budget). As an arid land, Actual evapotranspiration is strongly dependent on irrigation water quantity irrespective of rainfall in downstream sites. It should be stated that decreased irrigation water causes of increased aridity in the basin. This study confirmed that in arid and semi-arid regions with intensive agriculture, integrated

modelling is valuable for understanding water cycles in large basins.

Estimated groundwater recharge varied between 105-218 mm/year, making up 17-20% of the total water budget. The highest groundwater recharge occurs from March to May with an average of 90-60 mm/month.

Finally, an integrated hydrological model coupling with GIS was proposed to detect the spatial and temporal variation of groundwater level. The application of this model was demonstrated in Quyi Chirchik district to detect high groundwater table area spatially and to study the relationship between spatial and temporal variation of groundwater level and its quality.

The spatial analyses show southwestern part of Quyi Chirchik district is impacted by high groundwater table. In 925 ha area groundwater depth were estimated 2.5 meters in end of May. It should be noted that, about 86 % of these lands corresponds to irrigated agricultural lands.

The results shows that 75 % of water samples falls in “Fair” classification and 25 % samples falls in “Poor” categories of WQI. This shows that shallow groundwater in the study area is not suitable for drinking purposes. The study has revealed that good correlation exists the between groundwater table depth and total dissolved solids with 0.7 correlation coefficient.

The proposed integrated hydrological model coupling with GIS provides capability for spatial detection of high groundwater depth area. This method is oriented to solve one of the actual problems not only in the Chirchik River Basin but also other districts of Uzbekistan. Because these districts are also facing high groundwater table and salinity issues.

The comprehensive part of the research was the processing all required geospatial data (Soil type, land use, topography, geology, river network geometry and agricultural water use) into integrated numerical model. This is challenging because all these data have never been used together before in hydrological studies in the Chirchik River Basin.

The novelty of this study is a development of a local hydrological model for a relatively large river basin covering from upstream to downstream site of the basin and considering agricultural water use and administrative boundaries of the districts. This modeling approach is better describing formation, utilization and discharging of water resources under the impact of different land use process. This novel tool is urgent for integrated water resources management, particularly assessment of quantitative status of surface and groundwater resources.

6.2 Future works

In order to further improve the model performance and widening hydrological investigation scale, the following aspects are expected into consideration:

1. The existing hydrological model need to be updated with more detail information about operation of small irrigation canals, irrigation time and quantity, reservoirs and hydro-engineering structures within the Chirchik River Basin to minimize the estimated simulation errors and further explore uncertainty.
2. The further simulation should account the exchange between river water and saturated zone. To accomplish this task accurate geological data necessary to be used to construct geology of analytical layers of the hydrological model.
3. Using the model and model results, further steps of study should focus to predict effects of climate and land use change to the hydrological regime of the Chirchik River Basin. Apart from quantitative analyses, in future research should also consider surface and groundwater quality issues.
4. The GIS based hydrological model should be tested in other districts which is exposed high groundwater table and salinization issues in order to improve the model capability in different climatic regions.